

**New Jersey Water Resources Research Institute  
Annual Technical Report  
FY 2012**

# Introduction

The New Jersey Water Resources Research Institute (NJWRRI) supports a diverse program of research projects and information transfer activities. With oversight from the Advisory Council, which sets the Institute's Research Priorities, the available funds are divided between supporting faculty with 'seed' projects or new research initiatives, and funding graduate students to develop their thesis research. The funding is intended to initiate novel and important research efforts by both faculty and students, thus emphasizing new research ideas that do not have other sources of funding. We hope to support the acquisition of data that will enable further grant submission efforts, and, in the case of students, lead to research careers focused on cutting-edge research topics in water sciences.

Research projects span a wide range of topics in water resources. In the first faculty project, Bakacs characterized the types of pollutants associated with non-commercial carwash runoff and evaluated the potential of bioretention systems to treat this runoff. In the second faculty project, Hou developed a new carbon-based nanomaterial as an innovative sorbent with high capacity and activity to remove As and Pb contaminants from drinking water, and can be re-useable and manufactured with lower cost. In the final faculty project, Wei developed a novel hybrid material that integrates nanosized nHFO, microalgae and porous immobilization that could potentially remove arsenic from drinking water. Additionally, Deng and Rowe are providing updates for their projects continued from FY2011.

Graduate students have similarly carried out an impressive range of research. Falzone and his advisor sought to quantify matrix potential to predict groundwater flow within the vadose zone using nuclear magnetic resonance (NMR) relaxation times. Luther and her advisor studied the hydrolytic and fermentative stages of anaerobic digestion (AD), with a focus on the effect of free ammonia on these bacterial populations. From this research, they hope to develop a better understanding of the physiological response to ammonia stress, and to develop much needed molecular tools for process control of AD. Rattana and advisor developed techniques for improving anaerobic biodegradation of high N-wastes by enrichment of microorganisms responsible for rapid ammonia production from organic-N and tolerance to high ammonia concentrations. Shappell and her advisor sought to characterize the underlying mechanisms driving floral diversity, particularly invasive species dominance, which has great implications for the development of best management practices that maximize wetland services.

James A. Smith and colleagues from Princeton University received funding through the NIWR/USGS Program to develop statistical procedures for regional analysis of drought and flood in the eastern United States. Interim findings of this research are reported.

The goal of our information transfer program is to bring timely information about critical issues in water resource sciences to the public, and to promote the importance of research in solving water resource problems. The information transfer program continues to focus on producing issues of the newsletter that provide a comprehensive overview of a particular water resource topic, as well as one issue a year that highlights water research occurring in New Jersey. The program continues to develop the NJWRRI website ([www.njwrri.rutgers.edu](http://www.njwrri.rutgers.edu)) into a comprehensive portal for water information for the state. We also collaborate with other state and regional organizations in sponsoring and producing conferences.

## Research Program Introduction

The New Jersey Water Resources Research Institute has a policy, yearly reaffirmed by the NJWRRI Advisory Council, of using research dollars to promote novel directions of water resources research. To this end, three projects directed by research faculty at institutions of higher learning around the state were selected, and five grants-in-aid were awarded to graduate students who are beginning their research. In both cases, we expect that the research is exploratory and is not supported by other grants. The intent is that these projects will lead to successful proposals to other agencies for further support. The larger goal of the research component of the Institute's program is to promote the development of scientists who are focused on water resource issues of importance to the state.

A NIWR/USGS National Competitive Grant Program project from New Jersey received continued funding this year. Additional findings from that research are reported here. Also included are updates on two projects from FY2011.

# Scrap Tire and Water Treatment Residuals as Novel "Green" Sorbents for Removal of Common Metals from Polluted Urban Storm Water Runoff

## Basic Information

<b>Title:</b>	Scrap Tire and Water Treatment Residuals as Novel "Green" Sorbents for Removal of Common Metals from Polluted Urban Storm Water Runoff
<b>Project Number:</b>	2011NJ274B
<b>Start Date:</b>	3/1/2011
<b>End Date:</b>	8/31/2012
<b>Funding Source:</b>	104B
<b>Congressional District:</b>	NJ-008
<b>Research Category:</b>	Water Quality
<b>Focus Category:</b>	Methods, Water Quality, Non Point Pollution
<b>Descriptors:</b>	
<b>Principal Investigators:</b>	Yang Deng, Sudipta Rakshit, Dibyendu Sarkar

## Publication

1. Morris, Ciapha; Sudipta Rakshit; Yang Deng; Pravin Punamiya; Edward Landa; Dibyendu Sarkar, 2012, Sorption of Toxic Metals from Polluted Urban Stormwater Runoff using Two Recycled Waste-Based Sorbents - Water Treatment Residuals and Tire Rubber. 2012 Spring Annual Meeting of Hudson/Delaware Chapter - Society of Environmental Toxicology and Chemistry, Montclair, New Jersey. April 26-27, 2012. (Poster presentation)

## **4. PROJECT SUMMARY**

### **4.1 Problem and Research Objectives**

#### **4.1.1 Problem statement**

The United States is an extremely urbanized country. In 2000, over 75% of the total U.S. population was concentrated in more than 500 urban areas with a population density of  $> 390 /\text{km}^2$ . Among them, two-thirds lived in the 39 largest metropolitan areas (e.g. North Jersey-New York City Metro Area) with populations greater than 1 million. Despite many benefits, high urbanization has led to various environmental issues, such as polluted urban runoff. Urban runoff is the surface runoff of stormwater created by urbanization. Urban areas are characterized by high densities of impervious surfaces, such as buildings, parking facilities, urban streets, highways, or walkways. These impermeable surfaces can provide an effective environment to collect and accumulate constituents from atmospheric deposition, vehicular traffic or other sources. As a result, the impervious surfaces significantly increase the flow of urban runoff that efficiently transports numerous water quality constituents, and increases the variety and amount of pollutants in urban runoff, which are eventually transported to receiving waters without proper management and treatment. Increased pollutant loads can harm fish and wildlife populations, kill native vegetation, degrade the quality of drinking water supplies, and make recreational areas unsafe. Thus, urban runoff has been recognized among the major nonpoint sources of groundwater pollution (USEPA, 2009).

Heavy metals are pollutants of great interest in urban runoff due to their non-biodegradability, accumulation in the environment and toxicity. Copper (Cu),

zinc (Zn) and lead (Pb) are the most frequently found, among which Pb is the most toxic and has consistently ranked #2 in ATSDR's most hazardous chemicals list. The reported ranges of the three metals in urban runoff are summarized in Table 1.

**Table 1.** levels of common heavy metals in urban runoff in literature (unit:  $\mu\text{g/L}$ )

<b>Cu</b>	<b>Zn</b>	<b>Pb</b>	<b>Ref.</b>
34	144	160	USEPA, 1983
27	114	154	USEPA, 2006
390	160	1,300	Duke et al., 1998
97-104	120-2000	11-525	Gobel et al., 2007
0.06-1,410	0.7-22,000	0.57-26,000	Makepeace et al., 1995

Stormwater best management practices (BMPs) are control measures taken to address the quantity and quality issues of urban runoff. To remove metals from urban runoff, many structural BMPs have been attempted, including bioretention, wet ponds, constructed storm water wetlands, dry wells, extended detention basins, infiltration basins, and manufactured treatment (NJDEP, 2004). Some of the conventional structural BMPs are almost ineffective for metals, and many others, such as infiltration basins, are often impractical to implement in urban environments. These limitations have generated modifications to existing structural BMPs or led to the design of new BMPs that can properly treat urban stormwater constituents. Therefore, innovative, viable, cost effective, low-impact treatment options for heavy metals in urban runoff are in demand to improve the living quality of urban environments and safeguard the public health.

#### **4.1.2 Research objectives**

The long term goal of this study is to develop an effective, low-cost, and “green” BMP to sustainably address the issue of metal pollution in urban runoff. The primary objective of this study is to evaluate the performance of two recycled wastes,

aluminum-based drinking water treatment residuals (Al-WTR) and Tire Rubber (TR), in the adsorption of three major runoff metals (Cu, Zn and Pb), and to assess potential leaching of metals from spent sorbents. Our central hypothesis is that Al-WTR or/and TR can effectively and irreversibly adsorb Cu, Zn and Pb from USW runoff under a variety of relevant environmental conditions. The specific objectives are:

**Objective I:** to physically characterize TR and Al-based WTR surfaces by SEM, XRD, BET, and zeta potential analyses.

**Objective II:** to determine sorption/desorption of Cu and Pb by TR, and Cu, Pb and Zn by Al-WTR as a function of solution pH, ionic strength, solid:solution ratio, and temperature.

**Objective III:** to determine sorption/desorption of Cu, Pb and Zn by a composite TR/Al-WTR matrix from single and mixed-metal systems.

**Objective IV:** to assess potential leachability of the spent TR and Al-WTR using Toxicity Characteristics Leaching Procedure (TCLP) tests.

**Objective V:** to evaluate potential leachability of benzothiazole from TR and the effectiveness of Al-WTR in its retention.

## **4.2 Methodology**

### **4.2.1 Materials**

All the chemicals used are of analytical grade or above. Al-WTR and TR used in this study are shown in Figure 1. Al-WTR materials were collected from the Manatee County Water Treatment Plant in Bradenton, FL where they have been stockpiled following removal from storage lagoons. Once collected, the WTR was thoroughly mixed, air-dried, sieved through a 2-mm sieve, and finally ground into powder prior

to use. TR samples were provided from RubbeRecycle Inc., Lakewood, NJ. Prior to use, the TR was rinsed with Milli-Q water ( $18.2 \text{ M}\Omega\cdot\text{cm}$ ) twice and then air-dried.

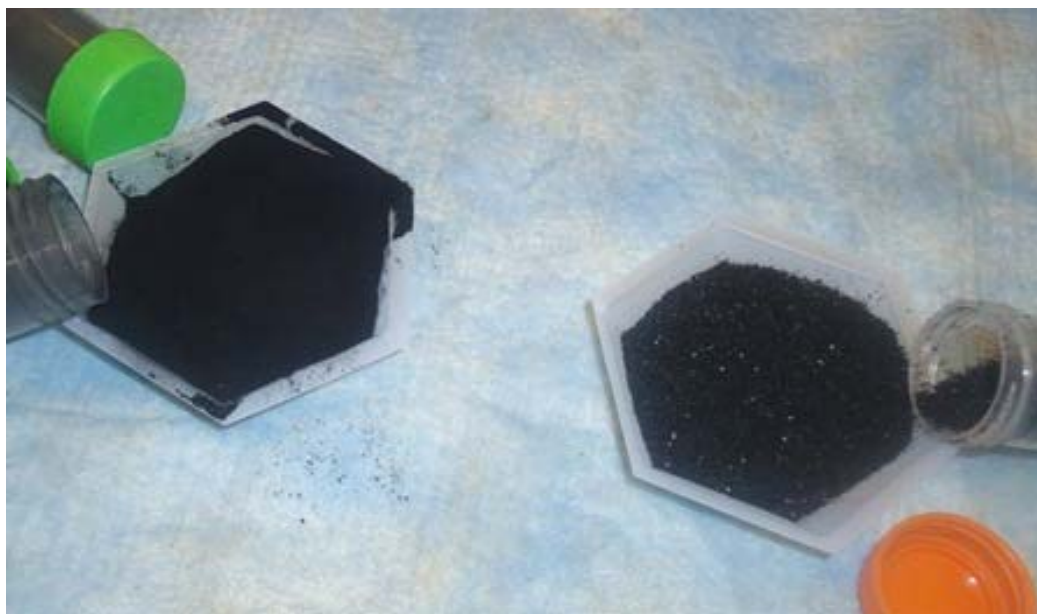


**Figure 1.** Al-WTR (left) and TR (right) used in this study.

#### **4.2.2 Adsorption tests**

Bench-scale batch experiments were carried out with triplicate samples with appropriate analytical controls and standards. All the adsorption kinetics and isotherm experiments were conducted in 15 mL centrifuge tubes containing 15 mL simulated metal-contaminated urban runoff. The simulated runoff solution was prepared by addition of specific amounts of  $\text{Cu}(\text{NO}_3)_2$ ,  $\text{Zn}(\text{NO}_3)_2$ , and  $\text{Pb}(\text{NO}_3)_2$  into Milli-Q water ( $18.2 \text{ M}\Omega\cdot\text{cm}$ ). The reactors were installed in a shaking water bath at  $25^\circ\text{C}$ . A rapid shaking speed ensured a completely mixing solution state. Initial solution pH was pre-adjusted to a desirable value with 1M NaOH and  $\text{HNO}_3$ , if needed. Solution pH was maintained during reactions using appropriate buffers such as PIPES. Desirable ionic strength was accomplished by addition of appropriate amount of  $\text{NaNO}_3$  into the simulated urban runoff. The adsorption reactions were initiated once certain amounts

of WTR and/or TR were added. In kinetics tests, at least three reactors were sacrificed at each designated sampling time. For adsorption isotherm experiments, shaking was stopped within a reaction time that allows the adsorption to reach a chemical equilibrium. Subsequently, 5 mL sample was collected from each reactor and then filtered through 0.45  $\mu\text{m}$  syringe membrane filter. The filtrate was stored in 2%  $\text{HNO}_3$  solution for metal analysis.

### **4.2.3 Analytical method**

Surface morphology of WTR and TR samples was characterized by scanning electron microscopy (SEM) (Hitachi S-3400N). Crystallographic structure of the materials was determined by X-ray diffraction (XRD) (Philips, X'Pert). Cu, Zn and Pb in water were quantified using an inductively coupled plasma mass spectroscopy (ICP-MS) (Thermo, X Series II, XO 472). Solution pH was measured with a Thermo Fisher Scientific ORION 5-Star multiparameter meter.

## **4.3 Principal Findings and Significance**

### **4.3.1 Principal findings**

**4.3.1.1 Surface characterization.** SEM images of WTR and TR materials are shown in Fig. 2 and 3, respectively. Al-WTR was composed of amorphous aluminum oxides whose sizes broadly ranged on an order of a few  $\mu\text{m}$  to mm. The WTR particles usually had a rough surface. In contrast, TR particles had irregular shapes, their sizes were on the order of a few mm, and they had less rough surface than WTR.

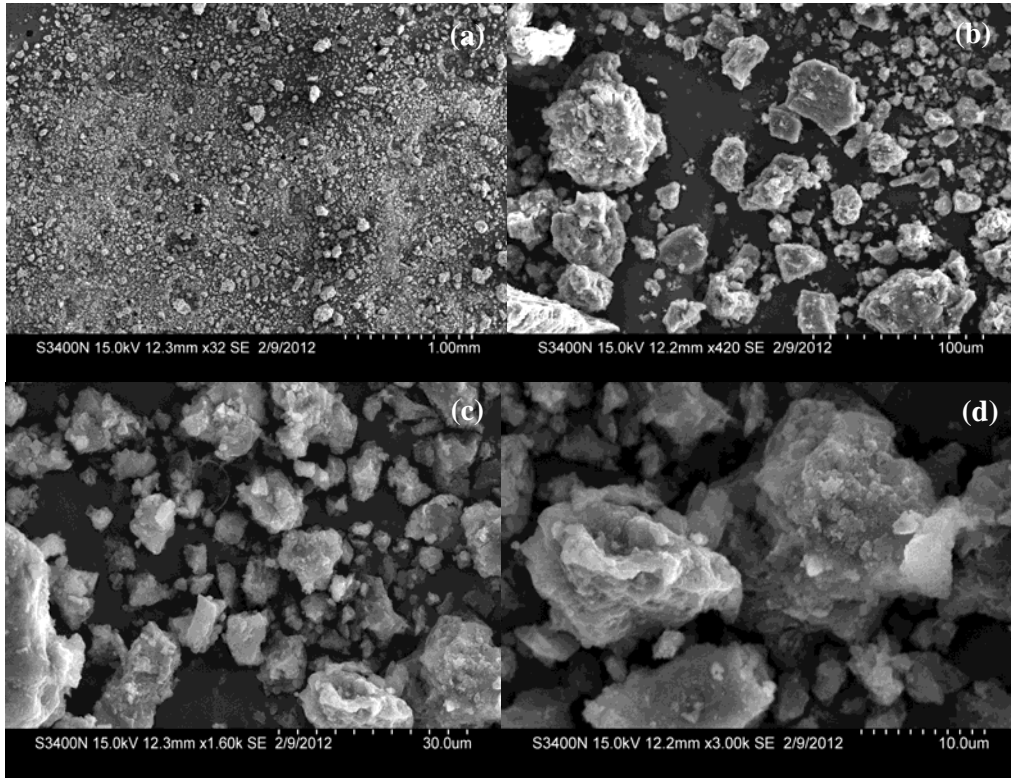


**Figure 2 (a)-(d).** SEM images of Al-WTR.

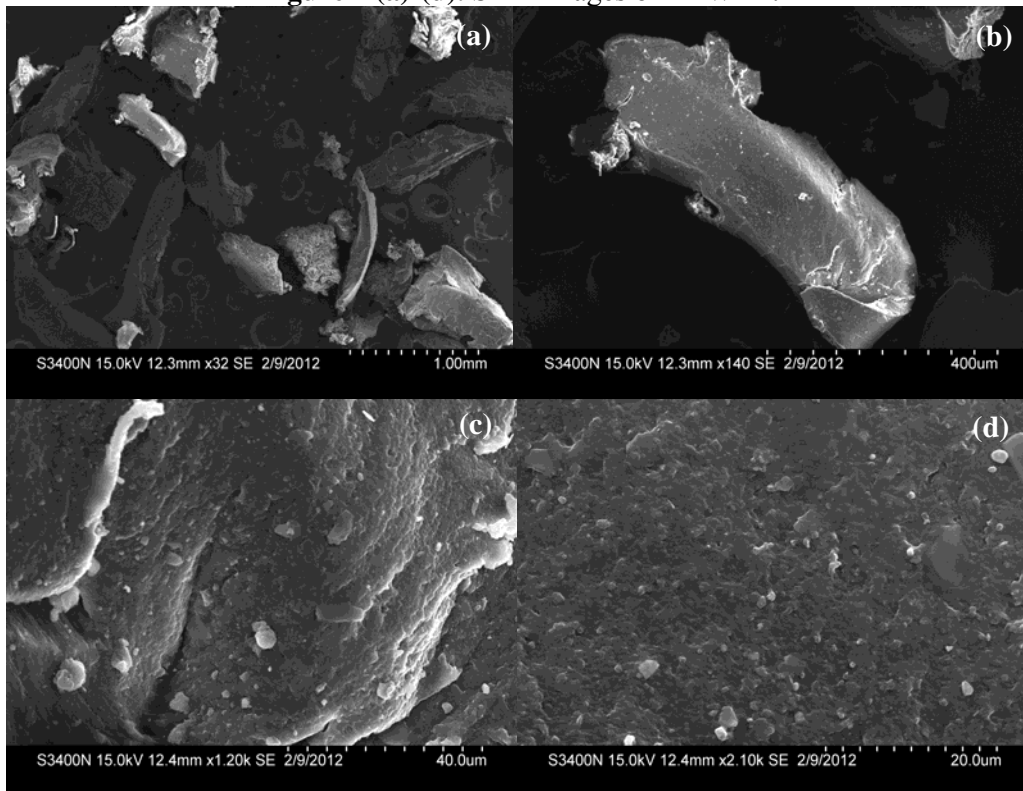


**Figure 3 (a)-(d).** SEM images of TR.

**4.3.1.2 Metal leaching from WTR and TR.** Metal leaching from 20 g/L WTR and TR in a Milli-Q water matrix is shown in in Fig. 4 and 5, respectively. Cu and Pb leaching from WTR and TR were negligible ( $< 0.2 \mu\text{M}$ ).The concentration of Zn released from WTR was also insignificant ( $2 \mu\text{M}$ ). However, Zn leaching from TR was noticeable. After 20 hours, Zn in 20 g/L TR solution reached  $156 \mu\text{M}$ .

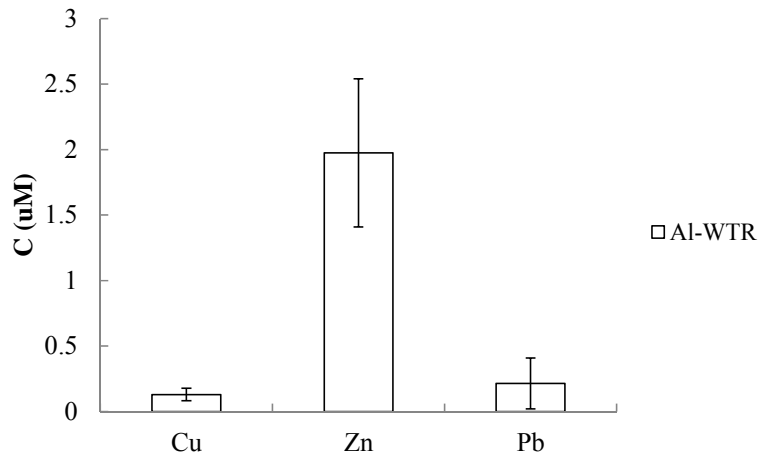


**Figure 4.** Leaching of different metals from Al-WTR in Milli-Q water (20 g/L WTR, reaction time = 20 hrs)

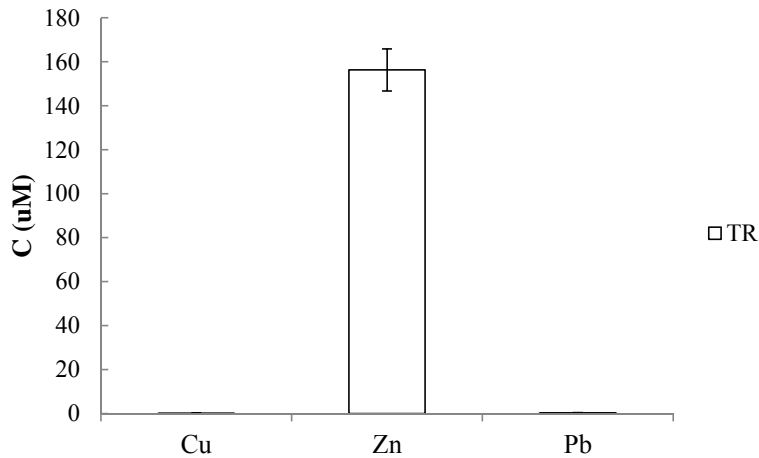


**Figure 5.** Leaching of different metals from TR in Milli-Q water (20 g/L TR, reaction time = 20 hrs)

**4.3.1.3 Kinetics tests .** Adsorption of Cu, Zn and Pb on WTR is shown in Fig.6. For all three metals, the adsorption reached equilibrium within one hour. Therefore, a removal efficiency of > 90% could be achieved within an hour. Within one hour, the removal efficiencies of Cu, Zn and Pb were 99.7%, 92.6% and 99.9%, respectively.

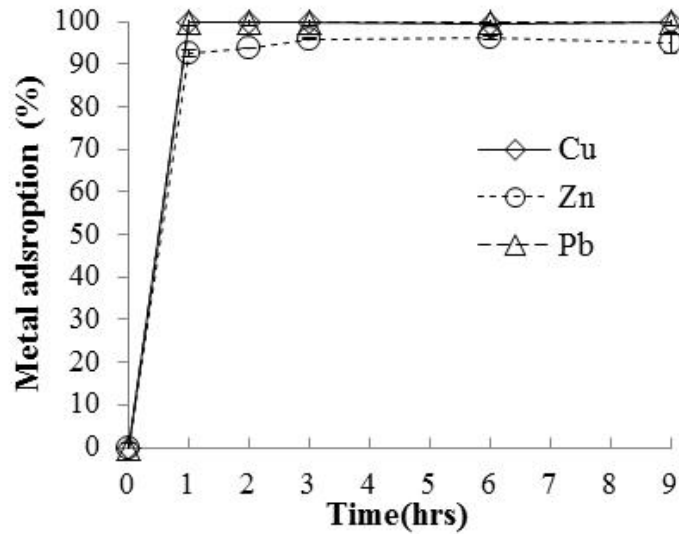


**Figure 6.** Metal adsorption by WTR with time (10 g/L WTR; initial Cu = 6  $\mu$ M, Zn= 6  $\mu$ M, and Pb = 2.45  $\mu$ M; initial pH 6.5)

Results of kinetic tests for adsorption of Cu and Pb on TR are shown in Figure 7. Adsorption efficiencies of Cu and Pb were gradually increased with time, and reached 97.4% and 97.2% after 9 hours, respectively. However, it is noted that Zn leached out from TR to enter the bulk solution, and the Zn concentration reached 170  $\mu$ M Zn within 9 hours.

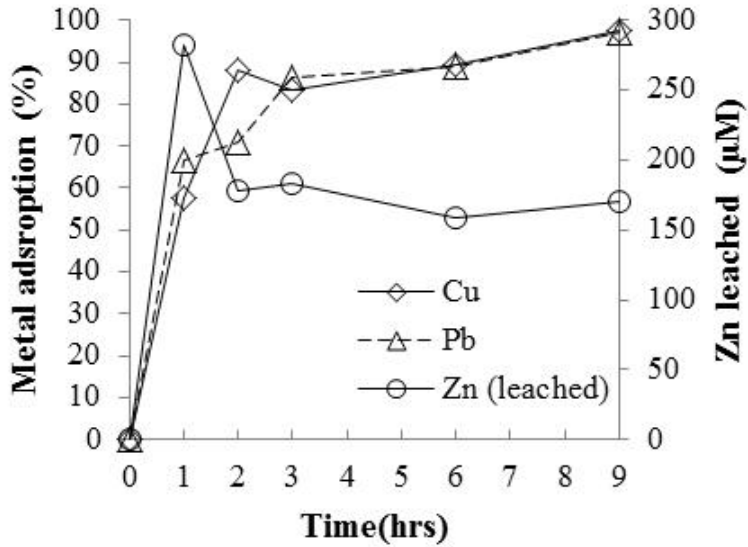


**Figure 7.** Cu and Pb adsorption onto and Zn leaching from TR with time (10 g/L TR; initial Cu = 6 µM, Zn= 6 µM, and Pb = 2.45 µM; initial pH 6.5)

**4.3.1.4 Adsorption isotherm experiments with WTR only.** Adsorption isotherms of Cu, Pb and Zn during WTR adsorption of a simulated Cu, Pb and Zn mixed runoff are shown in Figures 8-10, respectively. The adsorption isotherms exhibited a two-phase pattern. At a low metal concentration ( $C_e$ ) in bulk solution, the metal mass adsorbed per unit mass of adsorbent (i.e. WTR) ( $Q_e$ ) was dramatically increased. However, when  $C_e$  was over a critical value, the increase of  $Q_e$  was almost marginal.

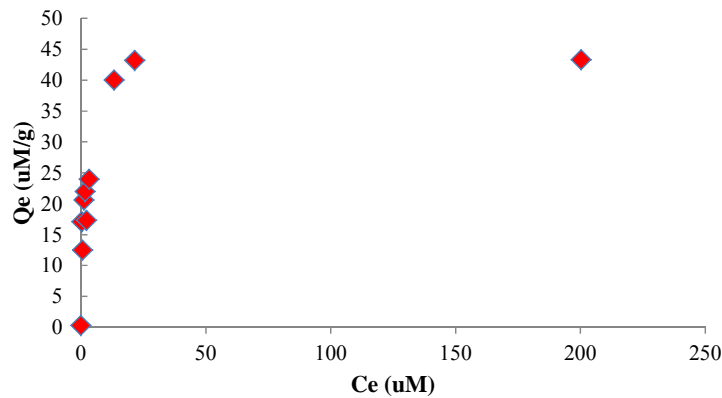


**Figure 8.** Cu adsorption isotherm on WTR (20 g/L WTR; initial pH 6.5)

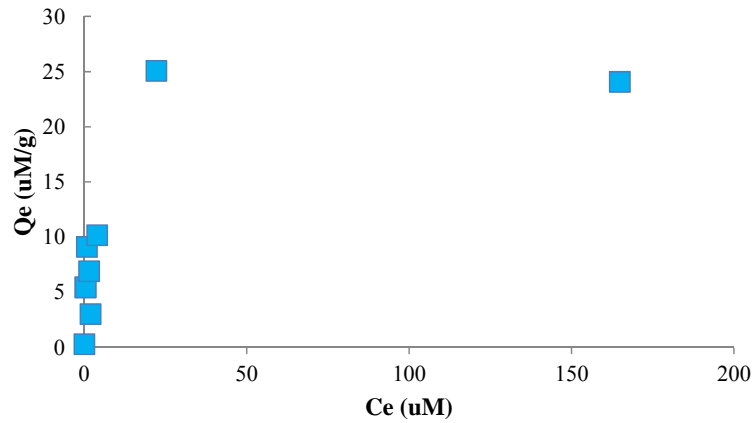


**Figure 9.** Pb adsorption isotherm on WTR (20 g/L WTR; initial pH 6.5)

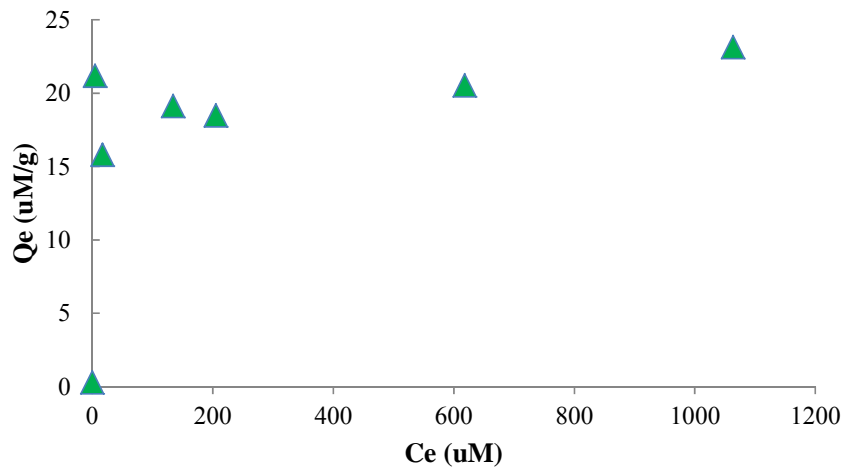


**Figure 10.** Zn adsorption isotherm on WTR (20 g/L WTR; initial pH 6.5)

**4.3.1.5 Adsorption isotherm experiments for TR only.** Adsorption isotherms of Cu and Pb during TR adsorption of a simulated Cu and Pb mixed runoff are shown in Figures 11 and 12, respectively. Similarly, the adsorption isotherms had a bi-phasic behavior. That is,  $Q_e$  was significantly increased with the increasing  $C_e$ , but plateaued at a high  $C_e$  level. Compared with WTR, TR exhibited a low adsorption capacity for both of the metals. For example, at  $C_e = 50 \mu\text{M}$ ,  $Q_e$  of the TR was  $\sim 3 \mu\text{M/g}$ , but  $Q_e$  of the WTR was  $\sim 45 \mu\text{M/g}$ .

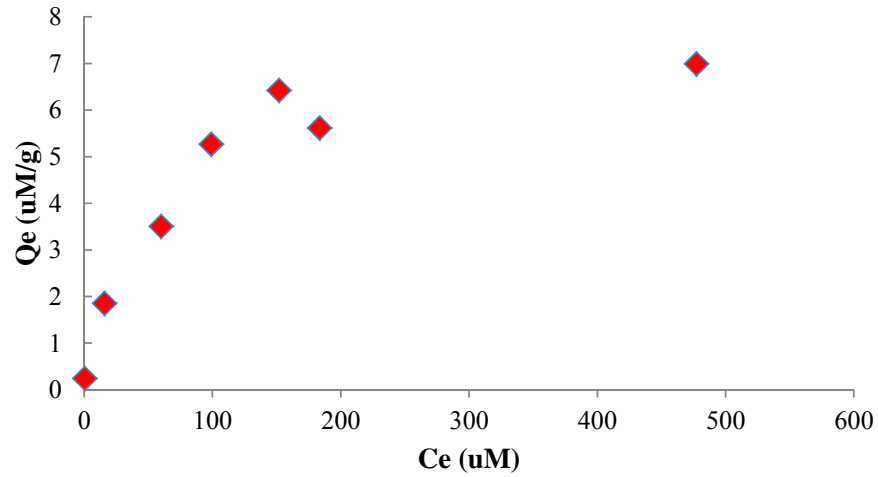


**Figure 11.** Cu adsorption isotherm on TR (20 g/L TR; initial pH 6.5)

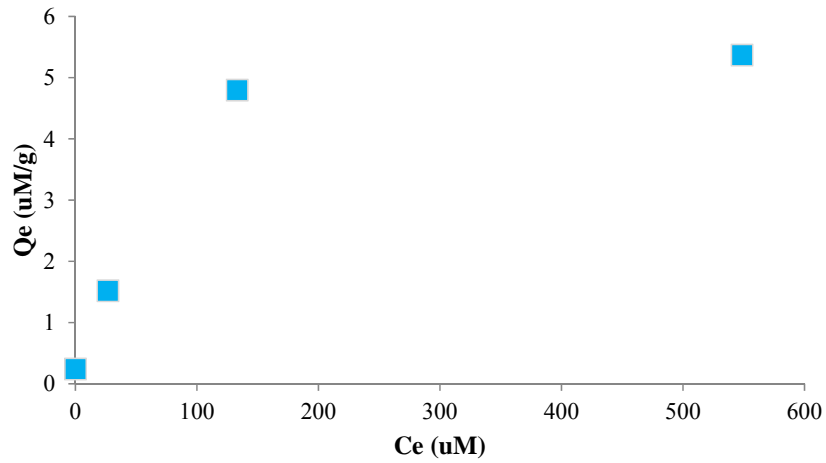


**Figure 12.** Pb adsorption isotherm on TR (20 g/L TR; initial pH 6.5)

The relationship of Zn leached out from TR and the initial combined Cu and Zn concentration is shown in Figure 13. In general, the level of leached Zn somewhat linearly increased with increasing combined Cu and Pb sorption.

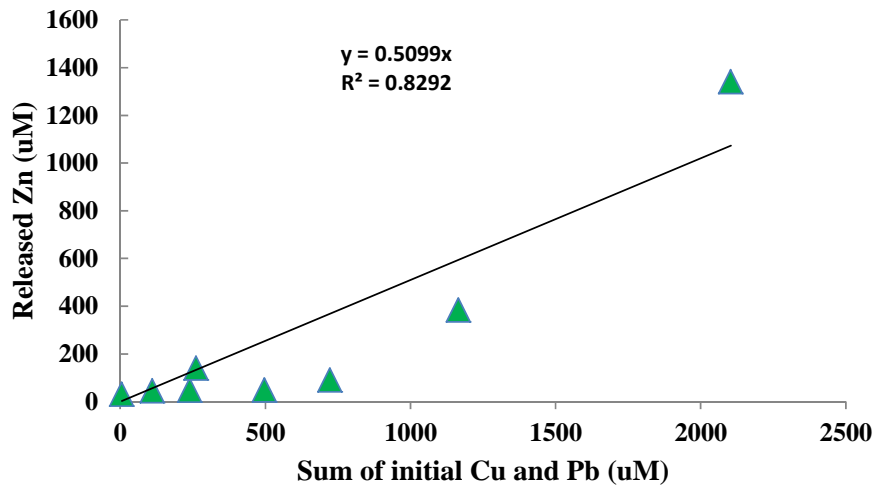


**Figure 13.** Sum of initial combined Cu and Pb vs. Zn leaching from tire during TR adsorption of Cu and Pb (20 g/L tire, pH = 6.5)

**4.3.1.6 Adsorption isotherm experiments for combined WTR and TR .** Adsorption isotherms of Cu and Pb during the combined WTR and TR adsorption of a simulated Cu and Pb mixed runoff are shown in Figures 14 and 15, respectively. The adsorption isotherms exhibited a two-phase pattern.

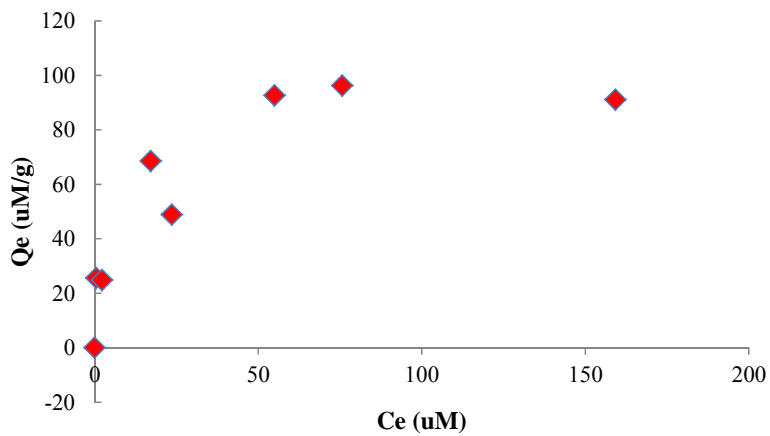


**Figure 14.** Cu adsorption isotherm on WTR and TR (20 g/L sorbents; mass WTR:TR = 1:1; initial pH 6.5)

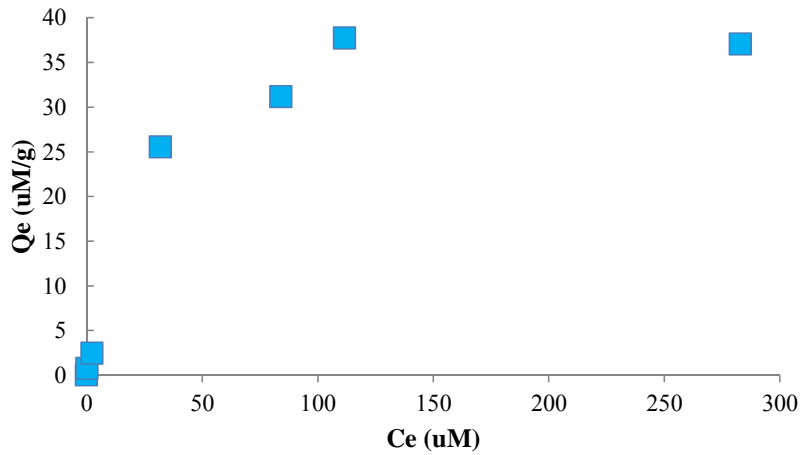


**Figure 15.** Pb adsorption isotherm on WTR and TR (20 g/L sorbents; mass WTR:TR = 1:1; initial pH 6.5)

The relationship of Zn leached out from TR and the initial combined Cu and Zn sorption is shown in Figure 16. Likewise, the level of leached Zn somewhat linearly increased with increasing combined Cu and Pb sorption. Of note, the amount of Zn leached out was much less than that in the treatment by TR adsorption alone, thereby indicating that WTR played a critical role to control Zn release from TR.

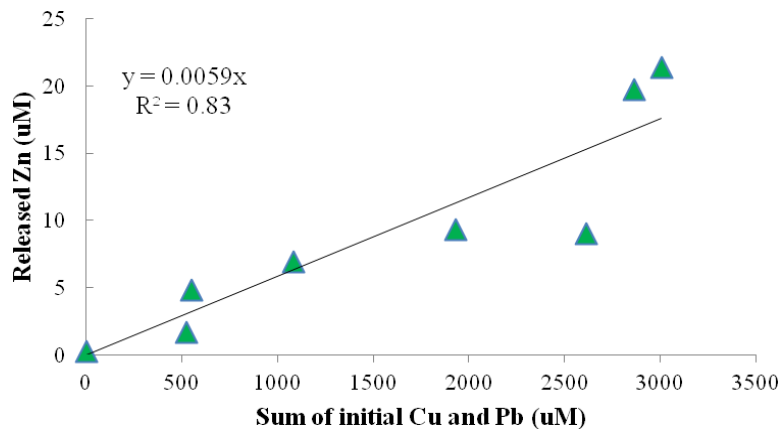


**Figure 16.** Sum of initial Cu and Pb vs. Zn leaching from tire during combined WTR and tire adsorption of Cu and Pb (10 g/L WTR, 10 g/L tire, pH = 6.5)

### 4.3.2 Significance

Based on the current data, a few significant outcomes are obtained, including:

- WTR can rapidly adsorb Cu, Zn and Pb from water. Moreover, it has high adsorption capacities for the metal of concern. Therefore, WTR appears to be an excellent remediation material to address the metal pollution in urban runoff.
- TR also adsorbs Cu and Pb in water. However, compared to WTR, its adsorption rate is relatively slow. Likewise, its adsorption capacity is lower than that of WTR. Accompanied with Cu and Pb adsorption on TR, Zn in TR gradually leaches out into bulk solution, implying that Zn leaching might have been enhanced by Cu/Pb-Zn exchange in TR.
- A mixture of WTR and TR are able to quickly and effectively adsorb Cu and Pb. In addition, in the presence of WTR, less Zn is leached, thus indicating that WTR can adsorb Zn released from TR. This finding suggests that TR should be used in conjunction with WTR, because the latter can minimize Zn release from TR.

Currently, this project is in progress. More outcomes are expected by the summer of 2012 when the project will be officially completed.

## REFERENCES

Duke, L.D., M. Buffleben, Bauersachs, L.A. 1998. Pollutants in storm water runoff from metal plating facilities, Los Angeles, California. Waste management 18:25-38.

Gobel, P., Dierkes, C., Coldewey, W. G., 2007. Storm water runoff concentration matrix for urban areas. Journal of Contaminant Hydrology 91 (1-2), 26-42.

Makepeace, D. K., Smith, D. W., Stanley, S. J. (1995) Urban stormwater quality: Summary of contaminant data. Critical Reviews in Environmental Science and Technology, 25 (2), 93-139.

U.S. EPA, 1983. Results of the Nationwide Urban Runoff Program, PB84-185552, Washington, D.C.

U.S. EPA. 2006. Urban Storm Water BMP Performance Monitoring. (<http://water.epa.gov/scitech/wastetech/guide/stormwater/monitor.cfm>)

US EPA. 2009. National Water Quality Inventory: Report to Congress 2004 Reporting Cycle, Office of Water Washington, DC 20460 (EPA 841-R-08-001).

## NEW FINDINGS SINCE 2012 ANNUAL REPORT

### BET tests for Al-WTR and TR.

BET specific surface areas of WTR and TR were measured in a commercial laboratory (Particles Technology Labs, Downers Grove, Illinois). Results of BET analysis are summarized in **Table 2**. Al-WTR used in this study exhibited a high specific surface area (SSA) at  $223.36 \pm 3.14 \text{ m}^2/\text{g}$ . In contrast, the TR used had a much smaller SSA at  $0.064 \text{ m}^2/\text{g}$ .

**Table 2.** BET characterization of Al-WTR and TR

Material	B.E.T Specific Surface Area ( $\text{m}^2/\text{g}$ )
Al-WTR	$223.36 \pm 3.14$
TR	0.064

### Desorption of adsorbed metals from used Al-WTR and TR.

During development of an adsorption process, desorption of adsorbed metal on sorbents into bulk solution under different conditions is extremely interesting. Desorption rate of a metal from the studied sorbents is defined as:

$$\text{Desorption rate} = \frac{\text{Amount of desorbed metal into bulk solution}}{\text{Amount of total adsorbed metal}} \times 100\% \quad (1)$$

Where, the “amount of total adsorbed metal” is the mass of metal that is adsorbed onto the adsorbent during adsorption isotherm tests; and the “amount of desorbed metal into bulk solution” is the mass of the adsorbed metal that is released into bulk solution under certain experimental conditions.

Desorption rates of Cu and Pb from WTR and TR in 0.02 M  $\text{NaNO}_3$  solution at WTR:TR = 1:1 or 1:4 are negligible (< 1%) (data not shown here). This finding

suggests that WTR/TR adsorption of Pb and Cu was somewhat strong and irreversible.

### Extraction of adsorbed metals from used Al-WTR and TR.

EDTA, a strong chelating agent, was added to the used WTR and TR. The amount of extracted metals from sorbent in the presence of EDTA provides information regarding how strong the bindings between these metals and our adsorbents are. Extraction rates of Cu and Pb from WTR and TR in 0.02 M EDTA solution at different mass ratios of WTR to TR are shown in **Figure 17**. As seen, 0.02 M EDTA extracted ~ 52% sorbed Cu and ~ 56% sorbed Pb into bulk solution, regardless of WTR:TR. These findings again suggest that the bindings between metals and WTR/TR are very strong, considering that EDTA is an extremely strong chelating agent.

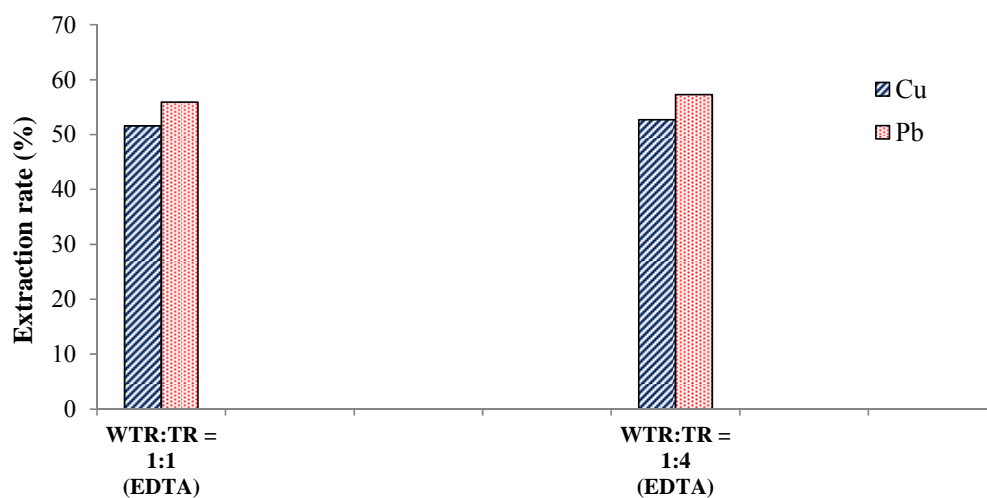


**Figure 17.** Extraction of Cu and Pb from WTR/TR sorbents in **0.02 M** EDTA at different WTR:TR ratios

### Effect of Varying Mass Ratio of WTR to TR

Cu and Pb adsorption isotherm data at different mass ratios of WTR to TR (WTR:TR) are shown in **Figures 18** and **19**, respectively. More Cu and Pb were adsorbed to the mixed adsorbent material at WTR:TR = 1:2 or 1:4 than at WTR:TR = 1:1. A WTR:TR of 1:2 was slightly better and 1:4 in terms of adsorption capacity. The experimental data better fit Freundlich isotherm models than Langmuir models. The parameters of the Freundlich isotherm models and regression coefficient ( $R^2$ ) are summarized in **Tables 3**.

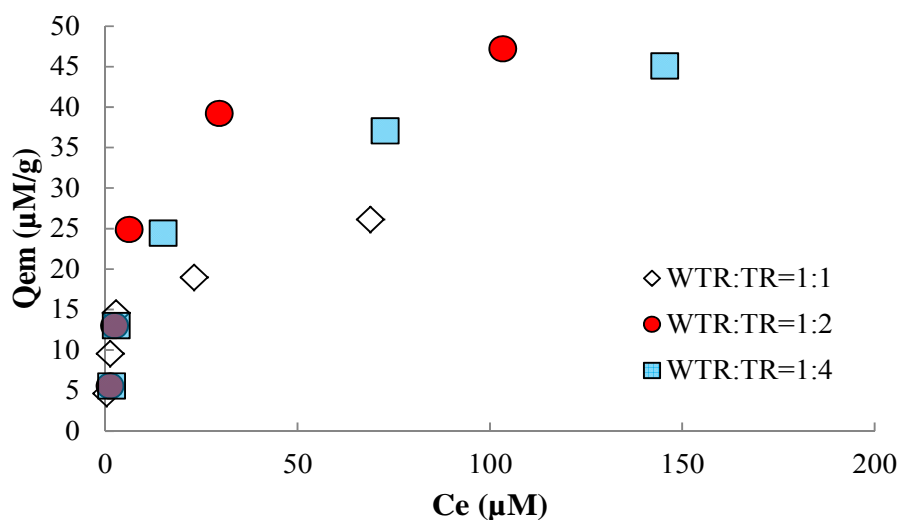


**Figure 18.** Cu adsorption isotherm at different mass ratios of WTR to TR (pH = 6.5, and 0.01M  $\text{NaNO}_3$ )

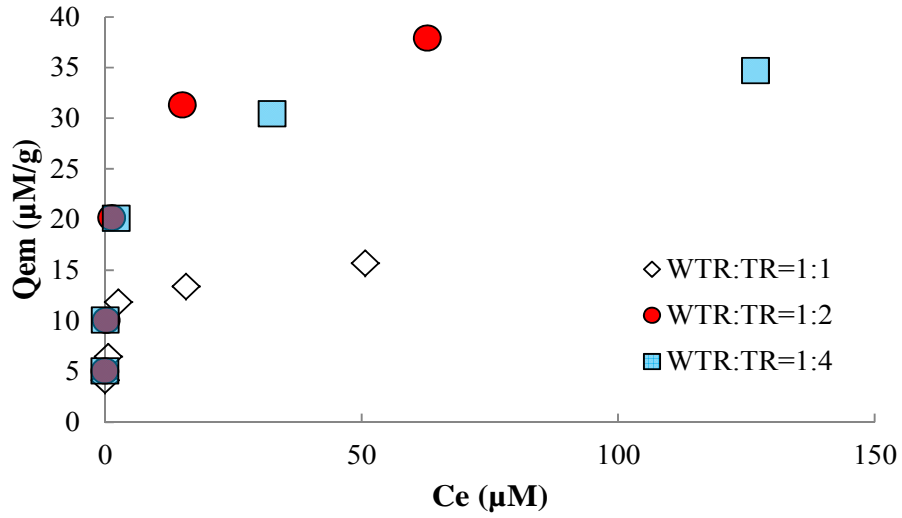


**Figure 19.** Pb adsorption isotherm at different mass ratios of WTR to TR (pH = 6.5, and 0.01M NaNO<sub>3</sub>)

**Table 3.** Parameters of the Freundlich isotherm models for WTR/TR adsorption of Cu and Pb at various mass ratios of WTR to TR (pH = 6.5, at ambient temperature)

Cu sorption onto various ratios of WTR/TR				Pb sorption onto various ratios of WTR/TR			
Ratio	1/n	K <sub>f</sub>	R <sup>2</sup>	Ratio	1/n	K <sub>f</sub>	R <sup>2</sup>
1:1	0.3073	7.731	0.8987	1:1	0.1840	8.056	0.9449
1:2	0.4587	7.228	0.8590	1:2	0.2464	15.31	0.9762
1:4	0.4237	6.160	0.9055	1:4	0.2179	13.94	0.9525

# Evaluation of organoclay in a permeable pavement system for removal of contaminants from urban stormwater runoff

## Basic Information

<b>Title:</b>	Evaluation of organoclay in a permeable pavement system for removal of contaminants from urban stormwater runoff
<b>Project Number:</b>	2011NJ275B
<b>Start Date:</b>	3/1/2011
<b>End Date:</b>	8/31/2012
<b>Funding Source:</b>	104B
<b>Congressional District:</b>	NJ-006
<b>Research Category:</b>	Water Quality
<b>Focus Category:</b>	Water Quality, Non Point Pollution, Water Supply
<b>Descriptors:</b>	
<b>Principal Investigators:</b>	Amy Rowe

## Publications

There are no publications.

**Project Summary:** This project has not yet started for a number of reasons. Late receipt of funding led to a delayed start, as well as extreme weather events the past two fall seasons. The experimental study site still has not been constructed, but as of this writing a contractor bid has been accepted and construction will begin in the next few weeks.

## Problem and Research Objectives

Permeable pavement can not only reduce stormwater volume, but can filter some contaminants from runoff as well. The addition of organoclay to the storage layer beneath the porous surface may adsorb typically hard-to-remove contaminants such as metals and hydrocarbons from infiltrating stormwater. It is expected that a permeable pavement system with an organoclay layer will remove hydrocarbons and metals more efficiently than one without any added organoclay. The pervasive presence of metals and hydrocarbons in urban runoff generally render it unusable, but the removal of these contaminants would possibly allow for the beneficial reuse of stormwater that would typically enter the sewer system.

The area underneath city sidewalks is generally an unexploited space with little to no value, and, at the same time, permeable pavement sidewalks have recently been gaining in popularity. These two tendencies could be combined to evaluate the possibility of a passive stormwater treatment system in an under-utilized piece of the cityscape. These treatment systems would not take up much space, would be underground, and would not spoil the aesthetic of the urban environment. These stormwater management systems would also be relatively easy to implement and cost-effective, as many cities have aging infrastructure and sidewalks that are in disrepair, so the installation could coincide with the regular sidewalk maintenance schedule. Finally, a permeable pavement sidewalk stormwater treatment system would not only reduce urban runoff volume, leading to a decreased burden on the combined sewer system, but the treated exfiltrate could be beneficially reused in community gardens or city landscape installations. It is expected that there would be many advantages to installing a permeable pavement sidewalk stormwater treatment system, but that there may be some unforeseen complications that may or may not outweigh those benefits.

## Specific study objectives

- Determine the removal efficiency of metals and hydrocarbons for a permeable pavement system cell with added organoclay compared to one without.
- Determine the practical feasibility of a permeable pavement sidewalk stormwater treatment system in terms of design and implementation.

## Methodology

No work has been done on this project at this time, but here is the intended methods description. Two side-by-side treatment cells will be installed below a pervious concrete surface. One cell will contain organoclay in the storage layer and the other will not. A perforated pipe will be placed at the bottom of each cell to allow for the capture of the exfiltrate, which will then be directed to the onsite rain garden or be sampled. This design will follow that of the U.S. Environmental Protection Agency (USEPA) permeable pavement demonstration site in Edison, NJ (Rowe et al., 2010). A curb cut will introduce stormwater runoff to the cells from Nye Avenue, which is a relatively busy street that runs through a densely-populated residential area

of Newark. The NJDEP stormwater quality design storm requires a rainfall depth of 1.25 inches with a total duration of 2 hours (NJDEP, 2004). The monitoring schedule will be weather-dependent, but it is expected that there will be at least one storm event per month that will satisfy the design storm requirements and will allow for sampling. Both the influent and effluent will be sampled in order to determine the pollutant removal efficiencies for the two cells. The samples will be analyzed for the following metals: copper, cadmium, lead, and zinc. Separate samples will be taken and analyzed for total petroleum hydrocarbons.

Principal Findings and Significance – no work has been done on this project at this time pending construction of the study site.

# Drought and Flood in the Eastern US

## Basic Information

<b>Title:</b>	Drought and Flood in the Eastern US
<b>Project Number:</b>	2011NJ292G
<b>Start Date:</b>	9/1/2011
<b>End Date:</b>	8/31/2013
<b>Funding Source:</b>	104G
<b>Congressional District:</b>	12th
<b>Research Category:</b>	Climate and Hydrologic Processes
<b>Focus Category:</b>	Drought, Floods, Water Supply
<b>Descriptors:</b>	None
<b>Principal Investigators:</b>	James Smith, Justin Sheffield, Eric Wood

## Publications

1. Kam, J., J. Sheffield, X. Yuan, and E.F. Wood. 2013. The Influence of Atlantic Tropical Cyclones on Drought over the Eastern US (1980-2007). *J. Climate*, 26 (10), 3067-3086.  
<http://dx.doi.org/10.1175/JCLI-D-12-00244.1>.
2. Wright, D.B., J.A. Smith, G. Villarini, and M.L. Baeck. 2012. The hydroclimatology of flash flooding in Atlanta. *Water Resources Research*, 48, W04524, doi:10.1029/2011WR011371.
3. Kam, J., J. Sheffield, X. Yuan, and E.F. Wood. 2012. The Influence of Atlantic Tropical Cyclones on Drought over the Eastern US (1980-2007), Abstract H51D-1369, 2012 Fall Meeting, AGU San Francisco, CA. 3-7 Dec. (poster presentation)

## **Problem and Research Objectives -**

We propose to develop statistical procedures for regional analyses of drought and flood in the eastern US based principally on USGS stream gaging data. We will focus on the interrelationships between drought and flood, with a particular emphasis on water supply systems for large urban centers of the eastern US. Procedures will exploit mixture distribution representations of flood and drought variables; these representations center on tropical cyclones, which are major rainfall and flood agents during summer and fall, and extratropical systems, which are major rainfall and flood agents during spring and fall in the eastern US. We adopt a regional approach covering the eastern US due to the scale of the weather and climate systems at play. Special emphasis will be placed in this study on the Delaware River basin (water supply for New York City), the Potomac River basin (water supply for Washington D. C.), the Catawba River basin (water supply for Charlotte, North Carolina) and the Chattahoochee River basin (water supply for Atlanta, Georgia). The procedures that we will develop are designed for broad use by USGS National and District offices for water resource assessment studies. Additional users will include river basin planning and management agencies (including the Delaware River Basin Commission and Interstate Commission on the Potomac River Basin), states and local municipalities.

The procedures will be used for regional assessments of drought and flood frequency, short-term (seasonal to interannual) characterization of drought and flood occurrence and long-term trend assessment of drought and flood variables. These procedures will provide capabilities for regional water resources analyses covering the eastern US. Detailed analysis capabilities will be developed for the Delaware, Potomac, Catawba and Chattahoochee River basins, providing information on drought and flood frequency for major urban centers of the eastern US.

The broad objective of this study is to develop statistical tools for characterization of water resources and flood hazards based on USGS streamflow records. The specific objectives of the study are to develop statistical procedures for: 1) assessing non-stationarities of drought and flood variables (in terms of change-points, slowly varying trends and long-term persistence), 2) characterizing spatial extremes of drought and flood and 3) characterizing the interrelationships between drought and flood, including their relationships to climate indices. The project will be carried out over a two year time period. Development of data sets and statistical procedures was completed during year 1. Implementation of procedures for assessing non-stationarities in drought and flood variables was also completed in year 1. In the second year of the project, we will complete analyses of the interrelationship of drought and flood for the eastern US, analyses of spatial extremes and analyses of drought and flood occurrence in terms of climate indices. We will also synthesize analyses for the Delaware, Potomac, Catawba and Chattahoochee River basins during year 2.

## **Methodology -**

For the drought analysis, we have focused in Year 2 on analyzing low flows and drought over the eastern US and evaluating the VIC land surface model in its simulation of low flows. The work on the influence of tropical cyclones on drought has been completed and published as a journal paper in *J. Climate* as Kam et al. (2013).

### *a) Analysis of Low Flows over the Eastern US*

Our goals were to 1) determine the spatial and temporal characteristics of low flows over the eastern US and 2) identify the spatial controls on low flow magnitudes and attribute temporal changes (abrupt, long-term trends and variability) to human and climate influences. To do this we (1) evaluated available data for low flows and drought studies in the eastern US, (2) carried out time series analysis of average daily discharge records, and (3) tested for non-stationarity in the mean and variance from change point and trend analysis tests. Low flows were calculated for n-day annual minimum flow values, where n is 1, 7, 30, and 90 days. A set of statistical methods were applied to the data to identify useable streamflow time series that were deemed to not have significant human influence, and explore factors that contribute to long-term trends and variability.

#### **1. USGS streamflow data**

4878 sites with daily streamflow records were retrieved from the United States Geological Surveys Hydro-Climatic Data Network (HCDN). All sites had Hydrological Unit Codes (HUC) of 01, 02, or 03, which are from the eastern US. We ended up with 523 sites based on the criteria of length of record, whether the site is currently active or stopped being active after year 2000, and the site should not have any missing year of daily data. The selected stations have a record of at least 50 years worth of daily data. Figure 1 shows the location of the remaining 523 sites colored by their drainage area [mi<sup>2</sup>]. Table 1 shows the statistics of the 523 sites.

Table 1: Record length statistics of the 523 study sites.

	<b>Min</b>	<b>Max</b>	<b>Average</b>	<b>Median</b>
<b>Years</b>	50	120	74	92

We analyzed four variants of low flows, based on different time scales. The 1-day  $Q_1$  minimum low flow is the annual minimum daily streamflow. For each year, two values were calculated: the flow on that day in [ft<sup>3</sup>/s] and the date ( $\in[1,365]$ ) on which it occurred. The other three variants  $Q_7$ ,  $Q_{30}$ , and  $Q_{90}$  are obtained by applying the same analysis to 7-day, 30-day, and 90-day moving average time series, as we now describe. The value of the 7-day averaged time series on a particular day is the average of that day's flow, the flows of the 3 following days, and the flows of the 3 preceding days; the 30- and 90-day averages are similar. Together, we refer to the four low flow variables as the n-day minimum low flows.

#### **2. Stationarity of low flows**

Estimation of low-flows and frequency analysis required an initial investigation of the raw low flow data and so we applied a combination of methods to identify non-stationarity to extract as much useful data as possible. We applied three tests to identify weak stationarity: (1) the Ljung-Box test, which tests for autocorrelation; (2) the Mann-Kendall test, which tests for overall

increasing or decreasing trends (change in the mean); and (3) the Pettitt test, which tests for abrupt changes or change points (change in the mean). An identified change in the mean by either of the first two tests would rule out stationarity, except in the case of autocorrelated data, for which the Mann-Kendall test will characterize too many sequences of the time series as having a trend. Therefore, analysis of autocorrelation was carried out before conducting the Mann-Kendall test. Even when a site is identified as being nonstationary, further analysis was required to understand the overall time regime of the data at such a site. For example, the time series may have two separate stationary regimes with one change point in between or an overall trend. By combining the Box test, the MK test, and the Pettitt test, we designed a recursive decomposition algorithm for testing for non-stationarity and assigned a decomposition index to the site. The algorithm for assigning an index value to a site is shown in Figure 2.

To quantify the magnitude of the variation in year-to-year changes in the time series, we also define a “volatility” index. For a time series with  $n$  observations of  $x_1, x_2, \dots, x_n$  and the standard deviation of  $\sigma$ , the volatility ( $V$ ) is calculated as:

$$V = (x_1 - x_2 + x_2 - x_3 + \dots + x_{n-1} - x_n) / (n-1) \sigma(x_1, \dots, x_n)$$

Volatility is positive number. The more correlated the previous observation is to the current observation, the less volatile the series is and therefore, we expect to see only small fluctuations in the time series. A highly volatile series shows that each year’s minimum flow day has an insignificant  $d$  with next year’s observation.

For each site, we also examined the date of occurrence, to test whether the timing of low flows was stationary or not. We used a measure of variability to determine, among all years, the size of the window of occurrence in which the flow occurs. The date of low flow in each year was compared to dates in adjacent years using the cyclic distance of the day of the year, rather than the absolute distance. If  $x_i$  is the day in the year when the low flow occurs, then the cyclic distance treats dates at the end of the year and the beginning of the year as close to each other:

$$\Phi(x_i, x_j) = \min(x_i - x_j, x_i - x_j + 365, x_i - x_j - 365)$$

For  $n$  low flow occurrence dates of  $x_i, x_j, \dots, x_n$ , we define the variability as the root mean square of the cyclic distance of the  $x_i$ . The low flow occurrence dates can be viewed in a polar plot as shown later.

## *b) Flood Studies*

Studies of flood climatology have focused on the Potomac River basin (Smith et al. 2013b and Hicks et al. 2013), the Delaware River basin (Smith et al. 2013a), Texas (Villarini et al. 2013), the Chattahoochee River basin (Wright et al. 2012) and Catawba River basin (Wright et al. 2013).

The Potomac River stream gaging stations at Point of Rocks, Maryland has one of the longest records in the stream gaging archive of the USGS. Furthermore, the Potomac River basin is one of the least “regulated” river basins in the eastern US, with a single reservoir (controlling less than 3% of the drainage basin) having been completed in the early 1980s. We have examined change points and trends in annual flood peak data and peaks-over-threshold flood data for the

Point of Rocks station. In addition to the Point of Rocks station, the Potomac River basin has a relatively large density of stream gaging stations with more than 50 years of record. We have carried out analyses of change points and trends for all of the “long” stream gaging records in the Potomac basin (Smith et al. 2013b). During the second year of the project, we have examined the role of orographic thunderstorm systems as catastrophic flood agents in the central Appalachians (Hicks et al. 2013).

The East Branch of the Delaware River basin is a critical water supply source for New York City and exhibits large spatial gradients in the runoff and flood magnitudes. There is a dense network of USGS stream gaging stations in the basin linked to assessments of hydrology and water quality of the Pepacton reservoir. The East Branch Delaware River basin has experienced a sequence of major flood events, with Hurricane Irene causing extensive damage and loss of life in August 2011. We have developed high-resolution rainfall analyses for major flood events in the East Branch Delaware and examined spatial variability and heterogeneity in extreme rainfall, runoff and flood magnitudes (Smith et al 2013a).

The Gulf of Mexico region experiences extreme rainfall and flooding from tropical cyclones, warm season thunderstorm systems and winter/spring extratropical systems. We have examined nonstationaries in annual flood peaks for stream gaging stations in Texas with long records. We have also examined the spatially varying role of tropical cyclones in the flood hydroclimatology of Texas (Villarini et al. 2013).

Atlanta, Georgia and Charlotte, North Carolina have been rapidly urbanizing regions of the southeastern US. We have examined the hydroclimatology and hydrology of flooding in the Atlanta metropolitan region (within the Chattahoochee River basin; Wright et al. 2012) and the Charlotte, Metropolitan region (within the Catawba River basin; Wright et al. 2013).

## **Principal Findings and Significance**

### *a) Analysis of Low Flows over the Eastern US*

Figure 3 shows the distribution of the categories of the 523 sites after the first recursive level of the decomposition algorithm. In this figure, all four types of low flows (i.e. Q1, Q7, Q30, and Q90) are presented. As expected, the higher the values of  $n$  in  $Q_n$ , the smoother the low flow time series and therefore, the higher the number of sites that appear stationary (Category 1). Conversely, as  $n$  increases, the number of sites in the category 4 (indicating an abrupt shift in the time series) decreases. The algorithm applies the Pettitt test on the sites with index 4 and splits the time series in to two parts. For example, 163 sites from the Q1 analysis are split into two parts: part one (P1) and part two (P2), which are further tested for non-stationarity.

Figure 4 summarizes the time periods of all sites for Q1. The gray dashed lines represent the original record length for each site. The vertical axis shows the site number from 1 to 523 ordered from lowest to highest latitudes. Therefore, site 1 is the site with the lowest latitude and site 523 is the most northerly one. The left panel of Figure 4 shows the record length of sites that in the first step of categorization had no significant autocorrelation. These sites are colored according to their MK values (Figure 5). MK values are equal to 0 (no significant trend with 95% confidence), -1 (significant negative trend), or 1 (significant positive trend). The right panel

of Figure 4 again shows the original record length for each site in gray, but highlights the sites identified with an abrupt change by the Pettitt test and which were split into two parts. For each part that exhibits no autocorrelation, the MK values are again calculated. The right panel highlights the portion of each non-stationary time series that was recovered by the decomposition algorithm.

Figure 6 shows a map of volatility of the sites for  $Q_1$  with decomposition categories of 1, 2, and 3 (not autocorrelated). Volatility tends to be higher in the northern part of the domain, but the lack of long-term time series in the south means that the sampling is poor in this region. Figure 7 shows an example of a highly volatile series. Site 01121000 is Mount Hope River near Warrenton, CT and it is only occasionally regulated. The trend of this site is stationary without any shift in its regime. Some extreme examples of variability in low flow timing are shown in Figure 8. The corresponding timing RMS values are 29.66 and 111.37. The lower the RMS, the more clustered the dates of low flow occurrence. Low flows for the site with minimum variability occur mostly from July 1 through November 1. The bigger the RMS the wider the window of occurrence of the dates of low flows. At the site with maximum variability, the low flows occur from August 1 to April 1. This site is located in the northeast for which the low flows are controlled by cold season processes in the late winter and early spring and late summer/early fall evaporative demands.

Figure 9 shows the spatial distributions of timing variability values for  $Q_1$  and  $Q_{90}$ . As  $n$  increases in  $Q_n$ , the variability in the southeastern US tends to get bigger. Only a few sites in the northeast fall in the lower range of variability implying that the date of low flow occurrence repeats every year within a narrow time frame. The highest variability occurs in the most northerly and southerly sites. Figure 10 shows the 1-day and the 90-day polar plots of site 01021000 selected from the most northern part (45.15N, -67.32W) and site 02312200 selected from the most southern site (28.57N, -82.16W). The variability of the low flows for both sites are very similar, but the times of occurrences are quite different. The low flows of the northeast site are mostly observed from July 1 to December 1 and for the southeastern site mostly from May 1 to November 1.

#### *b) Attribution of Abrupt Changes and Trends*

The decomposition algorithm allows us to find the subset of a time series that are likely hampered by management effects (non-stationary abrupt changes due to reservoir building and land use change), show long-term increases or decreases (non-stationary trends due to climate change or longer-term land use change) or are stationary. The latter set of sites is useful for low flow frequency analysis or generating flow duration curves, for example. Trends in low flows can be seen as potential evidence of climate change through changes in precipitation and temperature. Most of the sites (80%) in the eastern US do not show a significant trend. The other 20% of sites show increasing trends in low flows in the northeast and decreasing trends of low flows in the southeast. These results agree with those obtained from both observations and model simulations in terms of large scale changes in drought and mean flows (Andreadis and Lettenmaier, 2006; Dai et al., 2004; Milly et al., 2005). Our next step is to look at the consistency of these results with precipitation, as according to Andreadis and Lettenmaier (2006) these results should be consistent with changes in precipitation. The increasing trends in the northeast may also be related to increasing temperatures that are impacting freezing soils and snow cover (Hayhoe et al., 2007) and therefore the late winter/early spring low flow period.

The long-term trend results also are consistent with the pattern of land use change shown in Figure 11. The northeast and the southeast show the most overall land use-land cover change over the last decades, while the changes over the Appalachian Mountains was more heterogeneous. Further investigation of site-specific land use changes and timing is needed to provide more robust attribution of changes.

In most cases, larger dams have the most significant regulation impacts on the flows (Smakhtin, 2001), and these types of changes are generally identified in our analysis. Not only do dams break the natural hydrological cycle, but they also reduce runoff and sediment supply in the watershed, affecting land use (Poff et al., 1997). Reestablishment of a natural flow regime in smaller dams has been a useful management scheme in restorations of river systems. Statistically, many sites show stationary behavior after identification of a regime shift by the Pettitt test, suggesting that these sites are being effectively managed from the standpoint of the time series. A lower RMS in the date of occurrence of low flows for a site also suggests either evidence of stationarity or a properly human managed system. In a developed area, flows are often artificially evaluated above the natural levels of low flow to create “anti-droughts” (Bunn et al., 2006) such that low flows no longer occur with the usual seasonal patterns. For example, flow regulation in site 0108000 has changed low flow magnitudes relative to natural (unregulated) conditions. The USGS site notes also provide corroborating evidence of the impact of management, such as the year of construction of a dam. However, the site notes do not always match up exactly with the results from the Pettitt test, which may be because the regulation does not take effect immediately or combined effects from, for example, land use change dampen or delay the changes.

### *c) Flood Studies*

The East Branch Delaware River basin is an important water supply source for the New York City metropolitan region and contains a dense network of USGS stream gages (Figure 12). Hydroclimatological analyses of flooding in the East Branch Delaware have focused on nonstationarities in flood occurrence and spatial heterogeneities in precipitation, runoff and flood peaks (Smith et al 2013a). Orographic precipitation mechanisms play an important role in the flood hydroclimatology of the region. Rainfall analyses (see Figures 13 and 15) have been carried out for sequence of major flood events in the Delaware River basin and used to assess precipitation controls of the striking contrasts in runoff and flood peaks between Beaver Kill and the East Branch Delaware above Margaretville (Figures 14 and 16). Flooding from Hurricane Irene in August of 2011 produced the record flood peak at Margaretville and devastated portions of the upper Delaware basin (Figures 13 and 14). A principal conclusion of these analyses is that orographic precipitation mechanisms play a dominant role in determining spatial heterogeneities of flood hazards.

Hydroclimatological analyses of flooding in the Potomac River basin have focused on “mixture” distributions, change points and trends and controls of upper tail behavior of flood peak distributions (Smith et al. 2013b). The dominant flood agents for the Potomac River at Point of Rocks are winter/spring extratropical systems, like the March 1936 flood that produced record flood peaks throughout major drainages of the eastern US. Tropical cyclones play an important role in determining upper tail properties and contribute to a fall peak in flood frequency. Orographic thunderstorm systems determine the upper tail of flood peak distributions in “small”

(less than 100 km<sup>2</sup>), forested central Appalachian watersheds (Hicks et al 2013). Despite a history of major land use transformation, including deforestation in the late 19<sup>th</sup> and early 20<sup>th</sup> centuries, there is little evidence of nonstationarities in flood occurrences for the Potomac River at Point of Rocks.

Flood studies in Texas characterize the relative role of tropical cyclones as flood hazards. We have focused on spatial analyses of tropical cyclone flood hazards and demonstrated the sharp decrease in tropical cyclone flood frequency with distance from the Gulf Coast in Texas. Analyses of flood hydroclimatology in Texas have also highlighted the role of abrupt changes relative to slowly varying trends (Villarini et al. 2013).

Urban modification of land surface hydrology and precipitation hydroclimatology have profound impacts on flood hazards in major urban areas of the eastern US (Wright et al. 2012 and 2013). High-resolution radar rainfall fields provide useful tools for estimating flood frequency over urban drainage networks (Figure 17).

## Other References:

- Andreadis, K. M., Lettenmaier, D. P., 2006. Trends in 20th century drought over the continental united state. *Geophysical Research Letters* 33, 1–4.
- Bunn, S. E., Thoms, M. C., Hamilton, S. K., Capon, S. J., 2006. Flow variability in dryland rivers: boom, bust and the bits in between. *River Research and Applications* 22 (2), 179186.
- Dai, A., Trenberth, K. E., Qian, T., 2004. A global dataset of palmer drought severity index for 18702002: relationship with soil moisture and effects of surface warming. *American Meteorological Society* 5, 1117–1130.
- Hayhoe, K., Wake, C. P., Huntington, T. G., Luo, L., Schwartz, M. D., Sheffield, J., Wood, E., Anderson, B., Bradbury, J., Degaetano, A., Troy, T. J., Wolfe, D., 2007. Past and future changes in climate and hydrological indicators in the US northeast. *Climate Dynamics* 28, 381–407.
- Milly, P., Dunne, K., Vecchia, A., 2005. Global pattern of trends in streamflow and water availability in a changing climate. *Nature* 438-17, 347–350.
- Poff, N. L., Allan, J. D., Bain, M. B., Karr, J. R., Prestegard, K. L., Richter, B. D., Sparks, R. E., Stromberg, J. C., 1997. The natural flow regime: a paradigm for river conservation and restoration. *Bioscience* 47, 769–784.
- Rolls, R. J., Leigh, C., Sheldon, F., 2012. Mechanistic effects of low-flow hydrology on riverine ecosystems: ecological principles and consequences of alteration. *Freshwater Science* 31 (4), 1163–1186.
- Smakhtin, V. U., 2001. Low flow hydrology: a review. *Journal of Hydrology* 240, 147–186.
- Tallaksen, L. M., VanLanen, H. A. J., 2004. *Hydrological Drought, Processes and Estimation Methods for Streamflow and Groundwater*. Vol. 48. Elsevier Science.
- USGS, December 2012. Land cover change in the eastern united states. Electronic. URL <http://landcovertrends.usgs.gov/east/regionalSummary.html>

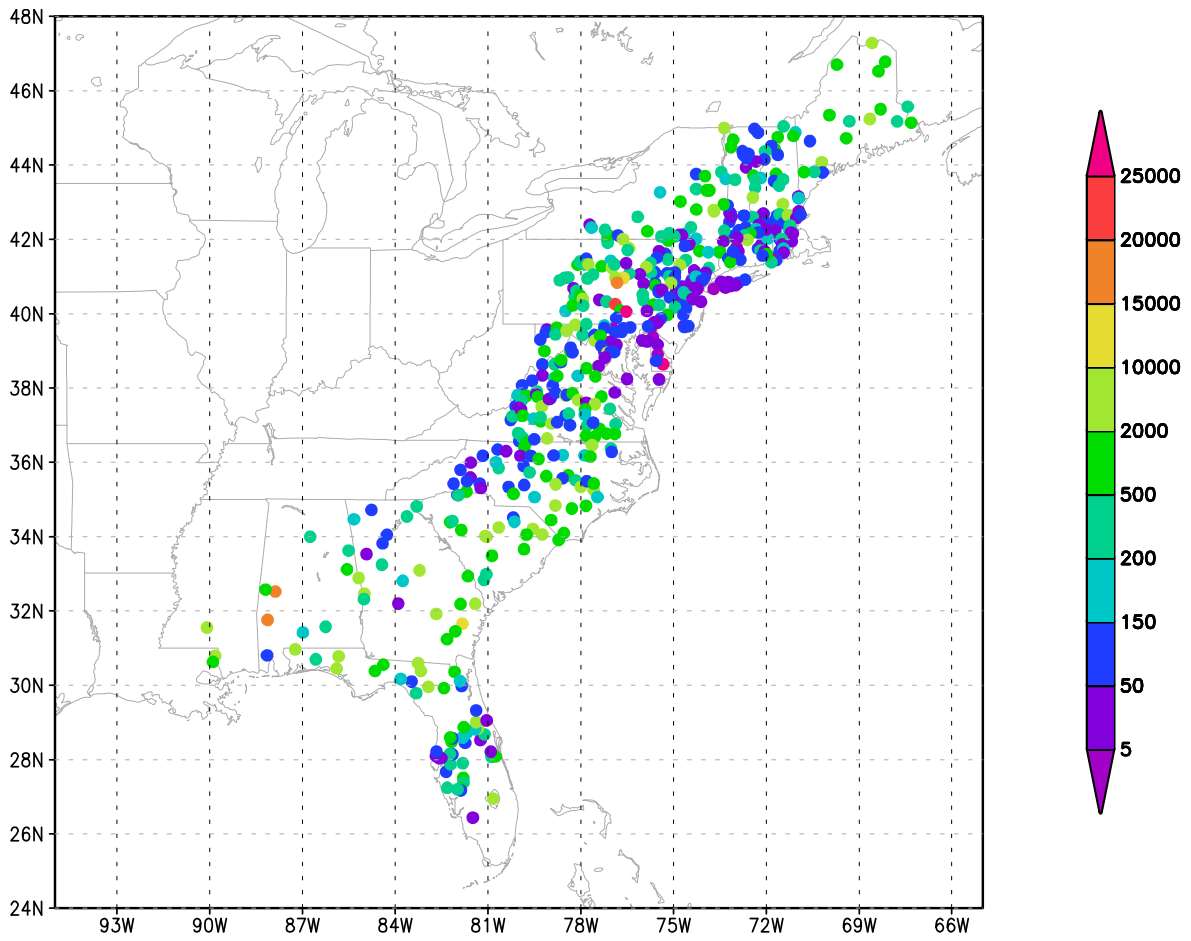


**Figure 1.** Location of 523 flow monitoring sites colored by the area of their corresponding watershed.

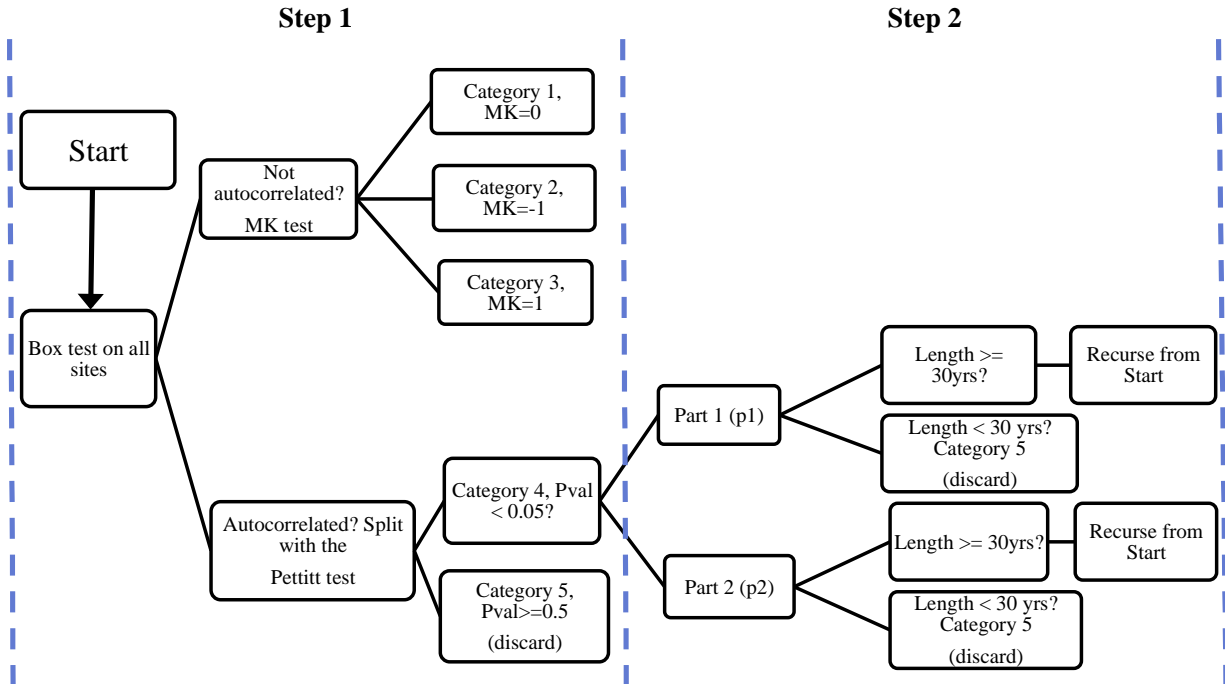


**Figure 2.** The recursive decomposition algorithm for identifying stationary, non-stationary and unusable sites. Each site's time series, possibly broken into pieces, is categorized as no trend (category 1), decreasing (category 2), increasing (category 3), or unusable (category 5).

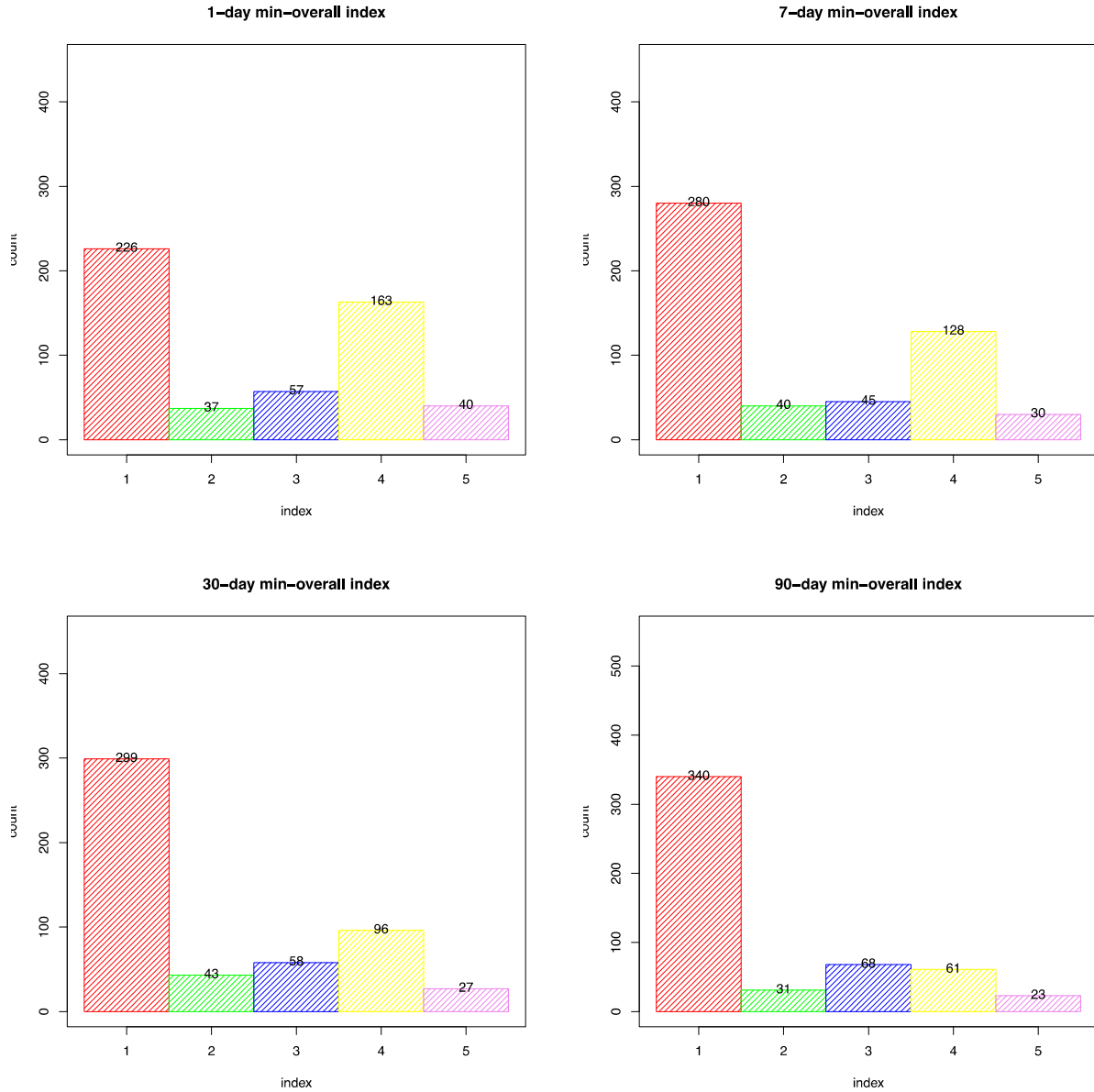


**Figure 3.** The histograms of time series categorization for  $Q_1$ . Red: no trend (category 1); Green: category 2 (MK =-1); Blue: category 3 (MK=1); Yellow: split by the Pettitt test (category 4); Pink: out of further consideration (category 5).

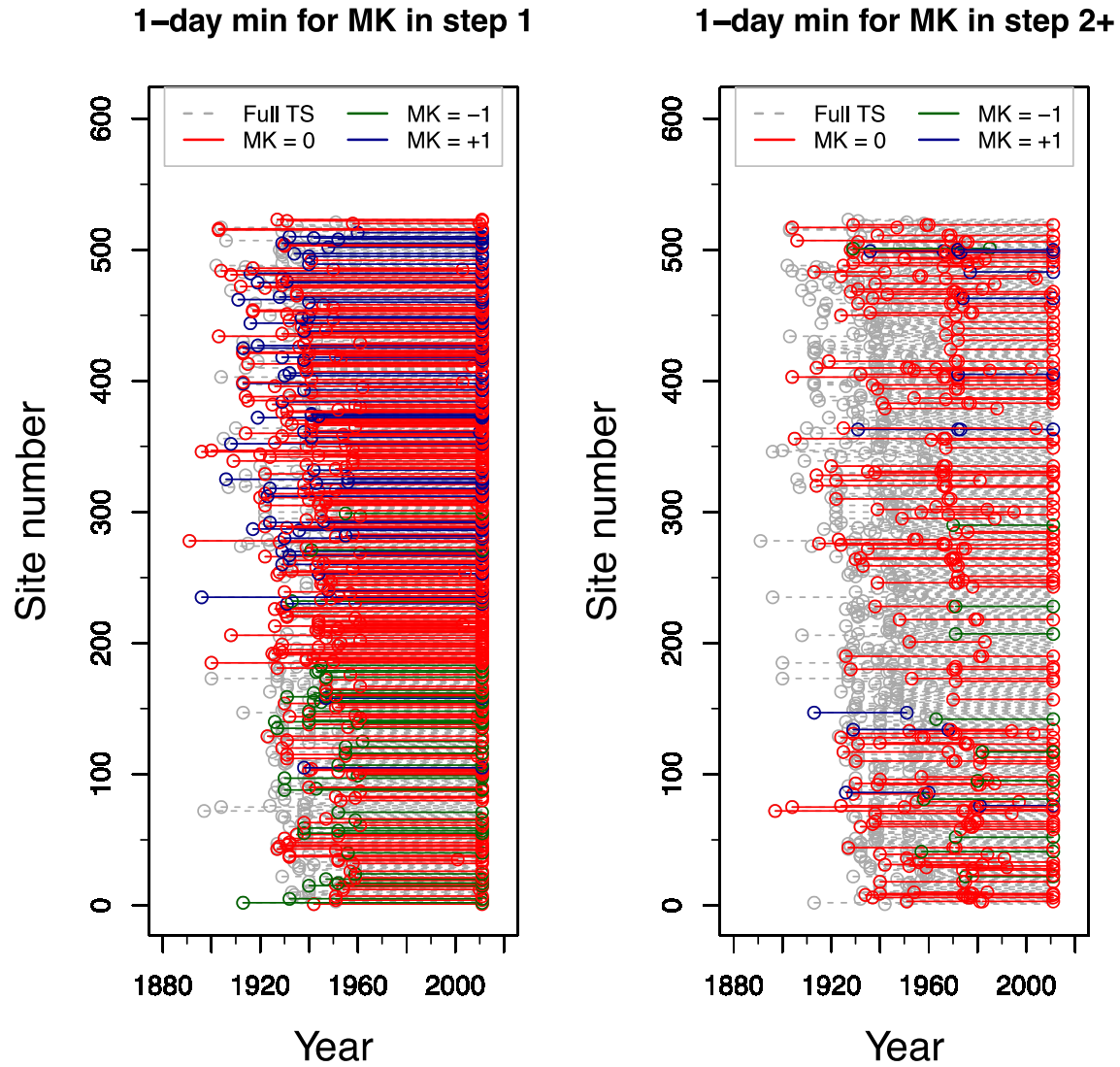


**Figure 4.** Range of years with MK=0, -1, or +1. The left plot shows the results of Step 1 of the decomposition algorithm. Sites are ranked by number from the most southerly to the most northerly. The right plot shows the sub series that are split recursively due to abrupt shifts. Gray dashed lines indicate the original length of the time series. The right panel shows the part of original time series that we were able to recover from regulated sites.

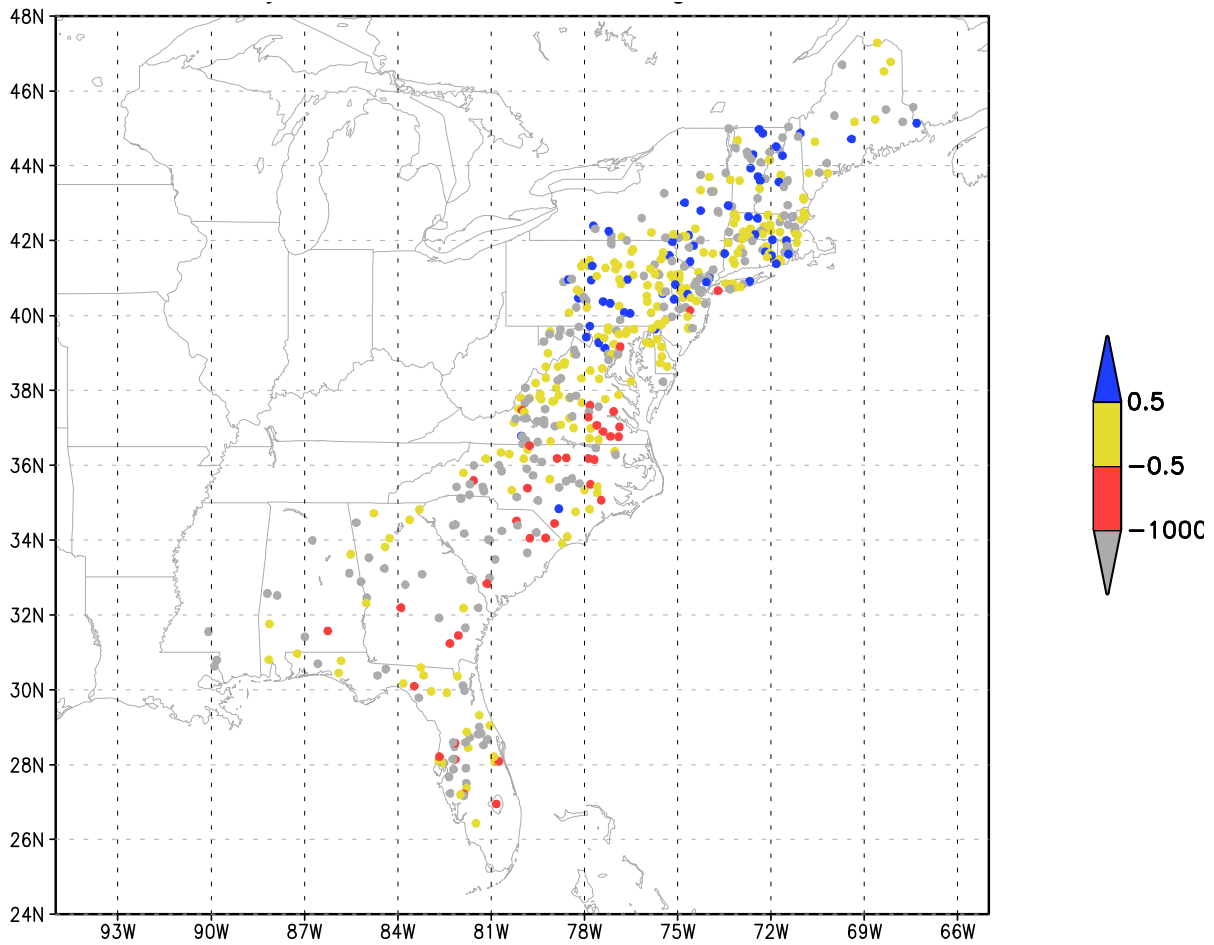


**Figure 5.** Overall trend of 1-day minimum time series after excluding sites with abrupt changes. Red shows a decreasing trend, blue shows an increasing trend and yellow shows no trend. Grey sites are those with significant autocorrelation and hence excluded from the MK test. The pattern of increasing trend in the northeast and decreasing trend in the southeast is apparent.

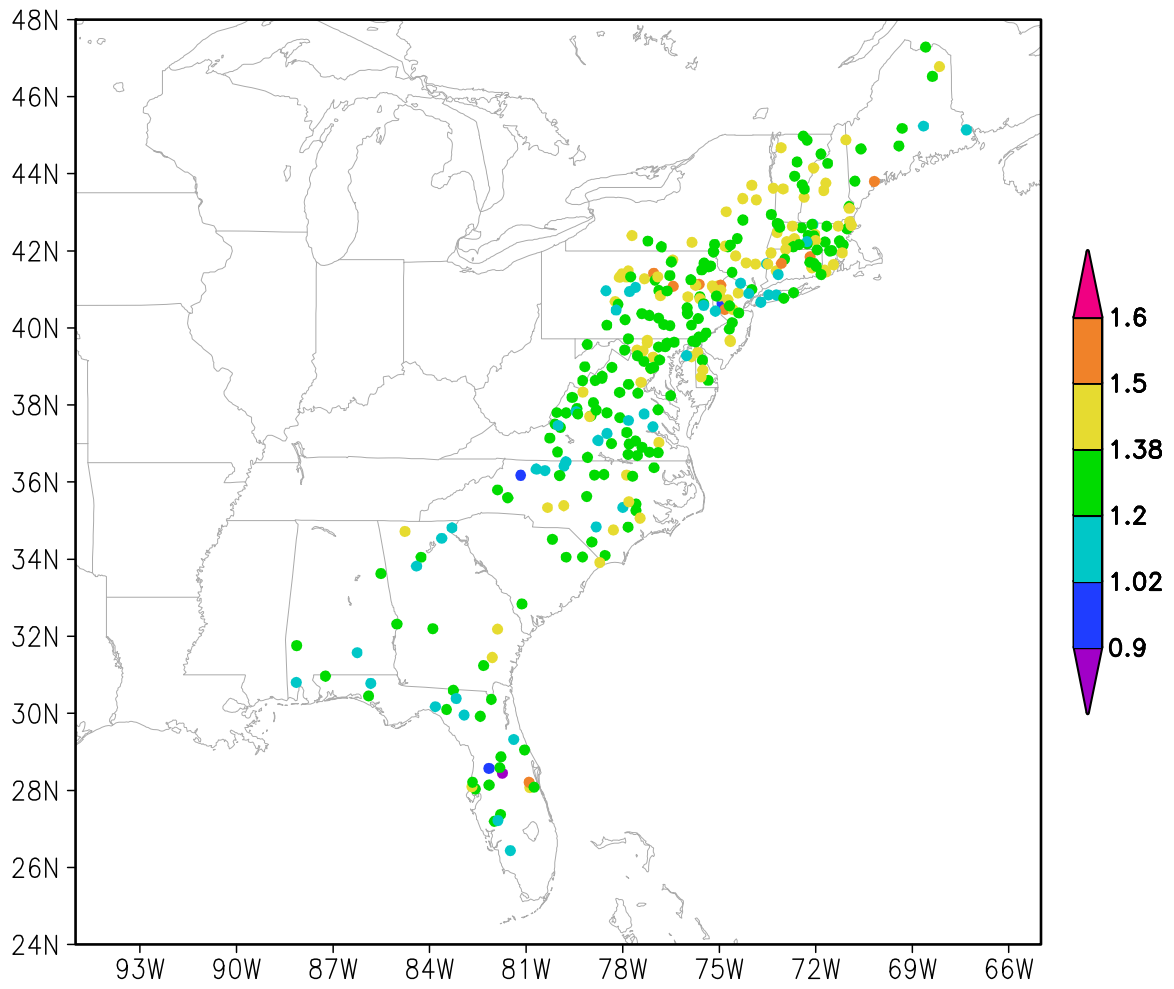


**Figure 6.** Spatial distribution of volatility values for  $Q_1$ .

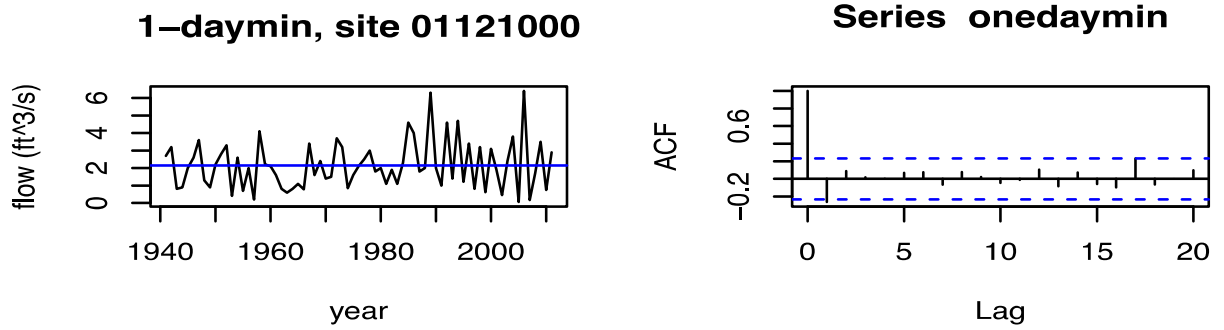


**Figure 7.** Time series of site 01121000 which has the maximum volatility (1.59) for  $Q_1$  among 318 sites. The left panel shows the time series and the right shows its autocorrelation plot.

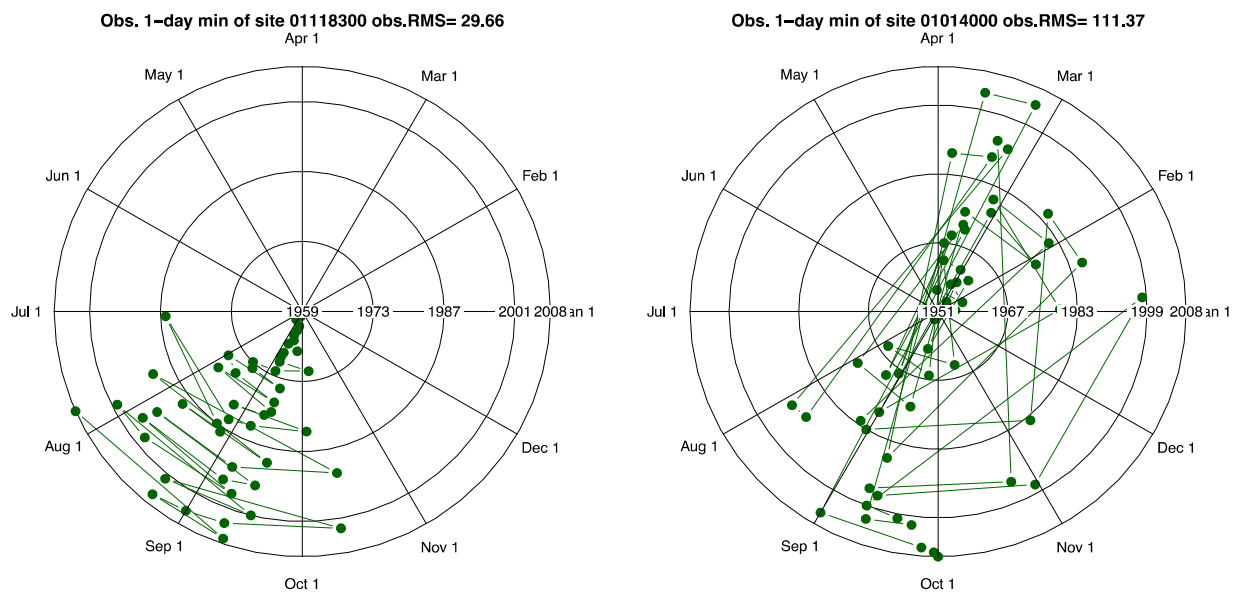


**Figure 8.** Date of occurrence of Q1 for two extreme sites: 01118300 (left) and 01014000 (right), with RMS variability values of 29.66 and 111.37, respectively.

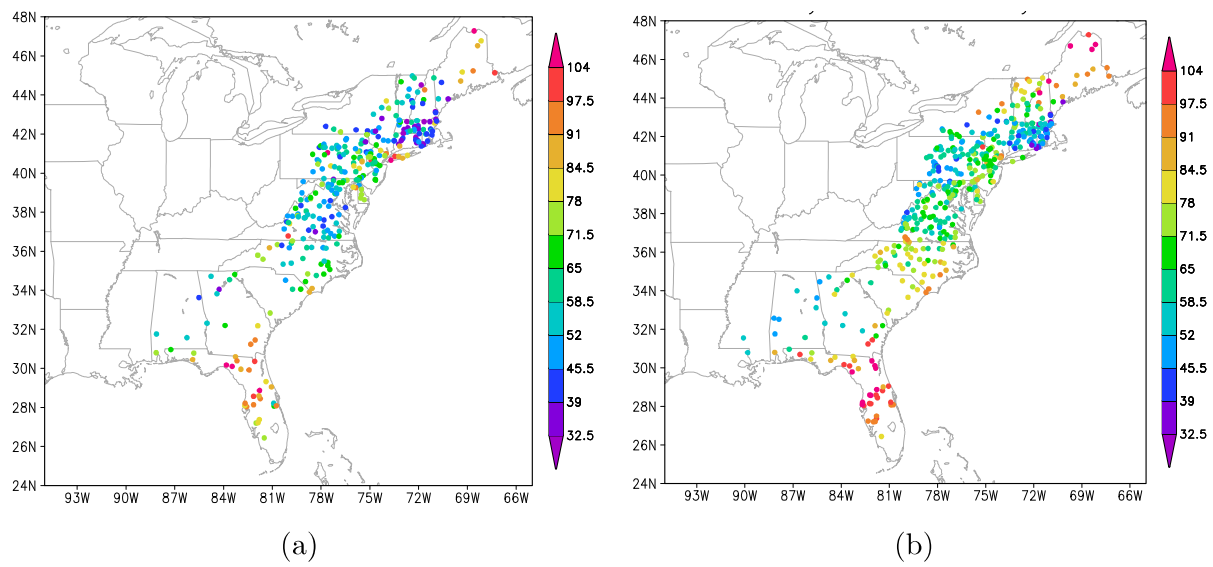


**Figure 9.** Spatial distribution of RMS values of date of occurrence for 1-day and 90-day low flows. The number of series that are used changes from 318 sites for 1-day to 437 sites for 90-day.

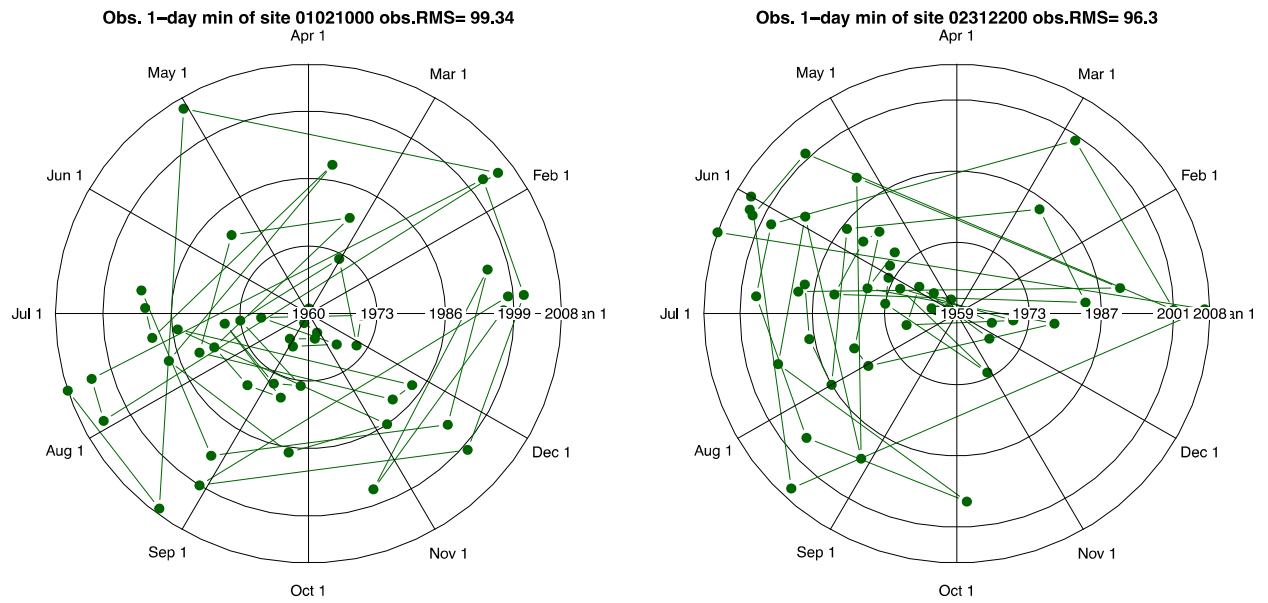


**Figure 10.** Left: date of occurrence of Q1 low flows for one of the most variable sites in the northeast. Right: for one of the most variable sites in the southeast.

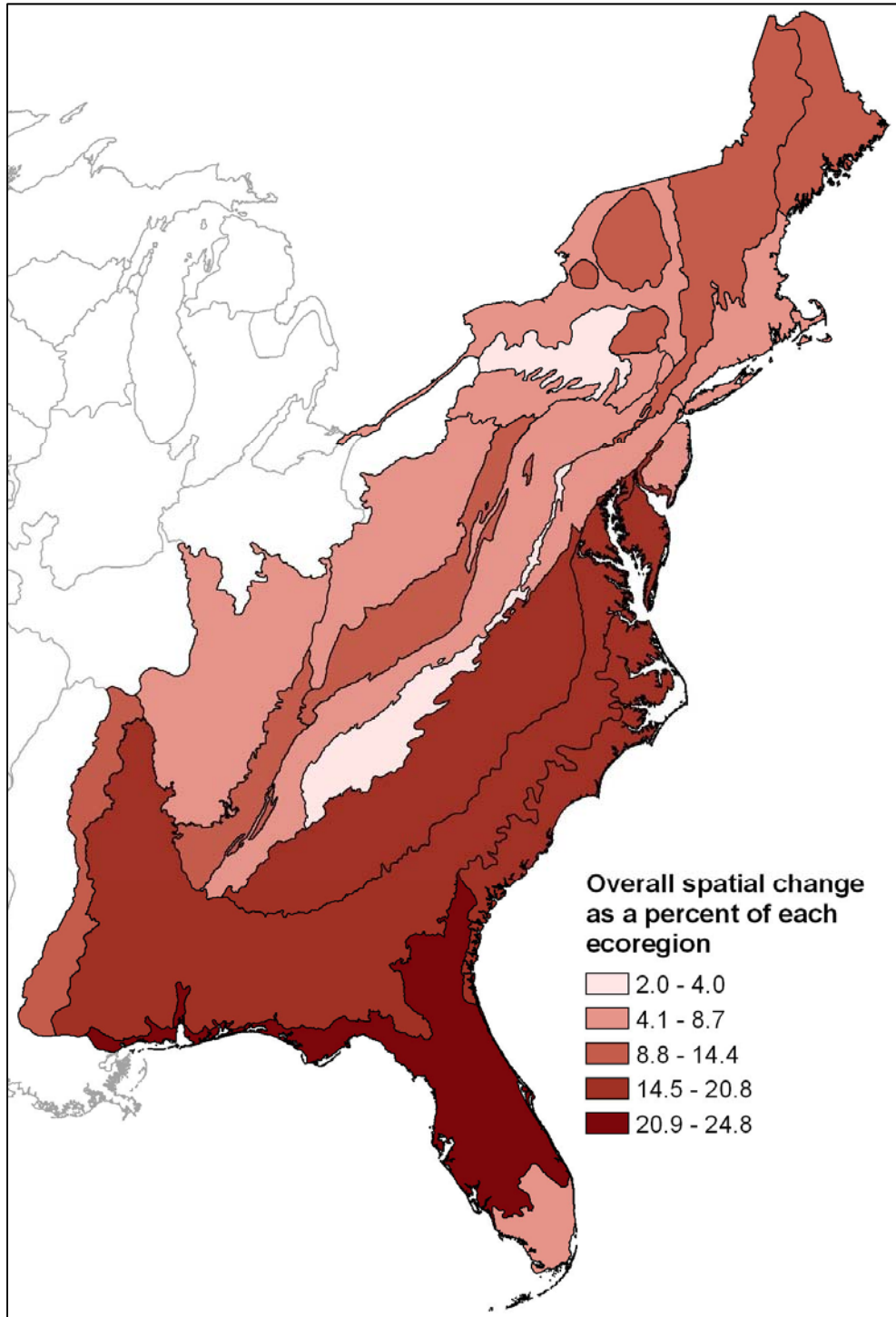


**Figure 11.** Overall spatial change in land use from 1973 to 2000 for all Eastern U.S. Most land use changes occurred in the northeast and the southeast. In the southeast changes were mostly in timber harvesting and urban growth. Large-scale timber harvesting is also done in the northeast (USGS, 2012).

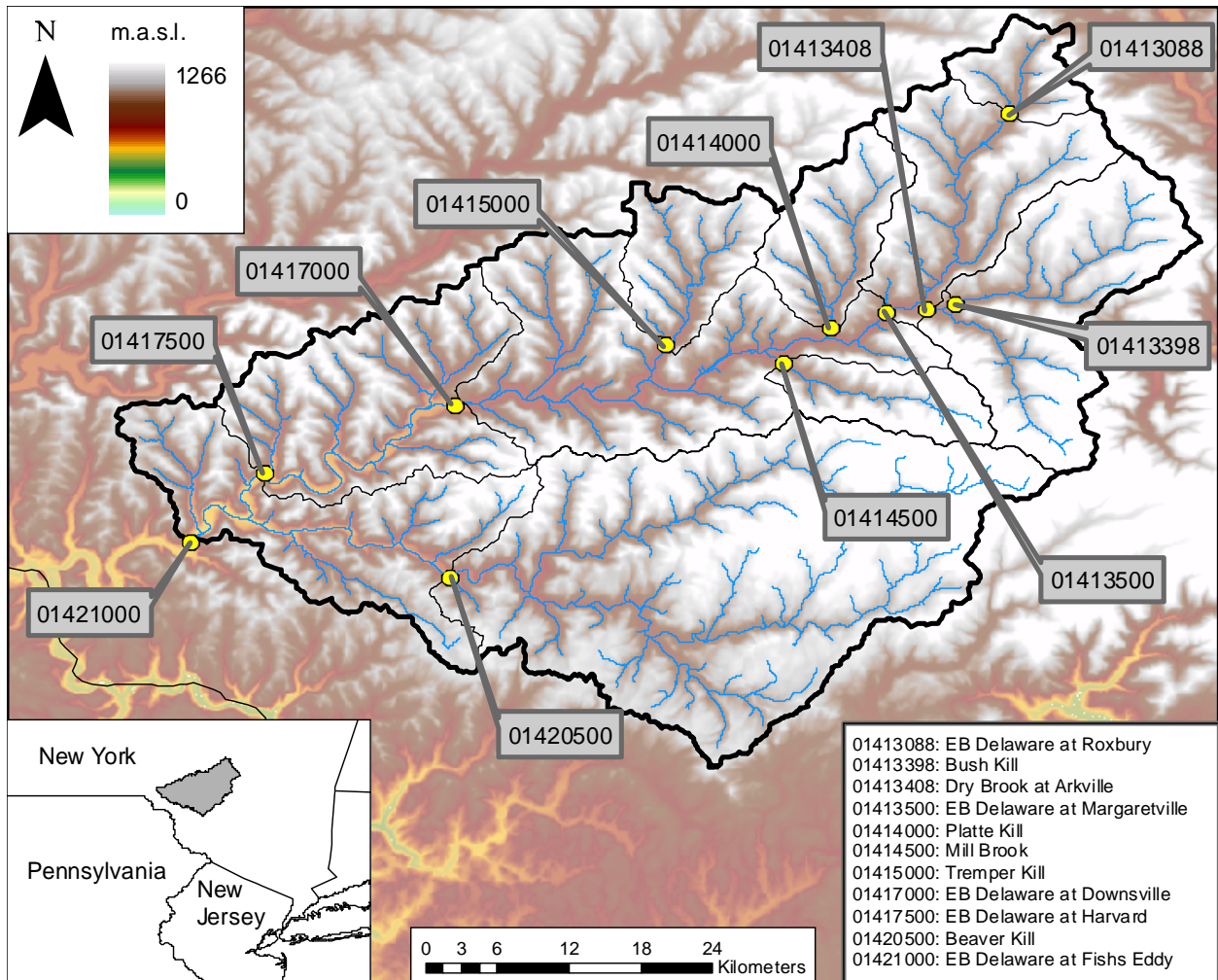


Figure 12. Location map for East Branch Delaware study watersheds, with USGS stream gaging locations.

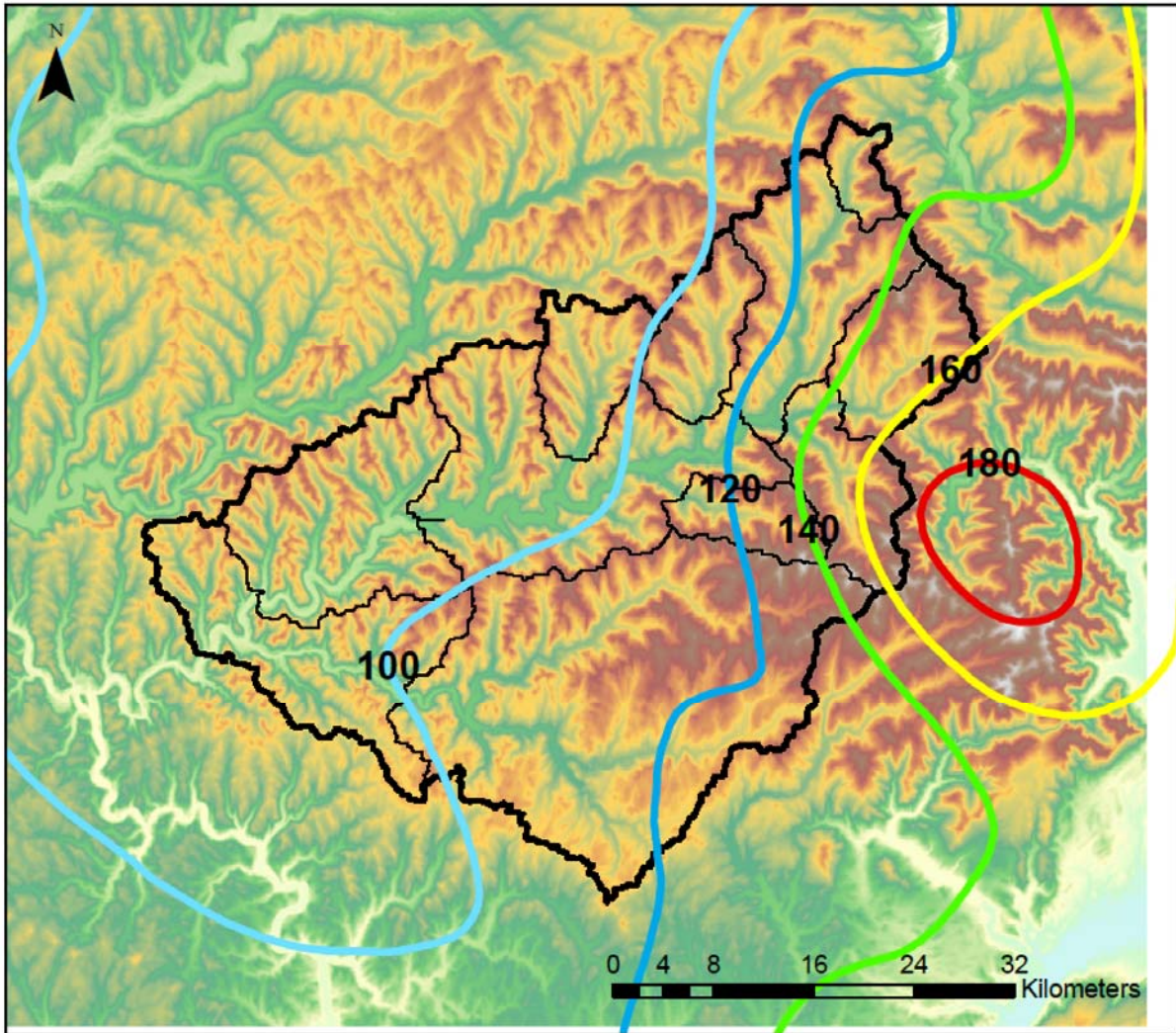


Figure 13. Storm total rainfall (mm) from Hurricane Irene (28-29 August 2011) based on bias-corrected Hydro-NEXRAD rainfall fields.

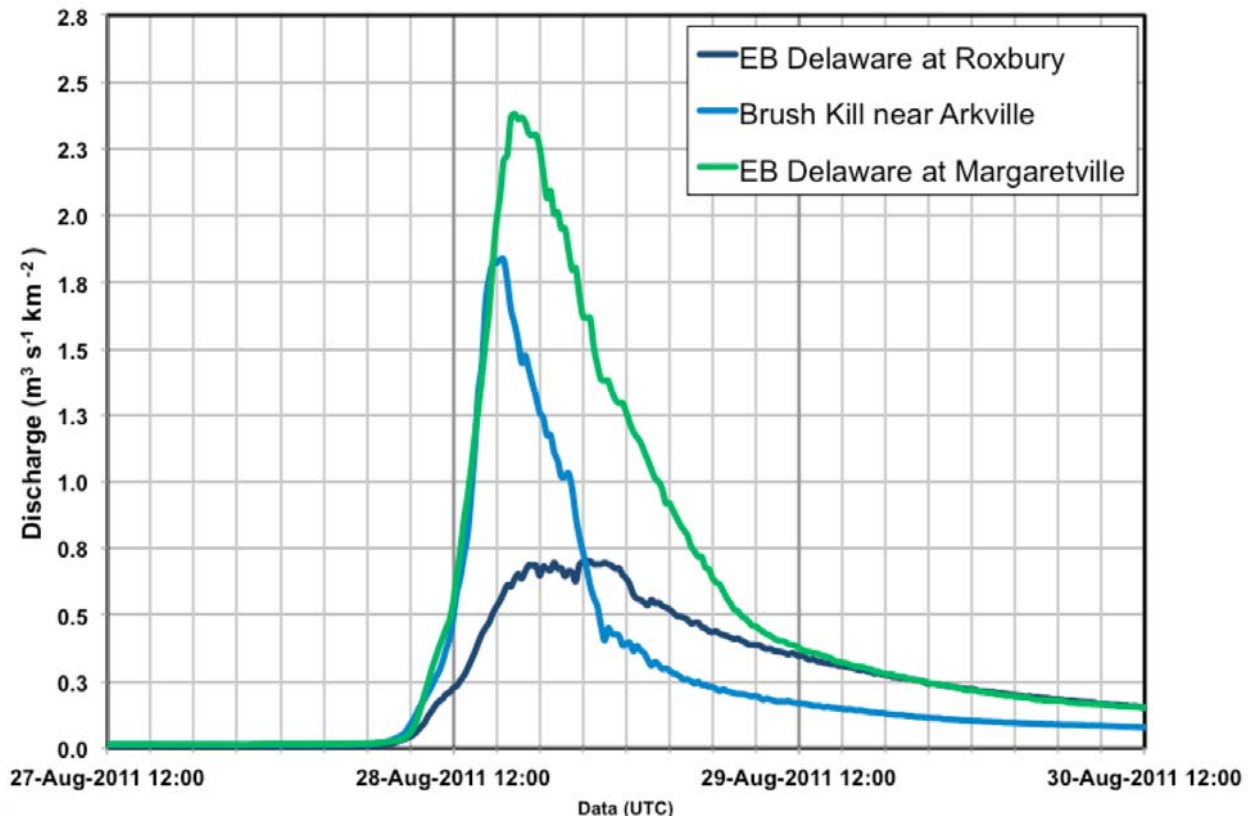


Figure 14. Discharge hydrographs (expressed as a unit discharge, i.e. discharge divided by drainage area) for Hurricane Irene in the East Branch Delaware at Margaretville (green), East Branch Delaware at Roxbury (black) and Bush Kill at Arkville (blue).

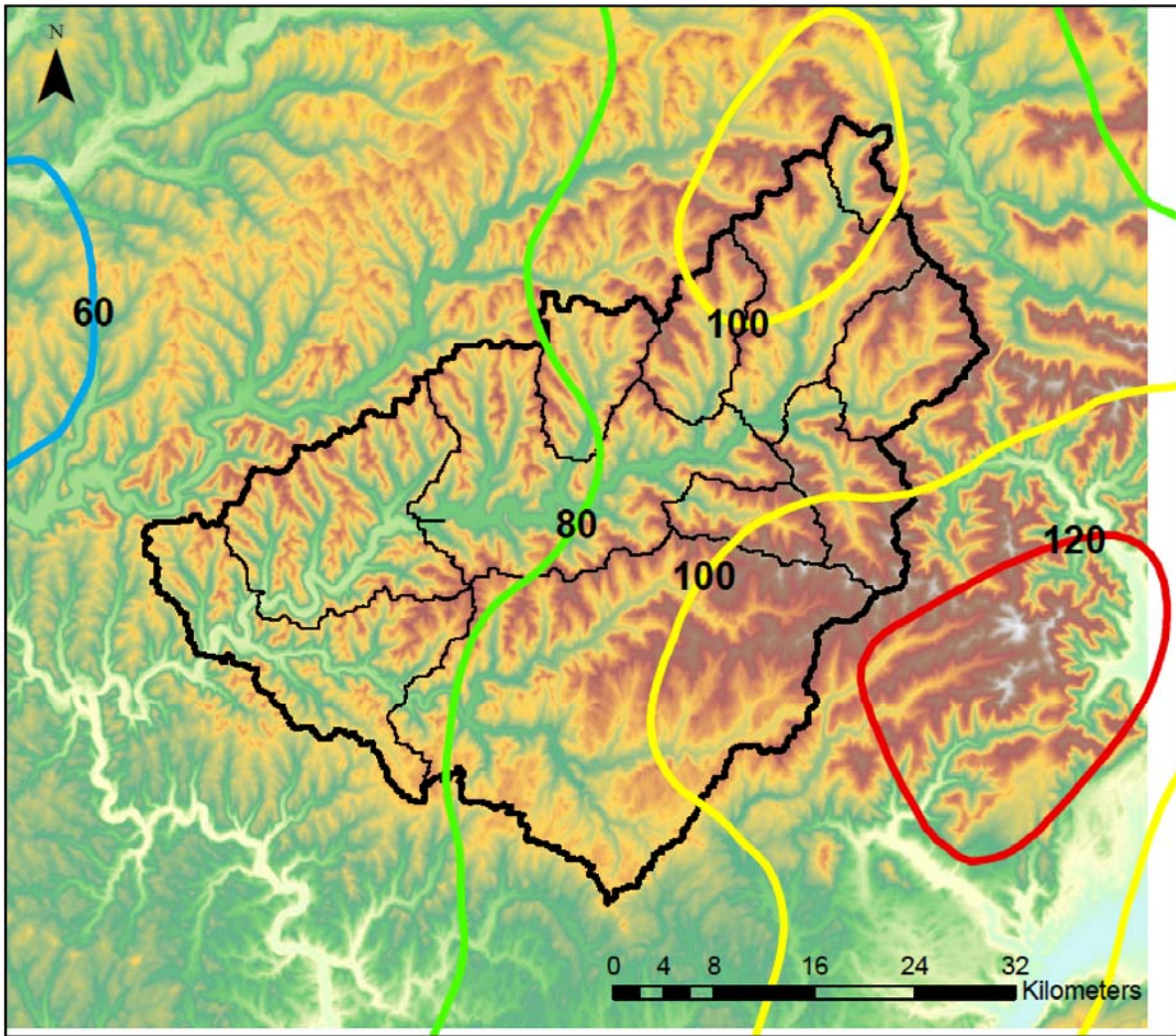


Figure 15. Storm total rainfall (mm) from April 2005 storm, based on bias-corrected Hydro-NEXRAD rainfall fields.

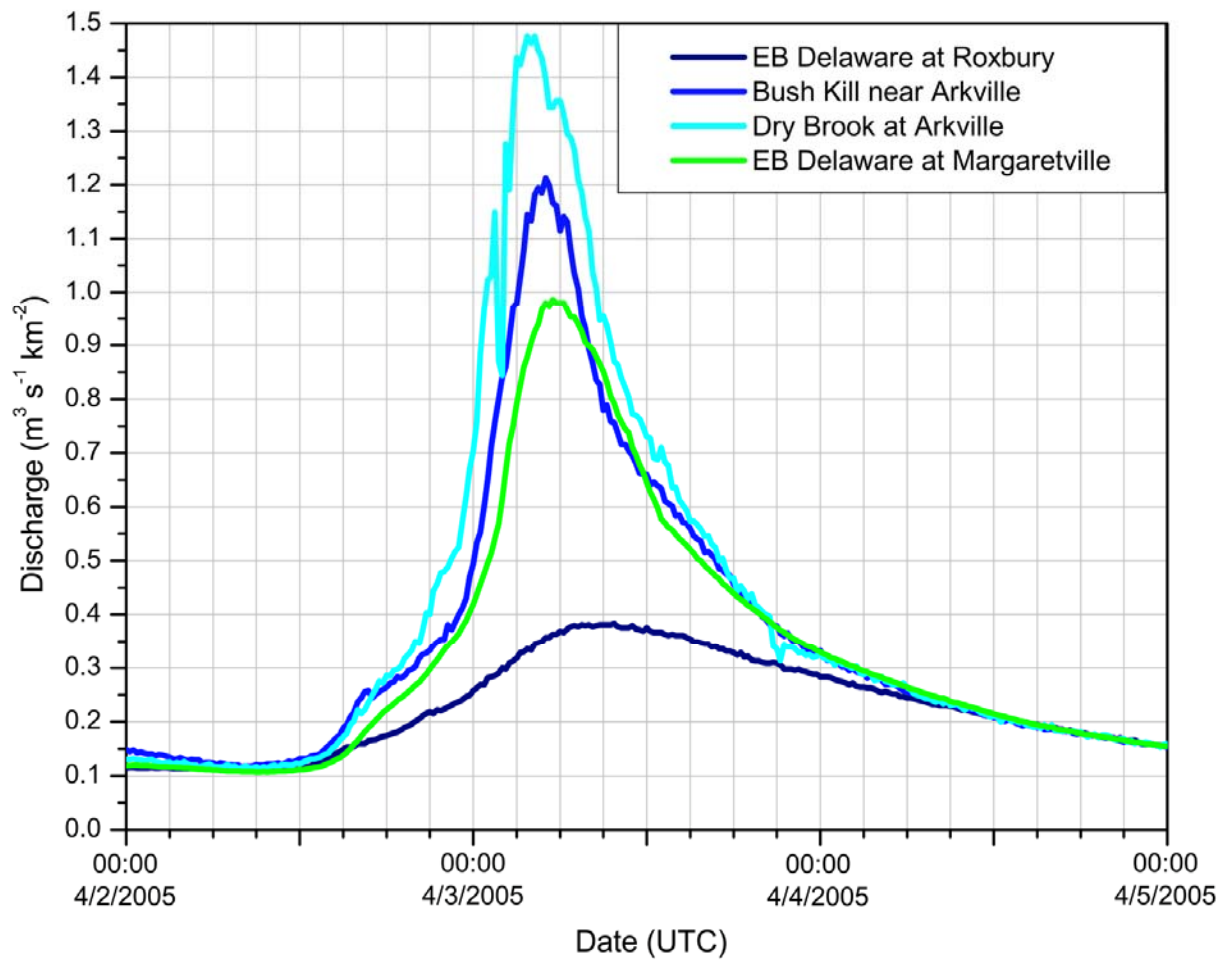


Figure 16. Discharge hydrographs (expressed as a unit discharge, i.e. discharge divided by drainage area) for April 2005 flood in East Branch Delaware at Margaretville (green), East Branch Delaware at Roxbury (black) and Bush Kill at Arkville (blue) and Dry Brook at Arkville (light blue).

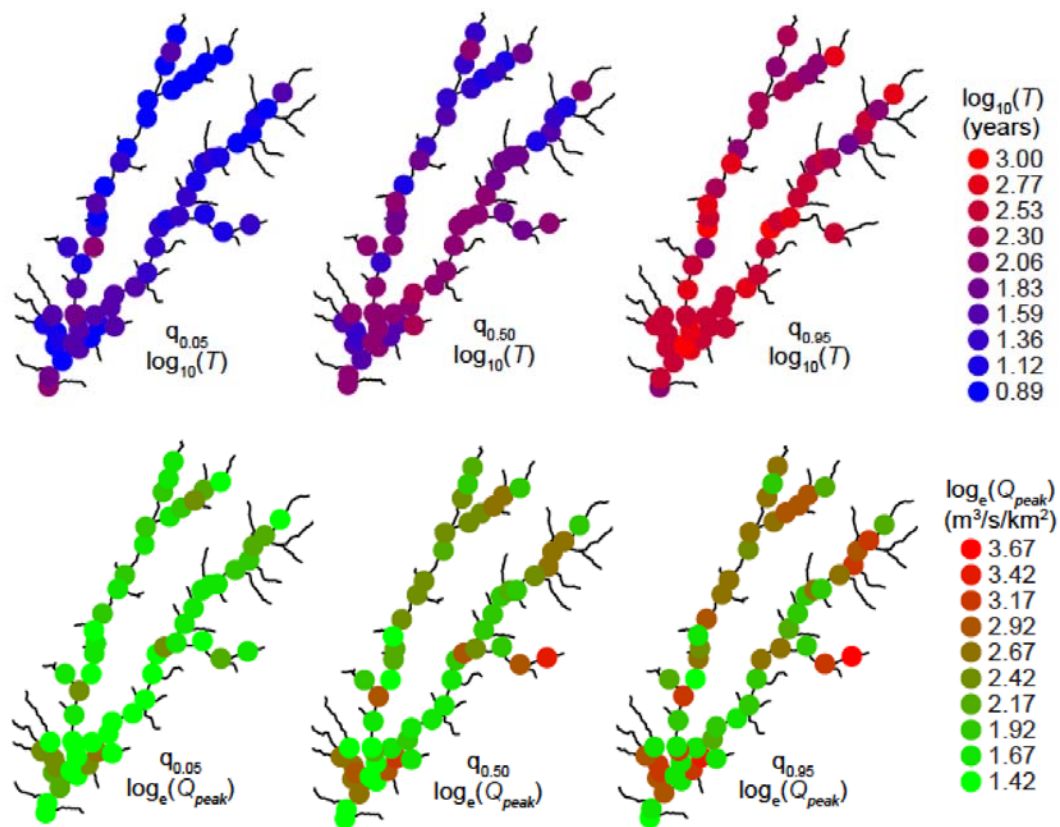


Figure 17. Spatial distribution of 0.05, 0.50, and 0.95 quantiles of return period  $T$  and area-normalized peak discharge  $Q_{peak}$ , estimated from the fifty events (one from each of fifty 1000-year SST realizations) that produced 100-year flood peaks at Little Sugar Creek at Archdale (Charlotte, NC).

# Performance Assessment of Bioretention for Car Wash Runoff Treatment

## Basic Information

<b>Title:</b>	Performance Assessment of Bioretention for Car Wash Runoff Treatment
<b>Project Number:</b>	2012NJ305B
<b>Start Date:</b>	3/1/2012
<b>End Date:</b>	2/28/2013
<b>Funding Source:</b>	104B
<b>Congressional District:</b>	NJ-006
<b>Research Category:</b>	Water Quality
<b>Focus Category:</b>	Non Point Pollution, Treatment, Methods
<b>Descriptors:</b>	None
<b>Principal Investigators:</b>	Michele Bakacs, Steven Yergeau

## Publications

1. Yergeau, S.E. 2013. Assessment of Car Wash Runoff Treatment Using Bioretention Mesocosms. New Jersey Water Environment Association (NJWEA) Conference. Atlantic City, NJ. Invited Presentation.
2. Bakacs, M., S.E. Yergeau, and C.C. Obropta. 2012. A Preliminary Investigation for Using Rain Gardens to Reduce Pollutants in Car Wash Runoff. Land Grant and Sea Grant National Water Conference. Portland, OR. (poster presentation)

## **Project Summary**

### *Problem & Research Objectives*

Recent investigations have shown that significant quantities of nonpoint source pollutants are generated from residential car washing (Smith and Shilley 2009). Car wash runoff has been shown to be a source of petroleum hydrocarbons, heavy metals, phosphorus, nitrogen, ammonia, total suspended solids (TSS), and surfactants from car wash soap. In New Jersey, as well as the nation as a whole, many groups hold car washing fundraisers unaware of the pollution issues associated with car wash runoff. Residential car washing and organized car wash events are currently exempt from the federal stormwater regulation program - the National Pollutant Discharge Elimination System Program. The most common pollution prevention strategies for car washing involve public education, partnering with commercial car washes for fundraiser events, use of storm drain inserts to collect wash water, and encouraging washing cars on lawns and other pervious surfaces. Little information exists on the effectiveness of using bioretention systems to reduce pollutants associated with car wash runoff.

This project's goal is to characterize the pollutants associated with car wash runoff and determining the efficiency of bioretention systems as a means to treat pollutants in this unique type of runoff. 'Car washing' and 'car wash' for this project are defined as the cleaning of vehicles by individuals either as the vehicle's owner or as part of a fundraising event, such as held by a school or other organization. The definition for this study does not include commercial car wash facilities which recycle water. This potential pollution source is estimated to be large, as runoff from residential car washing is estimated to produce an average of 20 gallons per vehicle and community fund raising events can produce up to 2,000 gallons per event (Kirschbaum and Fohn, 2009).

The objective of this project is to assess the ability of rain gardens to remove pollutants, specifically total phosphorus (TP), TSS, polycyclic aromatic hydrocarbons (PAHs), and surfactants, from car wash runoff. These parameters have been chosen based on prior research investigating contaminants associated with car wash runoff (Bakacs and Yergeau, 2011).

### *Methodology*

#### ***Experimental Set-Up***

Experiments were conducted at Rutgers University's Environmental and Natural Resource Sciences Building in New Brunswick, NJ using four bioretention mesocosms. The bioretention mesocosms were constructed in June 2011 using four 71.9 L "rope tub" containers, 56.5 cm in diameter and 41.9 cm high.



Figure 1: View of experimental set-up showing mesocosms after construction.

Design criteria for the mesocosms followed those used by Rutgers in its demonstration rain garden program (Obropta et al. 2008). Approximately 10.0 cm of washed  $\frac{3}{4}$ " gravel was placed in the bottom of each mesocosm to allow for sufficient drainage. Soil media used in the mesocosms follow bioretention guidelines established by the NJDEP (2009) for stormwater BMPs. Soil media consisted of 82% sand and 18% humus/manure mix by volume, which was hand-mixed on a tarp prior to installation in the mesocosms. Approximately 15.0 cm of soil media was added to each of the four mesocosms.

Four plants from each of three species were planted, for a total of twelve plants in each mesocosm: soft rush (*Juncus effusus*), switchgrass (*Panicum virgatum*), and black-eyed susan (*Rudbeckia lacinata*). These plants are typical for rain gardens designed in New Jersey. A 5.0 cm layer of wood mulch was applied on top of the soil media leaving approximately 12.0 cm of ponding depth for each of the rain garden mesocosms.

### ***Sample Collection and Analysis***

Runoff was generated by conducting car wash events on a vehicle selected from Rutgers University's Environmental Sciences Department so that one vehicle was washed per event. Rinsing and washing occurred on an impermeable tarp capable of containing and collecting the runoff water. This prevented contaminants and particles deposited on the pavement from contributing to the runoff so that contaminants from the vehicle itself were quantified during this study. A total of five car wash events have been conducted: three were performed in October

2011, prior to receipt of funding from NJWRRI and two events, one in September 2012 and one in October 2012. Currently, four more events are scheduled for 2013.

Car wash runoff was collected in a 71.9 L “rope tub” container and divided into three equal volumes based upon how much runoff was generated from each event (approximately 45 L to 60 L depending on the vehicle washing event). Each third of the runoff generated was applied to one of three mesocosms as influent. The fourth mesocosm had approximately 20 L of tap water (hereon in referred to as “clean water influent”) applied as a control for statistical comparison. Effluent samples from the four mesocosms were collected approximately 24 hours after addition to the mesocosms to allow for adequate treatment of the target contaminants (TP, TSS, PAHs, and surfactants). Samples for analysis were collected as grab samples while the effluent was flowing in appropriate containers by opening one of the four PVC ball valves located at the bottom of each mesocosm. Samples of the tap water used during the wash events and the runoff generated prior to treatment by the mesocosms were also collected to establish baseline data for the study. All samples were kept on ice after collection and until dropped off for sample analyses. Samples were analyzed for TP, TSS, PAHs, and surfactants by Accutest Laboratories (Dayton, NJ) and followed appropriate analytical and chain of custody procedures for TP (EPA Method 365.3), TSS (Standard Methods, 20<sup>th</sup> edition (SM20) Method 2540D), PAHs (SM20 Method 8270D), and surfactants (SM20 Method 5540C) (American Public Health Association 1998; United States Environmental Protection Agency 2012).

Pollutant removal was calculated as percent removal (%R) of the measured target contaminants (TC) in the runoff. All losses from the system through the various physical, chemical and biological processes were lumped together and the %R calculated as:

$$\%R = \frac{TC_{IN} - TC_{OUT}}{TC_{IN}}$$

TC was based on the concentrations of TP, TSS, and surfactants applied to and collected from each mesocosm. Data (both sample concentration and %R) were analyzed for significance ( $p < 0.05$ ) using analysis of variance (ANOVA: single factor). Statistical analyses were conducted using the statistical software package in Microsoft Excel<sup>TM</sup>.

Rain gardens remove pollutants through a variety of pathways (microbial processes, plant uptake, sedimentation, and absorption). Specific pollutants are removed through one of these specific pathways. One way to determine which removal processes are present is to measure indicators in the media to be studied. Oxidation-reduction potential (ORP) measurements were taken with a platinum combination electrode Ag+/AgCl Accumet (Fisher Scientific, Pittsburgh, PA USA) attached to a portable pH/voltage meter (Accumet AP62, Fisher Scientific, Pittsburgh, PA USA). High ORP is associated with an oxidized environment and promotes aerobic processes such as nitrification, while lower ORP values are linked to reduced conditions and promote anaerobic processes such as sulfate reduction and methanogenesis (Faulwetter et al. 2009). The portable pH/voltage meter was also used to measure pH and temperature, with the appropriate electrodes, of the mesocosm soil and car wash runoff water. A handheld meter (YSI 550A DO Meter) was used for DO measurements. Once the four rounds of sampling in 2013 are complete, these results will be evaluated as possible indicators of pollutant removal mechanisms occurring in the mesocosms.

### *Principal Findings & Significance*

Note: Results from all five sampling events conducted thus far (three in 2011 and two in 2012) are reported in the following sections, even though only the 2012 events were paid for with funding received from NJWRRI. Four additional rounds will be conducted in 2013.

### *Car Wash Runoff Characterization*

PAHs were not detected in the two rounds of sampling conducted in 2012, and were dropped from the sampling scheme. The mean pollutant concentrations from the car wash runoff exceeded New Jersey surface water quality standards for TSS and TP (Table 1; NJDEP 2011). New Jersey does not have a numerical standard for surfactants. Surfactants are considered to be toxic substances (general) and “should not be present in such concentrations as to affect humans or be detrimental to the natural aquatic biota, produce undesirable aquatic life, or which would render the waters unsuitable for the designated uses”. Varying toxicity levels have been reported in the literature for LAS (Venhuis and Mehrvar 2004). Lewis (1991) reported that chronic effects of LAS occurs at concentrations normally greater than 0.1 mg/L. Bjerregaard et al. (2001) reported that LAS concentrations in sewage effluent have a physiological impact on marine life when between 0.02-1.0 mg/L. Mean surfactant concentration for the car wash runoff was well above these thresholds at 10.56 mg/L.

Table 1. Mean pollutant concentrations in car wash runoff and estimated pollutant load per car wash fundraiser event. (+ indicates standard deviation).

Parameter	Standards for Fresh Waters (mg/L) <sup>b</sup>	Car Wash Runoff (mg/L)	Load per car <sup>a</sup> (kg)	Load per car wash event <sup>a</sup> (kg)
TP	0.1	0.12 ±0.11	0.0000066	0.00066
TSS	40.0	81.60 ±49.80	0.0045	0.45
Surfactants	n/a	10.56 ±2.99	0.00058	0.058

<sup>a</sup> Load is based on average volume applied to mesocosms (55.0 L ± 6.6) and an estimate of 100 cars per car wash event.

<sup>b</sup> NJDEP, 2011

Based on mean pollutant concentrations in the car wash runoff, an estimate of the potential pollutant loading from a typical car wash event can be determined (Table 1). Pollutant loading is estimated as the product of the average volume of car wash runoff discharged to the mesocosms during this study (55.0 L ± 6.6) and an estimate of 100 vehicles washed per car wash event held at the high school in Clark, NJ (S. McCabe, personal communication, May 30, 2012). Calculating percent watershed loading for these pollutants is beyond the scope of this study, but based on these estimates there is the potential for car wash fundraiser events to contribute significant quantities of pollutants to receiving water bodies.

### *Rain Garden Pollutant Removal Efficiencies*

Results shown in Table 2 indicate that mean TP concentration was higher in the car wash runoff than the clean water influent (tap water), although this difference was not statistically significant.

Since phosphate-free car wash soap was used during the car wash events, it is possible that the dirt residue on the vehicles might have been a source of TP to the runoff. Both mean TSS and mean surfactant concentrations for the car wash runoff were significantly higher in comparison to the clean water influent (Table 2).

Table 2. Comparison of mean pollutant concentrations for clean influent and car wash runoff. ( $n = 3$ ) (The  $\pm$  indicates standard deviation.)

Parameter	Clean Influent (mg/L)	Car Wash Runoff (mg/L)	$p$ -Value
TP	0.03 $\pm 0.00$	0.12 $\pm 0.11$	<i>ns</i>
TSS	2.40 $\pm 0.89$	81.60 $\pm 49.80$	$p < 0.01$
Surfactants	0.15 $\pm 0.10$	10.56 $\pm 2.99$	$p < 0.01$

Table 3 shows that for all mesocosms mean TP effluent concentrations were higher than the influent. The TP percent reductions for each mesocosm indicate that more TP was discharged from the mesocosms than entered, including the control mesocosm. It is most likely that the humus/manure mixture and mulch added to the media became a source of TP. Long term monitoring of the mesocosms in the current study is necessary to determine whether TP effluent concentrations decrease over time.

For mesocosms 1, 2, and 3, mean TSS effluent concentrations were significantly lower than the influent (Table 3). These results correspond well with other studies showing that bioretention basins effectively remove sediment from stormwater runoff (Davis et al. 2009; Hatt et al. 2009). Rain gardens would be an effective means of reducing TSS concentrations in car wash runoff.

Surfactant concentrations in the effluent were also significantly lower compared to the influent (Table 3) although the removals were not enough to reduce concentrations below aquatic toxicity ranges noted by researchers (Lewis 1991; Bjerregaard et al. 2001). Further research is needed to determine rain garden designs that sufficiently reduce effluent surfactant concentrations as well as whether surfactants effectively degrade within the rain garden media. Microbial breakdown of surfactants in the soil can be the primary mechanism for LAS removal (Holt et al. 1989). Removal occurs rapidly with half-life values for LAS observed between 7 and 22 days. Even in soils with little organic material and high sand content (between 77% and 96%), similar to rain garden designs for New Jersey, LAS concentrations rapidly degraded to below detection limits (Kuchler and Schnaak 1997). These results are important as they indicate that surfactants will most likely not accumulate in the rain garden nor will they be taken up by the plants themselves. Because aerobic activity is the primary mechanism for surfactant removal, it is essential for the rain garden to have proper drainage. Biodegradation of LAS under anaerobic conditions has not been demonstrated (Jensen 1999). Long term monitoring of the mesocosms, as well as monitoring of the rain garden installed as part of the high school car wash, will be necessary to confirm that surfactants do not accumulate in the rain garden over time.

Table 3. Summary of influent and effluent mean pollutant concentrations. ( $n=5$ ) (The  $\pm$  indicates standard deviation.)

Parameter	Influent (mg/L)	Effluent (mg/L)	Percent Reduction	$p$ -Value
Control Mesocosm				
TP	0.03 $\pm 0.00$	0.45 $\pm 0.24$	-1,706%	$p < 0.01$
TSS	2.40 $\pm 0.89$	9.20 $\pm 10.18$	-283%	$ns$
Surfactants	0.15 $\pm 0.10$	0.21 $\pm 0.09$	-38%	$ns$
Mesocosm 1				
TP	0.12 $\pm 0.11$	0.70 $\pm 0.43$	-463%	$p < 0.05$
TSS	81.60 $\pm 49.80$	7.20 $\pm 3.70$	91%	$p < 0.05$
Surfactants	10.56 $\pm 2.99$	0.37 $\pm 0.07$	97%	$p < 0.01$
Mesocosm 2				
TP	0.12 $\pm 0.11$	0.93 $\pm 0.47$	-647%	$p < 0.01$
TSS	81.60 $\pm 49.80$	14.40 $\pm 5.18$	82%	$p < 0.05$
Surfactants	10.56 $\pm 2.99$	0.48 $\pm 0.16$	96%	$p < 0.01$
Mesocosm 3				
TP	0.12 $\pm 0.11$	0.47 $\pm 0.42$	-277%	$ns$
TSS	81.60 $\pm 49.80$	14.20 $\pm 13.08$	83%	$p < 0.05$
Surfactants	10.56 $\pm 2.99$	0.77 $\pm 0.40$	93%	$p < 0.01$

Note:  $ns$ = not significant

### Conclusions/Summary/Recommendations:

This preliminary investigation demonstrates that rain gardens have the potential to effectively reduce some pollutants associated with car wash runoff, although the researchers acknowledge the small sample size ( $n=5$ ) on which the results are based. Surfactant concentrations were reduced by over 93%, although these removals were not enough to reduce concentrations below aquatic toxicity ranges. TSS was reduced by over 80% while TP concentrations were higher in the effluent than influent indicating that the organic medium might initially leach nutrients. Based on loading estimates, this study corresponds with prior research indicating that car wash runoff contributes significant quantities of pollutants, specifically TSS and surfactants, to receiving water bodies (Smith and Shilley 2009).

In addition to providing stormwater and water quality benefits, rain gardens are often installed on school grounds in order to engage students in hands-on activities and provide watershed and nonpoint source pollution education. Considering the popularity of car wash fundraisers for student activity clubs, an enormous potential exists to marry these two activities and utilize rain gardens to help reduce the negative impacts of car wash runoff contaminants. Car wash events could become an education and outreach opportunity not just for students, but also for parents who help organize these activities and drivers who have their cars washed. Often car wash events happen in the same location. Thus, when planning rain garden installations, effort should be made to place the rain garden where it can effectively capture and treat car wash runoff.

### **References:**

- American Public Health Association (APHA). 1998. *Standard Methods of Water and Wastewater. 20th ed.* L.S. Clesceri, A.E. Greenberg and A.D. Eaton, eds., Washington D.C.
- Bakacs, M.E. and S.E. Yergeau. 2011. Car Wash Runoff Sampling. Unpublished raw data.
- Bjerregaard, H., S. Stærmose, and J. Vang. 2001. Effect of Linear Alkylbenzene Sulfonate (LAS) on Ion Transport and Intracellular Calcium in Kidney Distal Epithelial Cells (A6). *Toxicology in Vitro.* 15:531-537.
- Davis, A.P., W.F. Hunt, R.G. Traver, and M. Clar. 2009. Bioretention Technology: Overview of Current Practices and Future Needs. *Journal of Environmental Engineering.* 135(3):109-117.
- Faulwetter, J.L., V. Gagnon, C. Sundberg, F. Chazarenc, M.D. Burr, J. Brisson, A.K. Camper and O.R. Stein. 2009. Microbial Processes Influencing Performance of Treatment Wetlands: A Review. *Ecological Engineering.* 35:987-1004.
- Hatt, B.E., T.D. Fletcher, and A. Deletic. 2009. Hydrological and Pollutant Removal Performance of Stormwater Biofiltration Systems at the Field Scale. *Journal of Hydrology.* 365:310-321.
- Holt, M.S., E. Matthijs, and J. Waters. 1989. The Concentrations and Fate of Linear Alkylbenzene Sulphonate in Sludge Amended Soils. *Water Research.* 23(6):749-759.
- Holt, M.S. and S.L. Bernstein. 1992. Linear Alkylbenzene in Sewage Sludges and Sludge Amended Soils. *Water Research.* 26(5):613-624.
- Jensen, J. 1999. Fate and Effects of Linear Alkylbenzene Sulphonates (LAS) in the Terrestrial Environment. *The Science of the Total Environment.* 226:93-111

- Kirschbaum, P. and M. Fohn. 2009. *Runoff from Fundraiser Car Washing: A Situational Analysis*. Kitsap County Public Works Surface and Stormwater Management Program. Port Orchard, WA.
- Kuchler, T., and W. Schnaak. 1997. Behavior of Linear Alkylbenzene Sulphonates (LAS) in Sandy Soils with Low Amounts of Organic Matter. *Chemosphere*. 35:153-167.
- Lewis, M.A. 1991. Chronic and Sublethal Toxicities of Surfactants to Aquatic Animals: A Review and Risk Assessment. *Water Research*. 25(1):101-113.
- Mungray, A.K., and P. Kumar. 2009. Fate of Linear Alkylbenzene Sulfonates in the Environment: A Review. *International Biodeterioration & Biodegradation*. 63(8):981-987.
- New Jersey Department of Environmental Protection (NJDEP). 2004. Chapter 9.5: Standard for Infiltration Basins. *New Jersey Stormwater Best Management Practices Manual*. Division of Watershed Management, Trenton, NJ.
- NJDEP. 2009. Chapter 9.1: Bioretention Systems. *New Jersey Stormwater Best Management Practices Manual*. Division of Watershed Management, Trenton, NJ.
- NJDEP. 2011. *Surface Water Quality Standards, N.J.A.C. 7:9B*. Division of Water Monitoring and Standards. Trenton, NJ.
- Obropta, C.C., M.F. DiNardo, and G.M. Rusciano. 2008. The Demonstration Rain Garden. *Journal of Extension*. 46(2):2TOT3.
- Smith, D. and H. Shilley. 2009. *Residential Car Washwater Monitoring Study*. City of Federal Way Public Works, Surface Water Management. Federal Way, WA.
- United States Environmental Protection Agency (USEPA). 2012. Phosphorus, All Forms, Colorimetric, Ascorbic Acid, Two Reagent. *Approved General-Purpose Methods*. [http://water.epa.gov/scitech/methods/cwa/methods\\_index.cfm](http://water.epa.gov/scitech/methods/cwa/methods_index.cfm) (Feb. 11, 2013).
- Venhuis, S.H., and S.H. Mehrvar. 2004. Health Effects, Environmental Impacts, and Photochemical Degradation of Selected Surfactants in Water. *International Journal of Photoenergy*. 6(3):115-125.
- Ying, G.G. 2006. Fate, Behavior and Effects of Surfactants and Their Degradation Products in the Environment. *Environment International*. 32(3):417-431.

# Application of Graphene-based Sorbents for Arsenic and Lead Removal from Drinking Water Resources

## Basic Information

<b>Title:</b>	Application of Graphene-based Sorbents for Arsenic and Lead Removal from Drinking Water Resources
<b>Project Number:</b>	2012NJ307B
<b>Start Date:</b>	3/1/2012
<b>End Date:</b>	7/31/2013
<b>Funding Source:</b>	104B
<b>Congressional District:</b>	NJ-008
<b>Research Category:</b>	Water Quality
<b>Focus Category:</b>	Toxic Substances, Treatment, Water Quality
<b>Descriptors:</b>	
<b>Principal Investigators:</b>	Shifeng Hou, Huan Feng

## Publications

There are no publications.

## **Project Summary:**

### **Problem and Research Objectives**

This project utilizes graphene as an environment treatment agent to develop chemically modified graphene with high capacity and activity as sorbents for removal of heavy metals.

The proposed approaches are to fabricate and synthesize graphene with special functional chelating groups.

The goal of this project is to make graphene into high capacity, wide-spectra, re-useable, and lower cost sorbents that are a new generation of graphene-based nanoparticle sorbents.

The objectives of this research include:

- 1) Designing surface groups of graphene oxide with chemical modification techniques;
- 2) Utilizing surface groups as chelating groups to remove heavy pollutants;
- 3) Utilizing hydrophobic domains of graphene for organic pollutant removal;
- 4) Optimizing various operating conditions to control the adsorption capacity and activity;
- 5) Synthesizing magnetic nanoparticles on graphene surface for actual environmental application;
- 6) Investigating the complexing mechanism and adsorption kinetics between the functional groups on the graphene surface and heavy metal cations and organic pollutants using synchrotron X-ray and synchrotron infrared spectroscopy techniques.

### **Methodology**

#### **The method includes**

##### **(1) New derivatives of GO:**

- ❖ Introduce functional groups onto the GO surfaces for arsenic removal.
- ❖  $-\text{PO}_3^-$ ,  $-\text{SO}_3^-$ ,  $-\text{NH}_2$  and  $-\text{SH}$  are linked to GO surface through covalent reaction.
- ❖ Silanization is applied to introduce various functional groups onto GO surfaces.
- ❖ N-(Trimethoxysilylpropyl)-ethylenediamine, triacetic acid (EDTA-silane) and 3-Tri-methoxysilyl-propyl-diethylenetriamine (Amine-silane) are used first, and 3-trihydroxysilyl 1-propanesulfonic acid and 3-trihydroxysilyl 1-propylmethylphosphonate are synthesized and these materials are investigated now.

##### **(2) Analytical methods:**

Analytical tools such as FTIR, UV-vis, XRD, TEM, SEM and AFM will be utilized to monitor the synthetic process and to characterize as-obtained compounds. The test of zeta potential and elements analysis will be used to analyze the density of surface functional groups and thus evaluate its adsorption properties.

##### **(3) Determine the physicochemical properties of the GO and FGO:**

Zeta potential, the point of zero charge (PZC), and the concentration of acidic and basic sites on sorbent surface will be tested and evaluated.

##### **(4) The adsorption mechanism**

##### **(5) Sorption Kinetics**

- (6) The effects of pH, the ionic strength, and the temperature on the adsorption properties  
 (7) Desorption Properties

### Principal Findings and Significance

Our initial research approaches include (1) designing the GO surface with specific functional groups, and (2) investigating the adsorption mechanism and kinetics for As, Ni(II), Cu(II) and Pb removal. We investigated the chemical and physical characteristics of functionalized GO; the interaction between toxic metals and the functional groups on GO and the effect of the GO structure on the adsorption capacities; and the adsorption kinetics and mechanism, and the renewable properties of GO-based sorbents.

The achievements thus far are listed below.

We synthesized new materials and investigated their potential application for Ni(II) and Cu(II) removal.

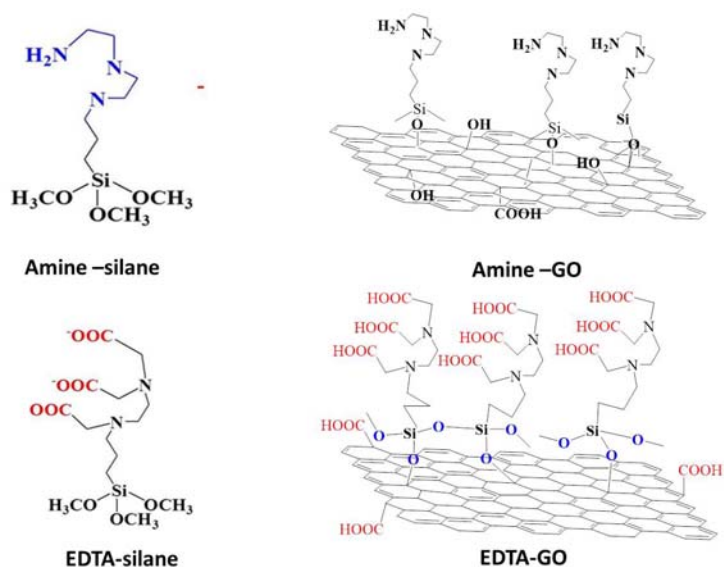


Figure 1. The chemical structure of Amine-GO and EDTA-GO.

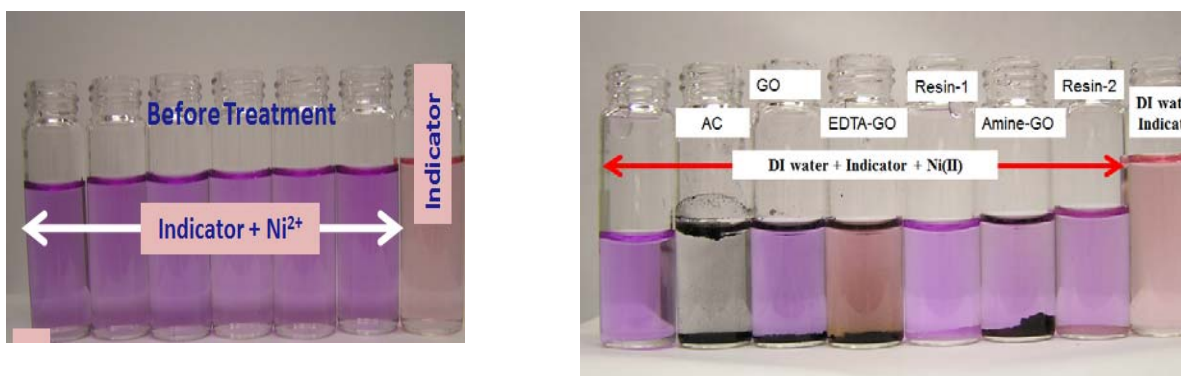


Figure 2. Various sorbent treated Ni (II) solutions.

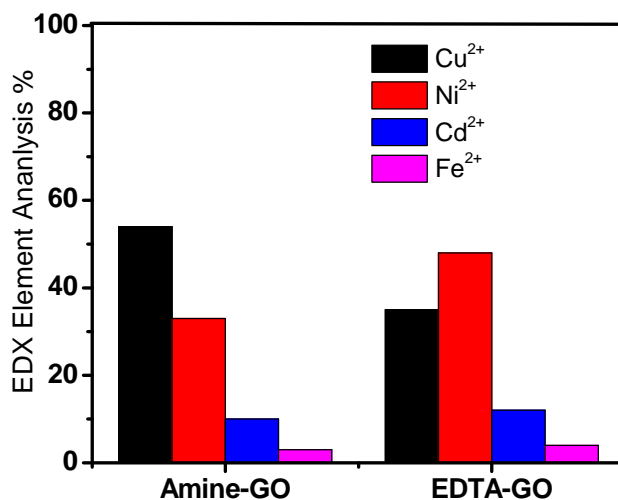
The adsorption behavior of Ni (II) on EDTA-GO fits the Langmuir equation well. The maximum adsorption capacities of EDTA-GO and amine-GO for Ni (II) are 103 mg/g and 86 mg/g, respectively, which are higher than that of GO, AC and other commercial products. The adsorption capacity varies with the pH value of the solution and these sorbents can be reused after washing with HCl. The simulation sample tests for Ni (II) removal demonstrate that at the same concentration level, 48% removed metals are Ni (II) at EDTA-GO. This research demonstrates that EDTA-GO can be a very effective sorbent for heavy metal removal and can be used to design some commercial products.

❖ It was found when four metal ions were co-existed at the same concentration, the percentage of Ni (II) on EDTA-GO surface (48%) was higher than all of the other three ions, which proved that EDTA-GO was a good sorbent for Ni (II) removal in a mixture solution.

❖ The percentage of Cu (II) on Amine-GO surface (52%) was higher than all other three ions, predicting that Amine-GO could be a good sorbent for Cu (II) removal in mixture solution.

❖ The above results suggested that GO modified with different functional groups could be designed for different heavy metal removal. Therefore, GO sorbent may provide selective separation of different metals from various waste water systems.

❖ The above materials to remove Arsenic are in progress. A final report with complete analysis will be provided in the near future.



❖

Figure 3. The EDXS element analysis of heavy metals on EDTA-GO and Amine-GO surface.

Initial concentrations of Cu<sup>2+</sup>, Ni<sup>2+</sup>, Fe<sup>2+</sup> and Cd<sup>2+</sup> were 50 ppm respectively, sample dose was 20 mg/20 mL, and temperature was 25 °C.

# nHFO-Microalgae and Immobilization for Water Quality Improvement

## Basic Information

<b>Title:</b>	nHFO-Microalgae and Immobilization for Water Quality Improvement
<b>Project Number:</b>	2012NJ308B
<b>Start Date:</b>	3/1/2012
<b>End Date:</b>	2/28/2013
<b>Funding Source:</b>	104B
<b>Congressional District:</b>	NJ-010
<b>Research Category:</b>	Water Quality
<b>Focus Category:</b>	Groundwater, Treatment, Methods
<b>Descriptors:</b>	None
<b>Principal Investigators:</b>	Liping Wei

## Publications

1. Thakkar, Megha; Varunpreet Randhaw and Liping Wei. 2012. Development and Characterization of ferrihydrite-microalgae Composite in Improving Water Quality. Passaic River Institute Symposium V, Montclair State University, Montclair, NJ. (poster presentation)
2. Thakkar, Megha; Varunpreet Randhaw and Liping Wei. 2012. Development and Characterization of ferrihydrite-microalgae Composite in Improving Water Quality. GSA Research Day 2012, New Jersey Institute of Technology, Newark, NJ. (poster presentation)

## Project Summary:

### Problem and Research Objectives

Groundwater arsenic contamination affects more than 30% of community water systems (CWSs) in the Piedmont (e.g. Bergen, Passaic, Essex, Union, Summerset, Mercer) and Outer Coastal Plain (e.g. Cumberland, Salem, Camden, Atlantic, Ocean counties etc.) regions, and 5 – 10% of CWSs in other areas of New Jersey (1, 2). Non-community water systems (NCWS, e.g. private wells, schools, parks) are also affected by groundwater arsenic (1, 2). It is critical to remove arsenic in drinking water, because of substantial health concerns from ingestion (skin, lung, liver, kidney urinary bladder cancers, diabetes, cardiovascular diseases, to name a few)(1). USEPA mandates arsenic below 10 ppb, while NJDEP allows for a maximum contaminant level of 5 ppb for drinking water (since 2006) (1).

The proposed research aims to develop and test a novel hybrid material that integrates nanosized hydrous ferric oxide (nHFO), microalgae and porous immobilization for effective arsenic removal. The proposed material takes advantage of (1) HFO particle's capability to strongly adsorb both As(III) and As(V) over a wide pH range as been demonstrated in granular ferric hydroxide sorbent (GFH), (2) increased surface area with nanosized HFO (nHFO has a reported surface area of up to 600 m<sup>2</sup>/g, twice that of GFH), (3) the potential to stably load nHFO particles on microalgae material, which is renewable and of low or negative carbon footprint, and (4) immobilization of nHFO-microalgae into porous granules is potentially durable without losing affinity to arsenic. Specific hypotheses are: (1) nanosize hydrous ferric oxide (nHFO) can be loaded on microalgae for immobilization into porous granular sorbent, and (2) both the intermediate product of nHFO-microalgae hybrid and the final granular sorbent will have high arsenic adsorption capacity.

### Methodology

**Adsorbents preparation.** Diatom *Phaeodactylum tricornutum* was cultured in the laboratory in synthetic seawater media Aquil (34) to stationary phase. Each 1-L culture of the diatom was flocculated with 0.4 mM FeCl<sub>3</sub>, pH 9 (adjusted with 1M NaOH), and conditioned overnight with shaking (150 rpm, 2280 VWR orbital shaker). The resulting diatom-HFO mixture was separated by gravitational settling and membrane filtration (< 5 psi, 0.2 μm PTFE filter), washed with 500 mL Milli-Q water, and the resulting slurry transferred to 2-mL microcentrifuge tube, moderately thermal treated at 60°C oven for 6 h, then dried overnight under vacuum in a speedvac (Savant AS160). The dried composite, named, CFe, was thus prepared. A diatom cell free adsorbent was prepared in the same way and was named Fe.

A bleached composite, BCFe, was prepared by bleaching CFe with 2 mL 30% H<sub>2</sub>O<sub>2</sub> in beaker for 40 min in fume hood, then dried in 70°C heat block.

Polysulfone was used to immobilize CFe and BCFe. Polysulfone was dissolved in dimethylformide at 100 g/L, then added to CFe or BCFe at 30% (i.e. 300 mg polysulfone per 700 mg CFe or BCFe). The mixture was stirred and beat into a thin paste, then sonicated (Fisher Scientific, Solid State/Ultrasonic FS-28) for 25 min while being further stirred every 10 min. The paste was injected drop-wise into a beaker of Mill-Q water (100 mL). A syringe with a 25 gauge

needle was used for stirring, beating, and injection. Micro-beads of polysulfone-CFe (PCFe) or polysulfone-BCFe (PBCFe) formed immediately as the phase inverted. The beads were left in water overnight for curing. The cured beads were collected into a 0.2  $\mu\text{m}$  membrane filter, and air-dried.

**Adsorption test and modeling.** Arsenate ( $\text{Na}_2\text{AsO}_4$ ) of selected concentrations were prepared in a 100 mL conical flask. Adsorbent (Fe, CFe, BCFe, PCFe, PBCFe) was added (upon suspending in MilliQ water). The mixture was placed on a shaker (New Brunswick Scientific G24 Environmental Shaker Incubator, 250 rpm). At various time intervals aliquots (5 mL) were withdrawn for arsenic quantification.

The adsorption of arsenite ( $\text{Na}_2\text{AsO}_3$ ) of selected concentrations and adsorbents was also tested with the same setting as described for arsenate.

Arsenic remaining in the media was quantified with ICP-MS (Agilent 7500i, Material Characterization Lab at NJIT). The aliquots were filtered through a 0.2  $\mu\text{m}$  syringe filter and stored in acid cleaned centrifuge tubes in the refrigerator until analysis (within 2 weeks). For ICP-MS standardization standards were prepared from multielement solution 2A (10 mg  $\text{L}^{-1}$ , Spex Certiprep), and internal standard mix (Li, Ge, Y, In, Tb, Bi) was added to each sample.

The sorption kinetics was modeled after pseudo-second order equation ( $t/q_t = 1/k_2q_e^2 + t/q_e$ ), where  $t$  is time,  $q_t$  and  $q_e$  are the amount of arsenic sorbed at time  $t$  and at equilibrium, respectively, and  $k_2$  is the rate constant of the second-order equation.  $C_e$  was then calculated from known  $C_0$  (initial concentration of arsenic),  $q_e$ , and amount of adsorbent.

$C_e$ , and  $q_e$  were fit to Langmuir model ( $q_e = q_m K_L C_e / (1 + K_L C_e)$ ) to get maximum monolayer biosorption capacity  $q_m$  and Langmuir constant  $K_L$ , a parameter that relates to sorption affinity.  $C_e$  and  $q_e$  was also fit to Freundlich model ( $q_e = K_f C_e^{1/n}$ ), which gives empirical parameters  $K_f$  on adsorption capacity, and  $1/n$  for sorption intensity, which varies with the adsorbent heterogeneity. D-R model ( $\ln q_e = \ln q_m - \beta \epsilon^2$ ) was also used to obtain the adsorption capacity  $q_m$  (mol/g, then unit convert to g/g) and the mean free energy of sorption (kJ/mol)  $E = (-2\beta)^{-1/2}$  to yield information about the sorption being physical or chemical interactions.

**Characterization of the adsorbents.** Adsorbent CFe, BCFe, PCFe, and PBCFe were characterized using Scanning Electron Microscopy (SEM) and Transmission Electron Microscopy (TEM) fitted with energy dispersive X-ray detector. Hitachi S-3400N variable pressure SEM and Hitachi H-7500 TEM with EDS detector were used. Samples for SEM were coated with carbon using Denton Desk II sputter.

Aqueous samples from the adsorption test were analyzed. The aqueous sample was sonicated for 5 - 10 min, and was repeatedly added on a carbon tape on a stud after drying from each addition until a visible layer of sample was seen. The sample was then coated further with carbon and viewed under a scanning electron microscope (SEM) fitted with energy dispersive X-ray spectrometer (EDS). For TEM, the aqueous sample was sonicated for 5-10 minutes and a few  $\mu\text{l}$

was added to the TEM grid, and viewed upon drying. When a diatom cell alone was viewed, uranium trioxide staining was performed.

Adsorbents were also examined for BET surface area. The amount of nHFOs loading was analyzed based on the acid digestion (10% HCl and 6-8 h equilibration) and ferrozine spectroscopic method (35) using a spectrophotometer (Perkin Elmer Ez301).

## Principal Findings

**Comparing CFe and Fe for arsenate adsorption.** Adsorption of 200 ppb arsenate on Fe and CFe rapidly approached equilibrium (Fig. 1A). The adsorption fit pseudo-second order kinetics,  $\frac{t}{q_t} = \frac{1}{k_2 q_e^2} + \frac{1}{q_e} t$  (Fig. 1B). Adsorption rate constants  $k_2$  were  $1.72 \times 10^{-4}$  and  $4.35 \times 10^{-5} \text{ g } \mu\text{g}^{-1} \text{ min}^{-1}$  for CFe and Fe, respectively. At equilibrium,  $q_e$  was 7,182 and 24,878  $\mu\text{g}$  per g adsorbent, or 122  $\text{mg g}^{-1}$  and 156  $\text{mg g}^{-1}$  when normalized to the amount of iron in the adsorbents, and similar  $C_e$ , for CFe and Fe respectively. Since the arsenate adsorption on CFe resulted in similar  $q_e$  (normalized to iron) and  $C_e$  as that for Fe, arsenate adsorption on CFe may be driven primarily by the iron oxyhydroxide within. Further, since CFe had 4-fold faster adsorption kinetics than Fe, it suggests dispersing iron oxyhydroxide on algal cell materials enhances adsorption kinetics.

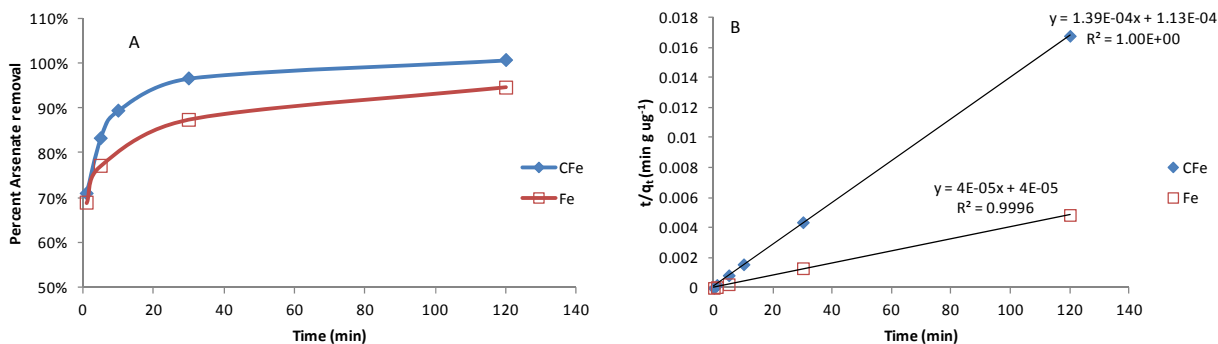


Figure 1. Adsorption kinetics of CFe and Fe.  $C_{0-As(V)} = 200$  ppb, volume  $V = 50$  mL, room temperature, amount of adsorbent used were 1409  $\mu\text{g}$  CFe and 383  $\mu\text{g}$  Fe, containing total 83  $\mu\text{g}$  iron (5.89%) and 61  $\mu\text{g}$  iron (15.93%), respectively.

**Comparing CFe and PCFe for arsenate adsorption.** Adsorption of 340 ppb arsenate on CFe and PCFe were compared. The amount of adsorbent addition was 15  $\text{mg L}^{-1}$  for CFe and 200  $\text{mg L}^{-1}$  for PCFe; the latter was equivalent to 136  $\text{mg CFe L}^{-1}$ , nearly 10 times of that in CFe. Arsenate adsorption quickly reached equilibrium with CFe and PCFe (Fig. 2 AB). On the basis of CFe, the adsorption rate constants  $k_2$  were  $1 \times 10^{-5}$  and  $4.6 \times 10^{-4} \text{ g } \mu\text{g}^{-1} \text{ min}^{-1}$ ,  $q_e$  were 18,907 and 2,348  $\mu\text{g}$

$g^{-1}$ , and  $C_e$  were 70 and 17 ppb for CFe and PCFe, respectively. Thus PCFe had more rapid adsorption kinetics and lower  $C_e$ ; this is likely because of 10-fold higher adsorbent in PCFe than CFe. Additional tests are needed to have similar CFe levels in the PCFe-arsenate and CFe-arsenate adsorption reactions to compare the adsorbent properties.

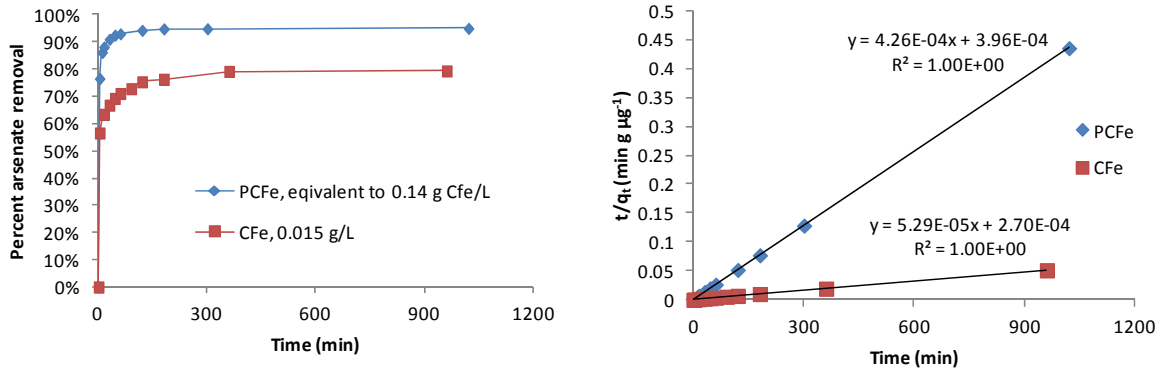


Figure 2. Arsenate adsorption kinetics of CFe and PCFe.  $C_{0-As(V)} = 340$  ppb, volume  $V = 100$  mL,  $20^\circ C$ , 150 rpm shaker. Adsorbent addition were 0.015 and 0.20  $g L^{-1}$  CFe and PCFe, respectively. The latter is equivalent to 0.14  $g CFe/L$ .

**Arsenate and arsenite adsorption on CFe.** The present removal of 68 – 342 ppb arsenate by a CFe addition of  $0.015 g L^{-1}$  was shown in Figure 2 A. The adsorption reached equilibrium quickly (Fig. 3A), and the adsorption fit pseudo-second order kinetics well (Fig. 3B), which revealed adsorption rate constants ranging from  $1.04 \times 10^{-5}$  to  $2.51 \times 10^{-4} g \mu g^{-1} min^{-1}$ , decreasing with increasing initial arsenate concentration. The kinetics also predicted a series of equilibrium adsorption  $q_e$  and  $C_e$ .  $q_e$  and  $C_e$  fit well with equilibrium models Langmuir  $q_e = \frac{q_m K_L C_e}{1 + K_L C_e}$  (Fig.

3C) to derive adsorption capacity  $q_m$  and adsorption affinity  $K_L$ , and Freundlich  $q_e = K_f C_e^{1/n}$  (Fig. 3D) for  $K_f$  and  $n$ , parameters related to adsorption capacity and adsorption intensity/heterogeneity of adsorption, respectively. Results show that the CFe adsorbent had maximum arsenate adsorption capacity of  $20.6 mg As(V) g^{-1}$  and affinity of  $0.096 g \mu g^{-1}$ , and the  $K_f$  and  $n$  were  $3.9 mg g^{-1}$  and 2.64 respectively (Fig. 3 C, D) The experimental data also fit well with D-R isotherm equation,  $\ln q_e = \ln q_m - \beta \varepsilon^2$  (Fig. 3E), where  $q_e$  ( $mol g^{-1}$ ) is equilibrium adsorption,  $q_m$  is adsorption capacity,  $\beta$  is activity coefficient related to the mean free energy of sorption, and  $\varepsilon = RT \ln(1 + 1/C_e)$  is Polanyi potential, [ $R = 8.314 J k^{-1} mol^{-1}$ ,  $T = 293k$ , and  $C_e$  is equilibrium concentration ( $mol L^{-1}$ )]. The  $q_m$  was found to be  $2.6 \times 10^{-3} mol g^{-1}$ , and mean free

energy,  $E = 1/\sqrt{-2\beta} = 15.7 \text{ KJ mol}^{-1}$ , indicating chemical adsorption process, potentially viacomplexation with iron oxyhydroxide.

The adsorption of arsenite, 63 – 283 ppb, by  $0.015 \text{ g L}^{-1}$  CFe addition was shown in Figure 3. The adsorption was slower to reach equilibrium as compared to arsenate (Fig. 4A). The predicted second order rate constant was nearly one order of magnitude lower than those on arsenate, i.e.  $1.85 \times 10^{-6} - 1.14 \times 10^{-5} \text{ g } \mu\text{g}^{-1} \text{ min}^{-1}$ , and decreased with increase initial arsenite concentration (Fig. 4B). The equilibrium adsorption  $q_e$  and concentration  $C_e$  fit well to Langmuir (Fig. 4C), Freundlich (Fig. 4D) and R-D (Fig. 4E) models. These equilibrium models revealed CFe had lower Langmuir adsorption capacity of  $q_{m-\text{As(III)}} = 6.3 \text{ mg As(III) g}^{-1}$ , and affinity  $K_{L-\text{As(III)}} = 0.014 \text{ g } \mu\text{g}^{-1}$ , as compared to the adsorption of arsenate (Fig. 4C).  $K_f-\text{As(III)}$  and  $n_{\text{As(III)}}$  were  $0.44 \text{ mg g}^{-1}$  and 2.25, respectively (Fig. 4D). The R-D model predicted an adsorption capacity of  $0.9 \times 10^{-3} \text{ mol g}^{-1}$ , nearly 3 times less than arsenate, and a free energy of  $13.5 \text{ KJ mol}^{-1}$ , weaker than arsenate, though indicative of chemical adsorption process dominating.

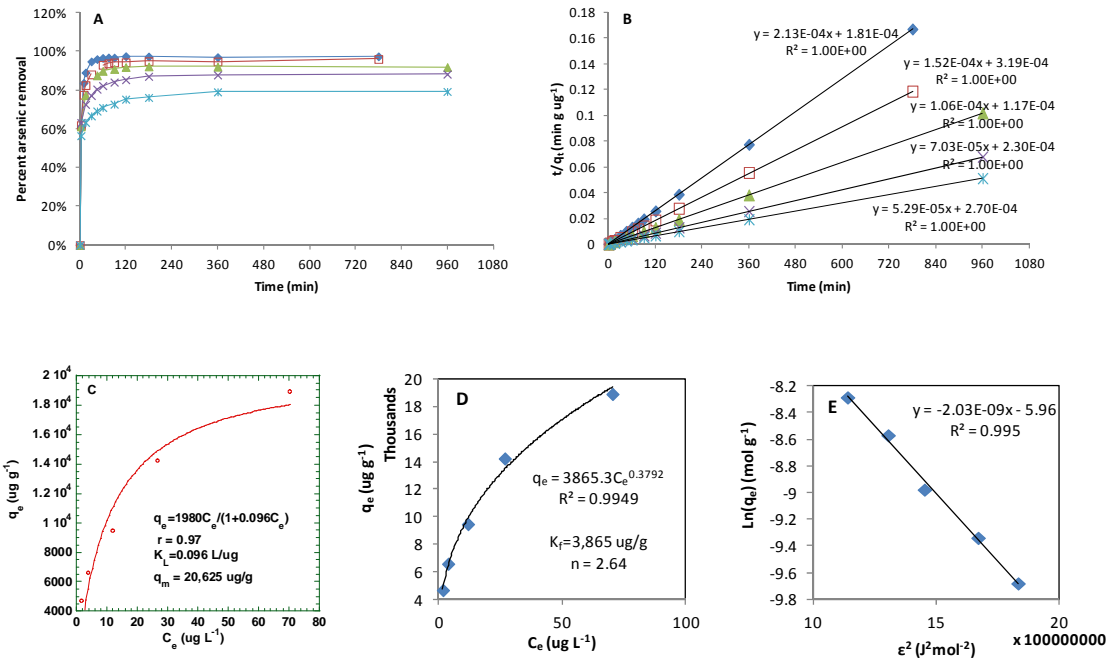
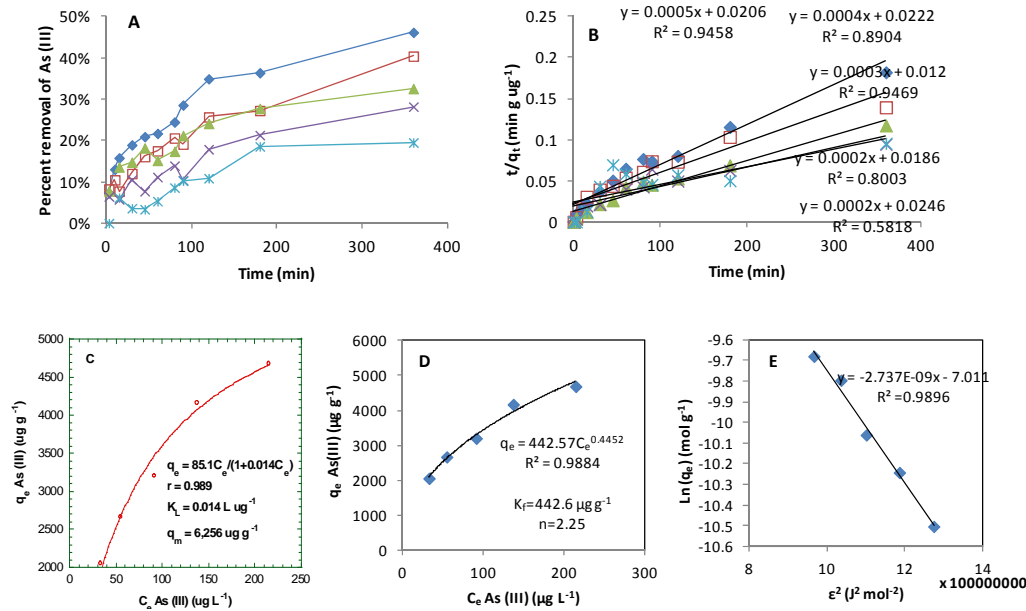
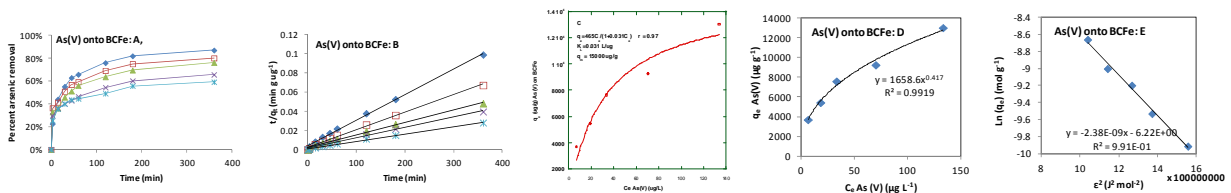


Figure 3. Additional adsorption kinetics (A, B) of arsenate (**As(V)**) on **CFe**.  $C_{0-\text{As(V)}} = 68$  ( $\blacklozenge$ ), 101( $\square$ ), 151( $\blacktriangle$ ), 228 ( $\times$ ), 342 ( $*$ ) ppb.  $V = 100 \text{ mL}$ , 150 rpm shaker,  $20^\circ\text{C}$ , adsorbent CFe addition at  $0.015 \text{ g L}^{-1}$ , equivalent to  $0.013 \text{ g L}^{-1}$  iron (8.58%). The adsorption equilibrium fit with the Langmuir model (C), and Freundlich model (D), and D-R model (E).



**Figure 4.** Adsorption kinetics (A, B) of arsenite (As(III)) on **CFe**.  $C_{0-As(V)} = 63$  (♦), 91(□), 138(▲), 198 (×), 283 (\*) ppb.  $V = 100$  mL, 150 rpm shaker,  $20^{\circ}\text{C}$ , adsorbent CFe addition at  $0.015$  g  $\text{L}^{-1}$ , equivalent to  $0.013$  g  $\text{L}^{-1}$  iron (8.58%). The adsorption equilibrium fit with the Langmuir model (C), and Freundlich model (D), and D-R model (E).

**Arsenate and arsenite adsorption on BCFe, as compared with CFe.** Since CFe potentially releases organic matter from the algae material, the BCFe was made by bleaching CFe with hydrogen peroxide. The experimental process that was used for adsorption kinetics and equilibrium of BCFe was also used for CFe for arsenate and arsenite removal (Fig. 5 and 6). A comparison on adsorption equilibrium was shown in Table 1. The comparison suggests that BCFe had slightly higher uniformity than CFe (from  $n$  value of the Freundlich model). For As(V) adsorption, CFe had higher adsorption capacity but lower affinity than BCFe, while the free energy term in the D-R model suggests stronger chemical interaction between CFe-As(V) than BCFe-As(V). Thus bleaching may not facilitate As(V) adsorption. For As(III), BCFe had greater adsorption capacity than CFe, and adsorption affinity and free energy were similar between CFe and BCFe. Thus the bleaching of the adsorbent does not affect As(III) adsorption.



**Figure 5.** Adsorption of arsenate (As(V),  $C_0 = 64 - 334$  ppb) on BCFe (0.0154 g/L). A: percent arsenate removal over time. B: second order adsorption kinetics. C: Langmuir model fit. D: Freundlich model fit. E: D-R model fit.

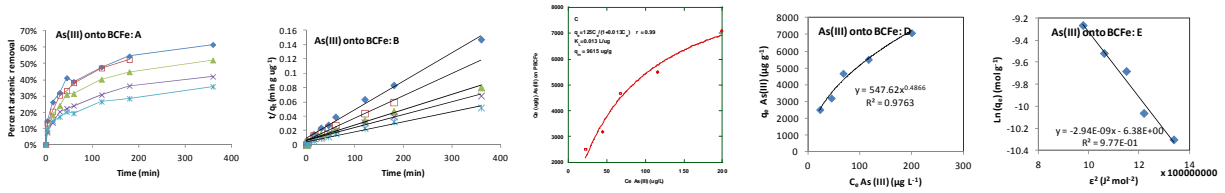


**Figure 6.** Adsorption of arsenite (**As (III)**,  $C_0 = 61 - 299$  ppb) on **BCFe** (0.0154 g/L). A: percent arsenite removal over time. B: second order adsorption kinetics. C: Langmuir model fit. D: Freundlich model fit. E: D-R model fit.

**Table 1.** Comparison on the adsorption of arsenate and arsenite on CFe and BCFE.

	Langmuir model		Freundlich model		D-R model	
	$q_m$ ( $\mu\text{g/g}$ )	$K_L$ (L/ $\mu\text{g}$ )	$n$	$K_f$	$q_m$ (g/g)	$E$ (kJ/mol)
As(V)-CFe	20625	0.096	2.64	3865	0.193	15.7
As(V)-BCFe	15000	0.031	2.40	1659	0.150	14.5
As(III)-CFe	6256	0.014	2.25	443	0.068	13.5
As(III)-BCFe	9615	0.013	2.06	548	0.127	13.0

**Characterization of the adsorbent materials.** When iron loading was low (10-times less than the target addition), a light microscope can clearly identify the cells and iron aggregation (Fig. 7; The adsorbent were made from diatom cells and 10-fold higher iron chloride addition than used in Fig. 7). The visual images of the adsorbent Fe, CFe and granular PCFe are shown in Figure 7 B and C.

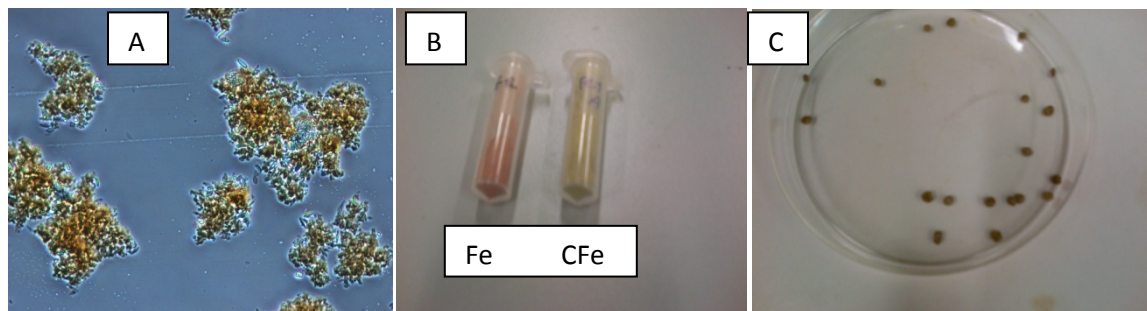


Figure 7. A: Light microscopic image on the precipitation of diatom cells by 10-time less iron chloride addition than the target iron loading. B: adsorbent Fe and CFe. C: granular PCFe in a petri dish.

TEM and SEM images of the adsorbent are shown in Figure 8. On TEM, the diatom cells appeared pale, and were of a few microns size (Fig. 8A). CFe appeared darker where iron content was higher (Fig. 8B). On CFe the micron-sized aggregation of HFO was based on cells (arrows), but also extended beyond the cell's boundary (Fig. 8B). The distribution of HFO on the cell surface may not be even (Fig. 8C). When polysulfone immobilization was applied, the nanosized HFO (nHFO) were immobilized on porous polysulfone (Fig. 8D-E for PFe and Fig. 8F for PCFe, algal cells were not readily identified on PCFe). Upon bleaching, the product BCFE did not look very different from CFe in TEM, except that BCFE may be a little more porous (Fig. 8G). The SEM images (Fig. 8 H -I) showed that the polysulfone made the adsorbent surface more smooth as compared to the raw adsorbent CFe (image not shown) or BCFE.

SEM-EDS analysis suggests that iron distribution on BCFE matched better with the distribution of Mg than Si (Fig. 9). After arsenic adsorption on PCFe, the distribution of As was not in perfect proportion to iron distribution (Fig. 10); the EDS data showed that atomic ratio of iron and arsenic on PCFe was about 110: 1.4. The EDS images also show that HFO was successfully loaded on CFe and PCFe and arsenic adsorption did take place.

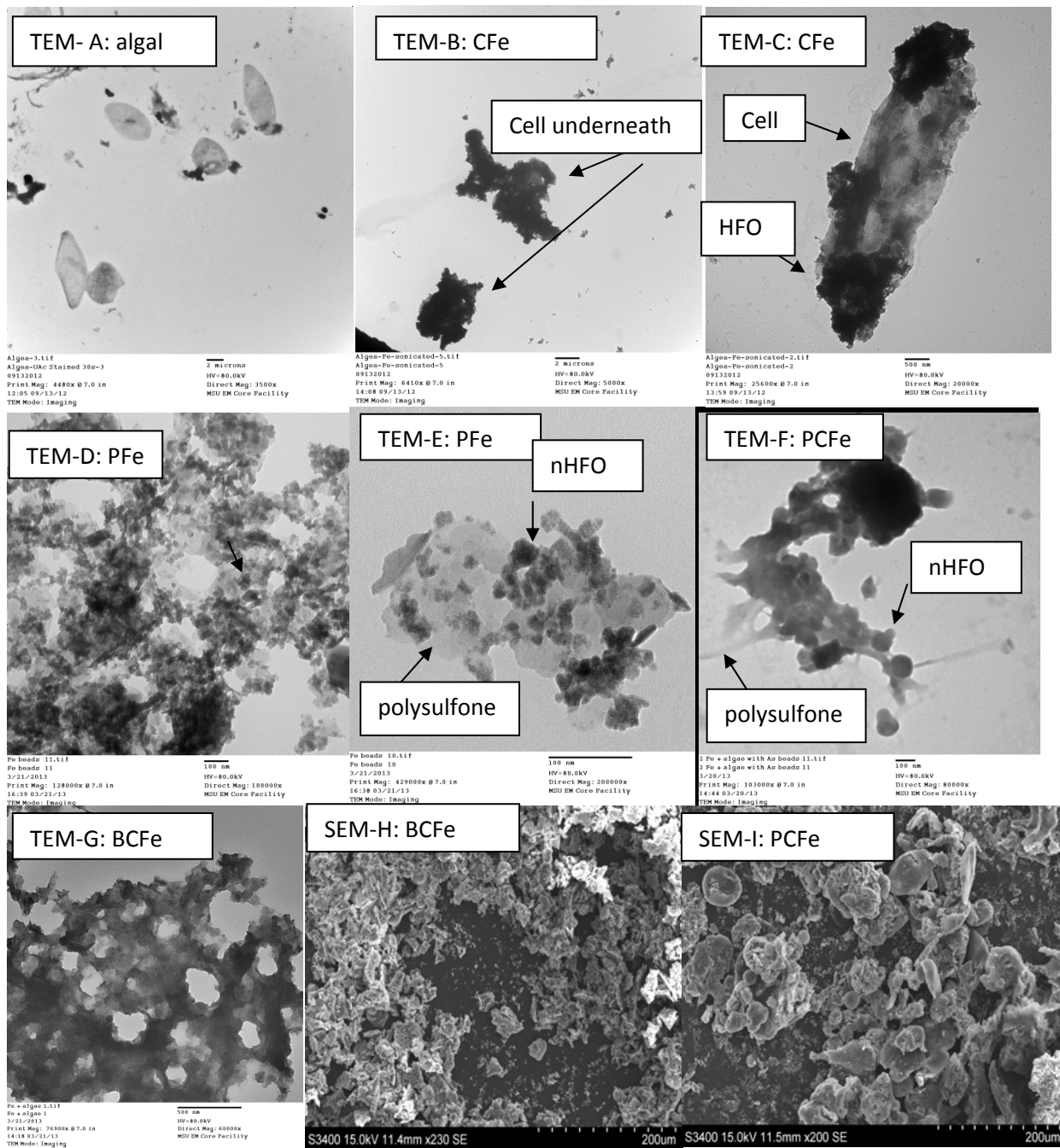


Figure. 8 TEM images of the diatom cell (A), CFe (B-C), PFe (D-E), PCFe (F) and BCFe (G), and SEM images for BCFe (H) and PCFe (I).

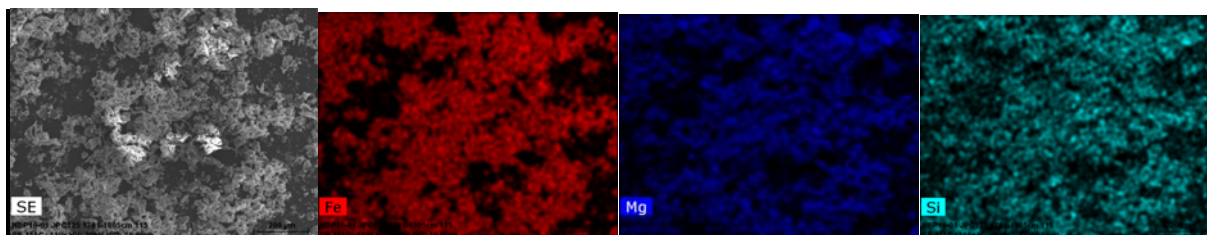


Figure 9. SEM-EDS images for CFe on Fe, Mg and Si distribution.

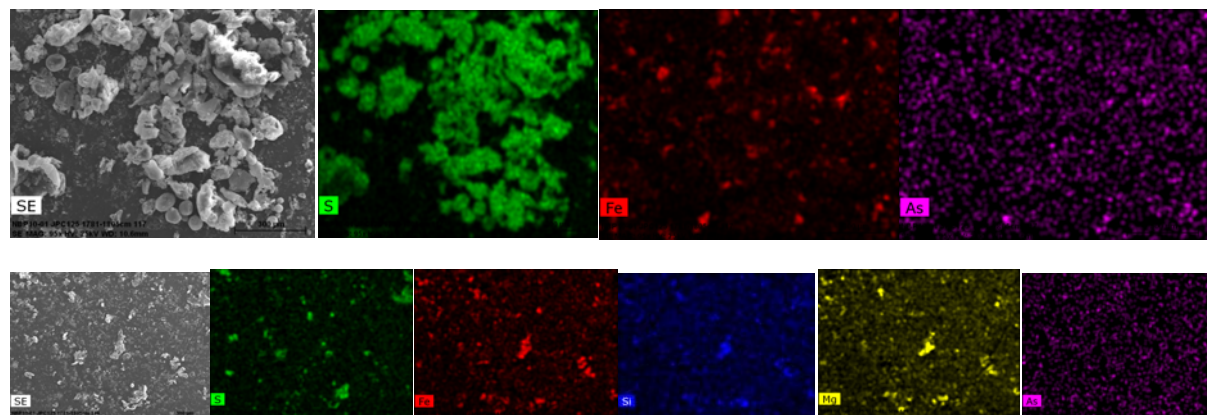


Figure 10. SEM-EDS images for PCFe after arsenate adsorption on the distribution of Fe, S and S (from polysulfone).

***Additional tests planned.*** Only preliminary adsorption tests were conducted on PBCFe. BET surface area quantification has not been completed, but will be in the future. Additional tests are needed to obtain a complete description of As(V) and As(III) adsorption behavior on PCFe and PBCFe. In addition, we need to test the effect of varying cell:iron ratio on As adsorption, and to understand mechanisms of As adsorption on polysulfone immobilized adsorbent by linking the information from images with the adsorption behavior.

## References

1. Mohan, D. and C.U. Pittman Jr, *Arsenic removal from water/wastewater using adsorbents—A critical review*. Journal of Hazardous Materials, 2007. **142**(1–2): p. 1-53.
2. NJDEP, *A homeowner's guide to arsenic in drinking water*. New Jersey Department of Environmental Protection, 2010. Office of Science (<http://www.state.nj.us/dep/dsr/arsenic/guide.htm>).
3. Mondal, P., C.B. Majumder, and B. Mohanty, *Effects of adsorbent dose, its particle size and initial arsenic concentration on the removal of arsenic, iron and manganese from simulated ground water by Fe<sup>3+</sup> impregnated activated carbon*. Journal of Hazardous Materials, 2008. **150**(3): p. 695-702.
4. Giles, D.E., et al., *Iron and aluminium based adsorption strategies for removing arsenic from water*. Journal of Environmental Management, 2011. **92**(12): p. 3011-3022.
5. NJDEP, *A homeowner's guide to arsenic in drinking water*. New Jersey Department of Environmental Protection Office of Science(<http://www.state.nj.us/dep/dsr/arsenic/guide.htm>). 2010.
6. NJDEP, *Evaluation and assessment of arsenic removal technologies for New Jersey drinking water*. New Jersey Department of Environmental Protection Malcolm Pirnie:1-93. 2003.
7. Sarı, A., Ö.D. Uluozlü, and M. Tüzen, *Equilibrium, thermodynamic and kinetic investigations on biosorption of arsenic from aqueous solution by algae (Maugeotia genuflexa) biomass*. Chemical Engineering Journal, 2011. **167**(1): p. 155-161.
8. Jang, M., et al., *Removal of Arsenite and Arsenate Using Hydrous Ferric Oxide Incorporated into Naturally Occurring Porous Diatomite*. Environmental Science & Technology, 2006. **40**(5): p. 1636-1643.

# Predicting the matric potential of unsaturated porous media using nuclear magnetic resonance

## Basic Information

<b>Title:</b>	Predicting the matric potential of unsaturated porous media using nuclear magnetic resonance
<b>Project Number:</b>	2012NJ309B
<b>Start Date:</b>	3/1/2012
<b>End Date:</b>	5/31/2013
<b>Funding Source:</b>	104B
<b>Congressional District:</b>	NJ-010
<b>Research Category:</b>	Ground-water Flow and Transport
<b>Focus Category:</b>	Groundwater, Hydrology, Methods
<b>Descriptors:</b>	
<b>Principal Investigators:</b>	Sam Falzone, Kristina Keating

## Publication

1. Falzone, S. and Kristina Keating. 2012. Laboratory measurements to explore the link between surface area, surface relaxivity, and NMR relaxation time in partially water saturation porous media. SEG-AGU Hydrogeophysics Workshop, Boise, ID. (poster presentation)

## (1) Project Summary:

### Problem and Research Objective

NMR is a unique geophysical method because it can directly detect water present within a sample volume (Dunn et al., 2002). NMR relaxation time, or the time by which the measured signal decays, is influenced by the distribution of water within the pore structure of soils, allowing the surface-area-to-volume ratio,  $S/V$ , of the sample to be determined in saturated samples (Brownstein and Tarr, 1979). Relaxation time is also affected by the paramagnetic content (i.e. iron (III)) of a sample, which directly effects the surface relaxivity,  $\rho_2$ , or the ability of the solid surface to enhance relaxation (Brownstein and Tarr, 1979). NMR measurements can be collected in the field, from the Earth's surface using surface NMR (SNMR) or in a borehole using logging instruments, and in the laboratory. Of interest in this research is developing NMR measurements that can be collected in the field using SNMR or in the laboratory to estimate the matric potential,  $\phi_{Matric}$ . The research outlined in this proposal is designed to test the following hypothesis: *NMR relaxation times can be used to determine matric potential.*

Two laboratory experiments and a field study have been designed to test the hypothesis. The first laboratory experiment will explore the effects of  $S/V$  and  $\rho_2$  on the relationship between saturation and NMR relaxation time. The second laboratory experiment is designed to develop an empirical relationship between NMR relaxation time,  $\phi_{Matric}$  and saturation. In the field study, SNMR measurements will be made during an infiltration experiment and used to determine changes in saturation and  $\phi_{Matric}$  over time. The results of this study will form a basis for developing methods for determining  $\phi_{Matric}$  on a field scale using SNMR. Ultimately, the conclusions reached in this study will provide the scientists with a better way of determining  $\phi_{Matric}$  in the vadose zone, which in turn will allow better monitoring of contaminants.

### Methodology

Nine sands were used to study the relative surface relaxation,  $T_{2S}$ , versus saturation curves of samples varying in both  $\rho_2$  and  $S/V$ .  $S/V$  was calculated from the specific surface area, measured with multi-point nitrogen BET absorption, and the porosity of the samples, determined gravimetrically. The value of  $\rho_2$  were calculated from the  $S/V$  and  $T_{2ML}$  measured from saturated sample using laboratory NMR measurements.

The relative  $T_{2S}$  versus saturation curves were created by measuring the NMR response as deionized water was pumped into each sand.  $T_{2S}$  was calculated by subtracting the inverse bulk relaxation, or the relaxation time of DI water, from the inverse  $T_{2ML}$  for each sand.  $T_{2S}$  and  $A_0$ , which will be used to calculate saturation, were determined from NMR measurements collected every thirty minutes during both imbibition of DI water. The plots of  $T_{2S}$  versus saturation from each sand were compared to evaluate the individual effects of  $S/V$  and  $\rho_2$ .

### **Principle Findings and Significance**

The proposal to NJWRRI outlined three phases for the research covered in this proposal. Of these three phases, the first phase, outlined in the methodology above, has been completed. Several presentations have been given at conferences concerning this research, and a manuscript has been submitted to Vadose Zone Journal presenting the key findings of this experiment. Of the remaining two phases, work is ongoing. All supporting equipment has been purchased and assembled. Data acquisition for the second phase will begin within the next two months. The data for the third phase has been collected, and is currently undergoing analysis. These findings will be prepared for submission to leading journals in the field of Geophysics and Soil Science, and will also be presented at relevant conferences, such as AGU 2013.

# Understanding metabolic flux dynamics during hydrolytic and fermentative digestion of wastewater treatment sludge for enhanced ammonia-nitrogen removal

## Basic Information

<b>Title:</b>	Understanding metabolic flux dynamics during hydrolytic and fermentative digestion of wastewater treatment sludge for enhanced ammonia-nitrogen removal
<b>Project Number:</b>	2012NJ310B
<b>Start Date:</b>	3/1/2012
<b>End Date:</b>	2/28/2013
<b>Funding Source:</b>	104B
<b>Congressional District:</b>	NJ-006
<b>Research Category:</b>	Water Quality
<b>Focus Category:</b>	Nitrate Contamination, Wastewater, Treatment
<b>Descriptors:</b>	None
<b>Principal Investigators:</b>	Amanda Luther, Donna E. Fennell

## Publications

There are no publications.

#### **4. Project summary**

Excess nutrient discharge into surface waters can have detrimental effects on aquatic ecosystems and water quality, and both nitrate and nitrite can be toxic to humans if these species accumulate in our drinking water. Removal of nitrogen and phosphorus during wastewater treatment often results in accumulation of these nutrients in the sludge, which is commonly treated by anaerobic digestion (AD). Through the sludge treatment and processing, these nutrients become re-solubilized and must be recycled through primary or secondary treatment, and can represent a significant additional nutrient load on the overall treatment system. This work is part of a larger project in our lab to develop a novel two-stage anaerobic digestion system for removal and recovery of ammonia from high nitrogen wastes. These studies are focused specifically on the hydrolytic and fermentative stages of anaerobic digestion, with a focus on the effect of free ammonia on these bacterial populations. The first experiment describes nitrogen flow, pH dynamics, and ammonia concentration in a single-stage batch reactor digesting casein as a model protein substrate. The second set of experiments described here focus on describing the physiology of a model protein fermenting hyper ammonia producing bacteria that will be used for a comparative transcriptomics experiment to identify specific genes involved in ammonia stress and tolerance. From this research, we hope to develop a better understanding of the physiological response to ammonia stress, and to develop much needed molecular tools for process control of AD.

##### **4.1 Problem and Research Objectives**

Discharge of nutrients, especially nitrogen (N) and phosphorus (P), into waterways, can cause eutrophication; depleting the waters of oxygen and detrimentally effecting fish and aquatic ecosystems. Ammonia can be directly toxic to these organisms, while nitrite is toxic to humans if it reaches high enough concentration in our drinking water. For these reasons, release of N and P in wastewater effluents is highly regulated, and wastewater treatment facilities must incorporate methods for nutrient removal in their processing systems. Most of the wastewater treatment facilities in New Jersey use an activated sludge secondary treatment process for biological oxygen demand (BOD) removal, followed by an anaerobic digestion process to treat the sludge generated in the primary and secondary treatments. Many facilities also are required to remove nitrogen and phosphorus before they can discharge the treated effluent, and as these standards get more stringent, such as with the recent decrease in P limits in NJ, these requirements can get too costly for the treatment plants to comply. Biological nitrification/denitrification are the most common processes for nitrogen removal, and this requires aeration. Aeration represents the largest cost for these facilities.

As a result of biological accumulation, precipitation, and sorption to settleable solids, N and P accumulate in the sludge and during anaerobic digestion. Through biological activity during treatment, and thickening and dewatering of the sludge following treatment, as much as 80% of these nutrients can be released to the soluble phase (Narayanan, 2006). This filtrate must be recycled to the primary or secondary influent for retreatment, introducing an additional nutrient load to the

system. This is not an insignificant load, and it can represent 20-40% of the plant's total nitrogen load (Stinson, 2006; Locke and Laquidara, 2006). The P load can range from 15-75% returned, depending on treatment methods and process design (Narayanan, 2006). Furthermore, this recycled filtrate has a low BOD: N/P ratio, and places an added carbon demand and alkalinity demand on the system (Stensel, 2006), both of which may prevent complete nitrogen removal in plants which utilize biological nitrogen removal. This excess nutrient loading puts added costs on the treatment facilities, and removal of these nutrients during AD could decrease or eliminate the added load providing much needed cost reductions and even revenues to treatment plants. Ammonia recovered from the system could be catalytically "cracked" to generate hydrogen, which could be used as an on site fuel source. Alternatively, ammonium and phosphorus could be removed by co-precipitation with magnesium in the form of struvite, which can be used as a fertilizer (Tong and Chen, 2009)

This project will examine a two-stage anaerobic system for enhanced ammonia-nitrogen removal, focusing on nitrogen flux and enhancement of ammonia release during hydrolysis and fermentation. Ammonia is known to inhibit methanogenesis at high concentrations (Chen et al., 2008; Babson, 2010), with different microbial populations appearing to have varying degrees of tolerance for ammonia. A series of recent papers from a research group in Japan have successfully demonstrated enhanced biogas production from a two stage AD process with *in situ* ammonia stripping (Abouelenien et al., 2010; Yabu et al., 2011; Nakashimada et al., 2008). Another group has looked at alkaline fermentation of waste activated sludge to enhance fatty acid production through biological processes (Yuan et al., 2006). Both groups have looked at microbial populations through sequencing of clonal libraries, but neither have taken it further by analyzing the overall metabolic pathway network in these two-stage systems. Indeed, there appears to be a lack of this type of analysis on the hydrolytic and fermentative processes in anaerobic digestion in general. A number of these studies have been performed in analysis of microbial gut communities, and photosynthetic systems for biofuel production. This type of analysis is necessary in order to develop better mechanisms for process control in anaerobic systems.

## 4.2 Methodology

*Task 1: determine flux of nitrogen, carbon under various nitrogen loads in batch and semi continuous cultures and monitor pH*

The first experiment completed towards this goal used 150 ml batch single stage systems to gather initial data on protein fermentation and ammonia release during the early stages of AD under different protein loads using digested sludge from a municipal WW treatment plant as the inoculum. Volatile fatty acids (VFAs) were measured by high performance liquid chromatography (HPLC), total ammonia nitrogen (TAN) by ion chromatography (IC), and pH was monitored using a pH electrode. The fraction of unionized ammonia ( $\text{NH}_3$ ) was calculated based on pH and temperature dependent equilibrium constants. Gas production in the reactors was measured by water displacement, and methane content of this gas was measured by

gas chromatography with a flame ionization detector (GC-FID). These parameters were measured over a three-week time period, where pH, ammonia, and VFA were measured daily. In order to perform a nitrogen balance, total nitrogen was measured at the beginning and end of this experiment by the standard Kjeldahl method.

#### *Task 2: Metabolic pathway analysis and identification of ammonia stress genes*

Work on task 2 has thus far focused on the identification of ammonia stress genes. In order to identify genes that may be involved in responding to ammonia stress we have chosen what we believe to be a good model peptide and amino acid fermenting bacteria. The species chosen is *Peptostreptococcus russellii*. This bacterium was isolated from a swine manure storage pit, an environment having a very high concentration of free ammonia. This species is described as a “hyper ammonia producing” (HAP) bacteria because it has a high rate of ammonia production from amino acid (AA) fermentation as compared to other AA fermenting bacteria. A number of growth experiments were completed in order to determine optimal growth conditions, ammonia tolerance, and ammonia production. Growth curves were generated by measuring optical density of cultures over time. Optical density was compared to direct cell counts to verify that OD would be an appropriate measurement of growth. Cell counts were performed by acridine orange staining and fluorescence microscopy. Ammonia tolerance was determined by comparing growth rates at TAN concentrations ranging from 1 to 14 g N-TAN/L. Further studies are underway to identify the critical level of unionized ammonia that results in a severe decrease in growth rate. Another set of growth experiments will be performed to differentiate between unionized ammonia and TAN toxicity if a difference exists. These experiments are done in preparation for an RNA-sequencing experiment that should be completed this summer. In this experiment *P.russellii* cultures will be grown under ammonia stress and non-stress conditions in order to determine differential gene expression in hopes of identifying ammonia stress related genes.

#### *Task 3: Set up two-stage system running at steady state to perform fundamental analysis of digester operation for both stages*

Work on task 3 has not begun.

### **4.3 Progress Report: Initial findings and significance**

#### *Objective 1: Understanding nitrogen flux and ammonia release during hydrolysis and fermentation*

The experiment performed under task 1 in which mixed batch reactors were run at different protein loadings showed inhibition of methanogenesis at TAN levels above ~3500mg N-TAN/L. Hydrolysis and fermentation of the casein to VFAs and ammonia did not appear to be inhibited based on continued production of ammonia and VFA above 3500mg N-TAN/L (VFA and ammonia are products of amino acid fermentation). A nitrogen balance on the system showed that between ~65-94 % of the nitrogen from the casein substrate was released as ammonia during the two month run (Table 1). These results support the vast amount of studies showing the

negative effect of ammonia on methanogenic activity, but also show that the activities of amino acid fermenting bacteria have a greater tolerance for ammonia. The upper level of tolerance was not reached in this experiment. These results are promising in the context of a two-stage digestion system designed to optimize ammonia release and recovery from nitrogenous wastes such as manures. At least for casein hydrolysis and fermentation, ammonia release is quite efficient with some of the reactors reaching over 90% release of nitrogen. In the highest loaded digesters TAN concentrations exceeded 6000mg N-TAN/L, and the efficiency of ammonia release appeared to slightly decrease with increased nitrogen load.

The results of this experiment suggests that the TAN concentrations are having an effect on fermentative activities, and so it will be important to perform further studies at higher nitrogen loads or at high TAN concentrations to determine the full pattern of this effect and the critical TAN concentrations that will inhibit growth of these populations.

Sample	%N-TAN released from Substrate	Standard Deviation
Sludge Only Control	0	n/a
10g/L Casein Bicarbonate Buffer	86.98	±8.43
10g/L Casein	88.13	±5.69
40g/L Casein	71.52	±5.84
60g/L Casein	78.35	±9.32

**Table 1:** AD of a model protein. Ammonia release shown as a percent nitrogen substrate added for different substrate loads.

*Objective 2: Metabolic pathways and ammonia resistance mechanisms in digester communities*

Experiments performed thus far towards this objective serve to define and optimize growth parameters for growing *P.russellii* under amino acid fermenting conditions with and without ammonia stress. In the growth studies exposing *P.russellii* to increasing levels of TAN, there was a clear negative correlation between free ammonia concentration in the media and growth rate. The critical concentration of free ammonia that appears to severely inhibit growth of *P.russellii* is ~2.5mM at near neutral pH. Further studies are underway to better support this observation, and to determine if this critical level may be different when growing at a different pH or with a different substrate. Another experiment will be performed to demonstrate that this effect on growth is in fact caused by increasing ammonia and does not result from a high salt concentration (ammonia is added to the reactors as ammonium chloride). Results of these growth studies will help define the physiology of a model HAP bacterium, and also will help in determining optimal

growth conditions for the RNA sequencing experiment. RNA extraction and mRNA enrichment methods are currently being standardized for *P.russellii* in preparation for sequencing. An example of a set of cultures used for the various growth studies is shown in Figure 1.



**Figure 1:** Example of culture set up for *P. russellii* growth studies

*Objective 3: Development of molecular techniques for process control and monitoring*

Work on this objective is directly dependent on the results from the sequencing experiment that is part of objective 2 and has not begun.

*Objective 4: Two-stage digestion: fundamental analysis of operating parameters and optimization for ammonia recovery*

Work on this objective is dependent upon the results of objectives 1 and 2 and therefore has not yet begun.

## References

1. Abouelenien, F., W. Fujiwara, Y.Namba, M.Kosseva, N.Nishio, and Y. Nakashimada. 2010. Improved methane fermentation of chicken manure via ammonia removal by biogas recycle. *Bioresource Technology*. **101**:6368-6373.
2. Babson, D. 2010. Enhancing energy recovery from biomass waste streams- from mega-landfills and biorefineries to microbial communities. PhD Dissertation, Rutgers University.
3. Chen, Y., J.J. Cheng, and K.S. Creamer. 2008. Inhibition of anaerobic digestion process: a review. *Bioresource Technology*. 99:4044-4064
4. Locke, E., and M. Laquidara. 2006. Three examples of wet weather mitigation evaluations. Session NI in WERF Workshop 05-CTS-1W, 2006.
5. Nakashimada, Y., Y.Ohshima, H.Minami, H.Yabu,Y.Namba, N.Nishio. 2008. Ammonia-methane two-stage anaerobic digestion of dehydrated waste-activated sludge. *Appl Microbiol Biotechnol*. **79**:1061-1069.
6. Narayanan, B. 2006. Solids treatment and recycle streams in BPR plants. Session P1 in WERF , 2006.
7. Stensel, H.D. 2006. Conditions for low N and effects of wet weather and recycle streams. Session NI in WERF Workshop 05-CTS-1W, 2006
8. Stinson, B. 2006. Alternatives to Mitigate the Impact of Recycle streams on nitrogen removal. Session NI in WERF Workshop 05-CTS-1W, 2006.
9. Tong, J., and Y. Chen. 2009. Recovery of nitrogen and phosphorus from alkaline fermentation liquid of waste activated sludge and application of the fermentation liquid to promote biological municipal wastewater treatment. *Water Research*. **43**:2969-2976.
10. Yabu, H., C.Sakai, T.Fujiwara, N.Nishio, and Y.Nakashimada. 2011. Thermophilic two-stage dry anaerobic digestion of model garbage with ammonia stripping. *Journal of Bioscience and Bioengineering*. **111**(3): 312-319.
11. Yuan, H., Y.Chen, H.Zhang, S.Jiang, Q.Zhou, and G.Gu. 2006. Improved bioproduction of short-chain fatty acids from excess sludge under alkaline conditions. *Environ Sci Technol*. **40**:2025-2029.

# Mitigation of Environmental Nitrogen Release by Enrichment of Hyper Ammonia Producing (HAP) Bacteria in Waste Treatment Systems

## Basic Information

<b>Title:</b>	Mitigation of Environmental Nitrogen Release by Enrichment of Hyper Ammonia Producing (HAP) Bacteria in Waste Treatment Systems
<b>Project Number:</b>	2012NJ311B
<b>Start Date:</b>	3/1/2012
<b>End Date:</b>	2/28/2013
<b>Funding Source:</b>	104B
<b>Congressional District:</b>	NJ-006
<b>Research Category:</b>	Water Quality
<b>Focus Category:</b>	Nitrate Contamination, Treatment, Water Quality
<b>Descriptors:</b>	None
<b>Principal Investigators:</b>	Sunirat Rattana, Donna E. Fennell

## Publication

1. Rattana, S. and D.E. Fennell. 2013. Mitigation of environmental release by enrichment of Hyper Ammonia Producing (HAP) bacteria in waste treatment systems. 2013 Symposium on Microbiology at Rutgers University. New Brunswick, NJ. January 31-February 1, 2013. (poster presentation)

## **Project Summary:**

### **Problem and Research Objectives**

Manure management from agriculture is currently being singled out for improvement since high ammonia and nitrogen levels in land-applied manure is associated with poor source water quality. Anaerobic processing is considered to be one of the alternative techniques for treating manure, sludge and other wastes. Anaerobic digestion can treat high N-waste and allow control and mitigation of nitrogen release into the environment. However, instability of anaerobic treatment processes is caused by high amounts of free ammonia released during the process (3, 9, 10). Therefore, it is vital to control ammonia concentrations while operating anaerobic reactors.

Although high ammonia concentration contributes to reactor failure, there are some possibilities for stable anaerobic treatment at high ammonia content. Gaining a better understanding of how to remove ammonia before operating the system will contribute to the improvement of waste treatment efficiency. Enabling production of high ammonia concentrations in waste treatment reactors could allow more efficient direct capture and re-use of ammonia as a fuel or fertilizer. Concentrating the ammonia for capture is preferable to its widespread release in dilute treated effluent.

The objective of this research is to develop techniques for improving anaerobic biodegradation of high N-wastes by enrichment of microorganisms responsible for rapid ammonia production from organic-N and tolerance to high ammonia concentrations. Studies on such organisms are needed to better understand how microorganisms play a role in recovering ammonia from sludge and manure. Isolation of these specific microorganisms will be applied to develop techniques for anaerobically treating high N-wastes and achieve the overall goals of waste treatment efficiency.

### **Methodology**

Task 1: Enrichment and investigation of amino acid-degrading microorganisms tolerant to high ammonia concentrations and responsible for rapid ammonia production

#### **Experimental Design**

*High Ammonia Concentration Reactors*

The 160-ml serum bottles were made anoxic and filled with 10 ml swine digestate as inoculum, 90 ml of anaerobic media recipe for methanogenic bacteria (3), 10 mM glutamate sodium salt stock solution as the sole of carbon and energy source, and a different concentration of  $\text{NH}_4^+\text{-N}$  (0.5, 1, 2.5, and 5 g/L). Triplicate reactors were tested for each  $\text{NH}_4^+\text{-N}$  concentration, and incubated at mesophilic conditions. A hydraulic retention time (HRT) of 70 days was maintained by a fill and draw exchange of 10 percent of the medium every seventh day. The glutamate solution and ammonium chloride were also added at each fill and draw event to achieve semi-continuous operation.

#### *Salt Effects to Reactors*

Reactors were set up at  $\text{NH}_4^+\text{-N}$  concentration of 2.5 and 5 g/L. Then magnesium salt ( $\text{MgCl}_2$ ) and calcium salt ( $\text{CaCl}_2$ ) were maintained at 5 mM and 10 mM of  $\text{MgCl}_2$ , and 20 mM and 40 mM of  $\text{CaCl}_2$  in each reactor set.

#### *Analytical Method*

Analytical techniques were performed to determine volatile fatty acids and methane production as a result of anaerobic digestion processes. Reactors were sampled every seventh day. Volatile fatty acids such as acetate, propionate, and butyrate were measured using High Performance Liquid Chromatography (HPLC). Methane was measured by Gas Chromatography-Flame Ionization Detection (GC-FID). In addition, the amount of released total ammonia nitrogen (TAN) was measured by Ion Chromatography (IC) occasionally to make sure that ammonia was maintained to the desired concentrations. pH and reactor gas volume were also measured by a pH meter and water displacement equipment, respectively. Those parameters were quantified based on five-point standard calibration curves.

Task 2: Identification and characterization of amino acid-fermenting microorganisms tolerant to high ammonia concentrations

Enriched microorganisms from Task 1 were analyzed for microbial communities using Polymerase Chain Reaction (PCR) coupled to Denaturing Gradient Gel Electrophoresis (DGGE). DNA extraction from the microcosm samples was performed using the PowerSoil™ DNA Isolation Kit from a 1 mL slurry sample according to the manufacturer's instruction. The DNA extracts were analyzed by 1.5% agarose gel electrophoresis. The DNA was electrophorized in the gel by staining in 0.1% ethidium bromide (EtBr) solution for 30 min and visualized using UV on a Molecular Imager Gel Doc XR system. Primers were used to amplify 16S ribosomal

RNA (16S rRNA) genes of members of the bacteria in DNA extracts by means of Polymerase Chain Reaction (PCR). The PCR amplification of partial bacterial 16S rRNA genes was performed with forward (338-GC F) and reverse primers (519 R). Denaturing gradient gel electrophoresis (DGGE) of PCR amplified community DNA was carried out and dominant bands were excised and sequenced to examine the community diversity by comparing sequences with those available in the 16S rRNA gene libraries of Genbank (<http://blast.ncbi.nlm.nih.gov/Blast.cgi>).

### **Principal Findings and Significance**

The effects of high ammonia concentrations on the performances of anaerobic reactors were studied. Anaerobic reactors inoculated with swine digestate were operated for 240 days under ammonia concentrations of 0.5-5 g/LNH<sub>4</sub><sup>+</sup>-N. Using glutamate sodium salt solution as the sole of carbon and energy source, it was found that there are amino acid-fermenting microorganisms in swine digestate that can tolerate high ammonia concentrations in waste treatment systems.

#### *Methane Production*

The results revealed that ammonia concentrations play a role in methane production. Figure 1 shows the methane production from a 1 g/L NH<sub>4</sub><sup>+</sup>-N reactor. There was a longer lag phase for methane production at higher NH<sub>4</sub><sup>+</sup>-N concentrations. At 1 g/L NH<sub>4</sub><sup>+</sup>-N, it took about 20 days to reach the exponential phase and maintained at steady state after day 80. Methane production at 5 g/L NH<sub>4</sub><sup>+</sup>-N was the lowest compared to other ammonia concentrations. The salt experiment revealed high methane production for some conditions.

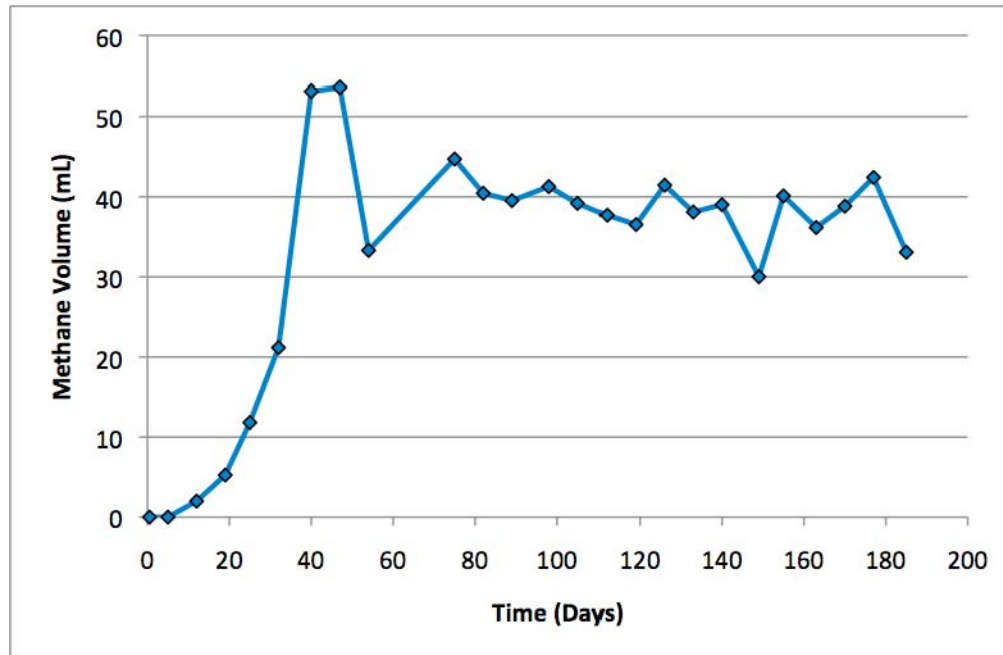


**Figure 1.** Methane production from a 1g/L  $\text{NH}_4^+\text{-N}$  reactor

#### *Volatile Fatty Acids Analysis*

Volatile fatty acids concentration is a key indicator of system performance. It determines degree of fermentation and toxicity to the reactor. Acetate, propionate, and butyrate are three main volatile fatty acids identifying anaerobic digestion. The results indicated that more acetate and propionate accumulated at higher ammonia concentrations. This result relates to the fact that acetate-utilizing methanogens have been shown to be sensitive to ammonium (1, 8). Figure 2 shows volatile fatty acids concentration of a 1 g/L  $\text{NH}_4^+\text{-N}$  with time. Acetate concentration was at 2600 mg/L around day 33 before decreasing to steady state at day 75, while propionate tended to accumulate less and reached steady state at day 75. Butyrate appeared to have high concentration at the beginning and decreased to reach steady state at day 80. Addition of salt to high ammonia reactors showed interesting volatile fatty acids accumulation patterns compared to controls.

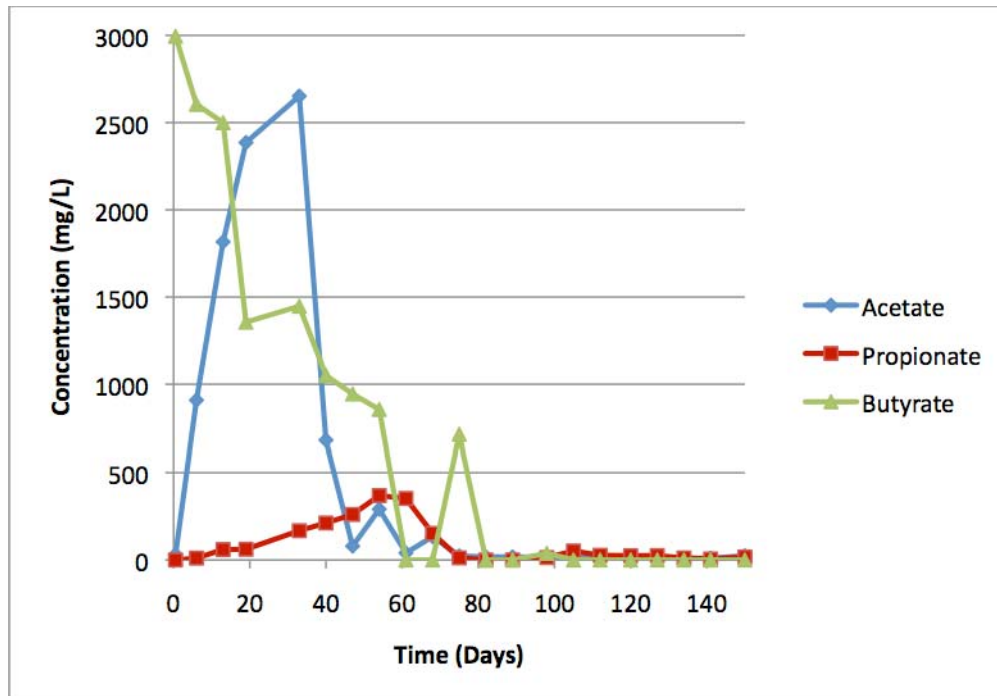


**Figure 2.** Volatile fatty acids concentration with time

### *Molecular Techniques*

Microbial communities of enriched microorganisms were investigated by using 16S rRNA based molecular methods such as PCR coupled to DGGE. Changes in microbial communities were found in conditions tested (Figure 3). Other studies on the reactor stressed by high concentrations of ammonia also indicated changes in microbial population and shifts of the most abundant members (2, 11). This phase of study is ongoing to complete bacterial and methanogenic archaeal communities analysis.

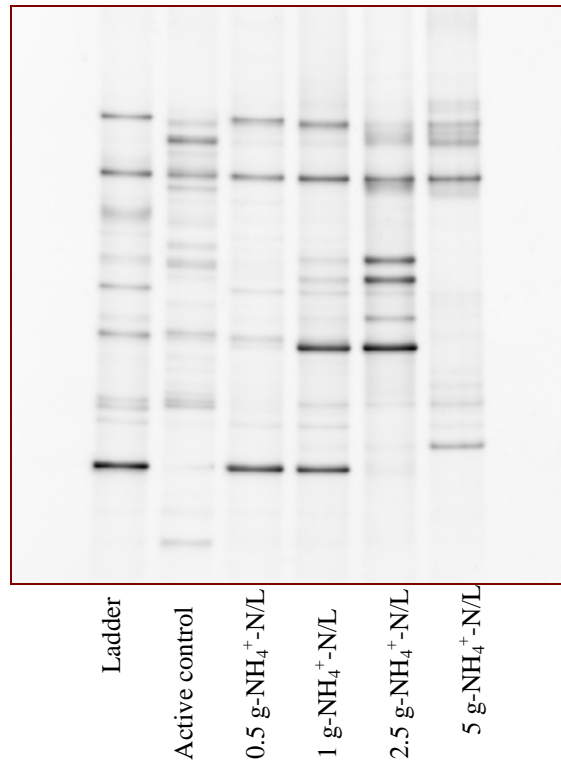


**Figure 3.** DGGE bands of samples day 164

We have successfully enriched microorganisms tolerant to high ammonia concentrations. These microorganisms will be further identified and characterized. It is expected that they are also responsible for rapid ammonia production known as Hyper Ammonia Producing (HAP) bacteria as found by other studies (5, 6, 7). However, the results from this study will be the first report involving glutamate-degrading microorganisms from swine digestate in mesophilic condition. The knowledge of microorganisms tolerant to high ammonia concentrations and ammonia production will allow engineering to enhance the efficiency of waste treatment and achieve nitrogen removal from wastes.

## References

1. **Calli, B., Mertoglu, B., Inanc, B. Yenigun, O.** 2005. Effect of high free ammonia concentrations on the performances of anaerobic bioreactors. *Process Biochemistry* 40:1285-1292.
2. **Calli, B., Mertoglu, B., Inanc, B. Yenigun, O.** 2005. Methanogenic diversity in anaerobic bioreactors under extremely high ammonia levels. *Enzyme and Microbial Technology* 37:448-455.
3. **Chen, Y., Cheng, J.J., and Creamer, K.S.** 2007. Inhibition of anaerobic digestion process: A review. *Bioresource Technology* 99:4044-4064.
4. **Fennell, D. E., J. M. Gossett, and S. H. Zinder.** 1997. Comparison of butyric acid, ethanol, lactic acid, and propionic acid as hydrogen donors for the reductive dechlorination of tetrachloroethene. *Environmental Science and Technology* **31**:918-926.
5. **Plugge, C.M., Erwin, G.Z., and Alfons J.M., S.** 2000. *Caloramator coolhaasii* sp. nov., a glutamatedegrading, moderately thermophilic anaerobe. *International Journal of Systematic and Evolutionary Microbiology* **50**:1155–1162.
6. **Plugge, C.M., Melike, B., Erwin, G.Z., and Alfons J.M., S.** 2002. *Gelria glutamica* gen. nov., sp.nov., a thermophilic, obligately syntrophic, glutamate-degrading anaerobe. *International Journal of Systematic and Evolutionary Microbiology* **52**:401-407.
7. **Russell, J.B., Herbert, J.S., and Guangjiong, C.** 1988. Enrichment and isolation of a ruminal bacterium with a very specific activity of ammonia production. *Applied and environmental microbiology* **54**:872-877.
8. **Schnurer, A., Zellner, G., Svensson, B.H.** 1999. Mesophilic syntrophic acetate oxidation during methane formation in biogas reactors. *FEMS Microbiology Ecology*. 29:249-261.
9. **Siles, J.A., Brekelmans, J., Martin, M.A., Chica, A.F., and Martin, A.** 2010. Impact of ammonia and sulphate concentration on thermophilic anaerobic digestion. *Bioresource Technology* 101:9040-9048.
10. **Sung, S., and Liu, T.** 2003. Ammonia inhibition on thermophilic anaerobic digestion. *Chemosphere* 53:43-52.
11. **Westerholm, M., Muller, B., Arthurson, V., Schnurer, A.** 2011. Changes in the acetogenic population in a mesophilic anaerobic digester in response to increasing ammonia concentration. *Microbe Environment* 26: 347-353.

# Urban wetland plant assemblage species diversity and invasive species dominance as expressions of flood regime

## Basic Information

<b>Title:</b>	Urban wetland plant assemblage species diversity and invasive species dominance as expressions of flood regime
<b>Project Number:</b>	2012NJ312B
<b>Start Date:</b>	3/1/2012
<b>End Date:</b>	2/28/2013
<b>Funding Source:</b>	104B
<b>Congressional District:</b>	NJ-006
<b>Research Category:</b>	Biological Sciences
<b>Focus Category:</b>	Wetlands, Invasive Species, Ecology
<b>Descriptors:</b>	None
<b>Principal Investigators:</b>	Laura Shappell, Lena Struwe

## Publication

1. Shappell, L.J. and J.G. Ehrenfeld. 2012. Urban wetlands: hope on the invasion front. Ecological Society of America Annual Meeting. Portland, OR. (invited poster presentation)

# 1. PROJECT SUMMARY

## Research Problem

Floodwater storage and water quality protection are often cited as reasons for conserving and restoring wetlands. Ecosystem services provided by wetlands play an integral role in water quality and water supply reliability, particularly within urbanized areas such as central New Jersey (Ehrenfeld, 2004). Preserving and restoring wetlands within New Jersey headwater complexes may prove the most cost-effective for watershed managers. For example, water quality models have suggested that second-order streams receive approximately 65% of their nitrogen input from headwater streams (Alexander et al., 2007). The ability of urban wetlands to buffer high water volumes and pollutant loads is a function of overall ecosystem health, or the level to which human modifications have affected system processes (Hogan and Walbridge, 2007). Wetlands within developed landscapes experience shorter, shallower, and more frequent flooding; that is, a high intensity, short-duration hydrologic disturbance (Ehrenfeld and Schneider, 1993; Ehrenfeld et al., 2003; Groffman et al., 2003). Wetland ditching/drainage, and subsequent lowering of the water table, affects soil processes and plant species composition (Groffman et al., 2003). Invasive plant species dominance can alter processes within wetlands, such as soil nutrient pools (Weidenhamer and Callaway, 2010) and water table levels (Zedler and Kercher, 2004). Previous research highlights the variation among urban wetland structure (e.g., floral composition) and function (e.g., hydrology), emphasizing the need for site-specific research to understand mechanisms shaping these novel ecosystems (Ehrenfeld and Schneider, 1993; Woodward and Wui, 2001).

Human-modified disturbance patterns and low levels of environmental stress are hypothesized to increase invasibility of a given habitat (Alpert et al., 2000). Some hypothesized mechanisms for invasive species establishment include local scale environmental variables, biodiversity, and disturbance (Lockwood et al., 2007). The low flood tolerance characteristic of competitive invasive species may buffer forested wetlands against invasion (Barden, 1987; Price et al., 2011). In the absence of abiotic stressors, non-native invasive plant species may have a competitive advantage over native stress-tolerating wetland flora (Grime, 1977). Previous research generally supports these hypotheses (Ehrenfeld and Schneider, 1993; Owen, 1999). However, the extent to which hydroperiod may provide resistance to invasion has not been well established, though the management implications of such findings are significant.

Invasive plant species can alter soil properties and nutrient processes – this effect has been demonstrated for species found in New Jersey such as garlic mustard (*Alliaria petiolata*), Japanese barberry (*Berberis thunbergii*), and Japanese stiltgrass (Ehrenfeld et al., 2001; Kourtev et al., 2003; Rodgers et al., 2008). In addition, researchers have found reduced structural complexity in the wake of invasive dominance for species such as oriental bittersweet (*Celastrus orbiculatus*) (Fike and Niering, 1999) and Japanese stiltgrass (Adams and Engelhardt, 2009; Flory and Clay, 2010). This structural shift is particularly important in wetlands because vegetation strongly influences the rate of evapotranspiration and the quantity of surface flow (Chapin et al., 2002). Thus, invasive species common in NJ and other Mid-Atlantic states may create a positive feedback whereby species alter water dynamics, nutrient cycling, and vegetation structure in a manner that supports invasive population growth, and disrupts ecosystem services.

## Objectives & Research Questions

- 1) Characterize wetland hydroperiod at sites previously surveyed for vegetation structure.

What is the nature of the hydrologic conditions (flooding duration, depth, and frequency) within and among my wetland sites?

- 2) Identify how hydroperiod conditions affect floristic diversity and invasive dominance.

To what extent are floristic diversity and invasive plant species dominance reflective of site hydrologic condition?

## Methods

Research was conducted in six headwater mineral flat wetlands located in urban central New Jersey. Dominant wetland plant assemblages within my research sites include deciduous swamps, scrub-shrub, and emergent. Hydroperiods range from saturated to seasonally flooded (*sensu* Cowardin et al., 1979). Wetland patch sizes are categorized as large (>125 ha, n = 2), medium (<35 ha, n = 2), and small (<15 ha, n = 2). Sample point placement for the initial vegetation surveys (2008-2010) lay along a regular 400-m grid. Hydrology monitoring occurred within the largest subareas of each wetland; two to four subareas per wetland were monitored depending on wetland size. The fifteen points selected for monitoring correspond to my previously sampled vegetation plots (707 m<sup>2</sup>). Floristic diversity, vegetation structure, invasive plant species dominance were assessed within each plot. Topography was measured within each plot along cardinal directions at 5-m intervals (plot n = 12), providing data on plot-scale topographic variation (range). Ecotone water wells were affixed to a PVC stake at the lowest altitude within each plot, and programmed to log data hourly. iButtons were waterproofed with a rubber coating of Plastidip, and affixed to the stake 1 cm and 90 cm above the soil surface, with the latter serving as an aerobic control. iButtons arrays were deployed at points of interest such as vernal pools, plot center (i.e., topography reference point), and patches of invasive plants (Figure 1).

## Principle findings and significance

*Object 1: Characterize hydrology.*

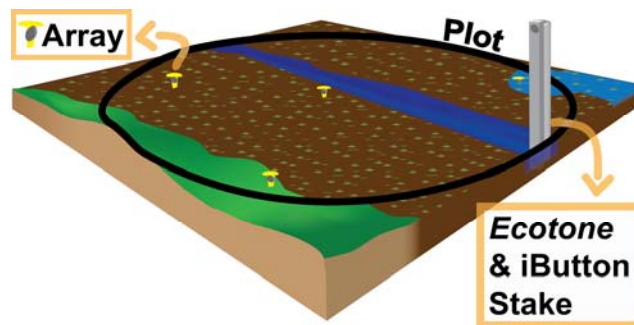


**Figure 1:** Sample diagram of hydrology monitoring plot design (15-m radius). Ecotone installed at ephemeral stream, arrays deployed in a vernal pool, patch of Japanese stiltgrass (green area), and plot center.

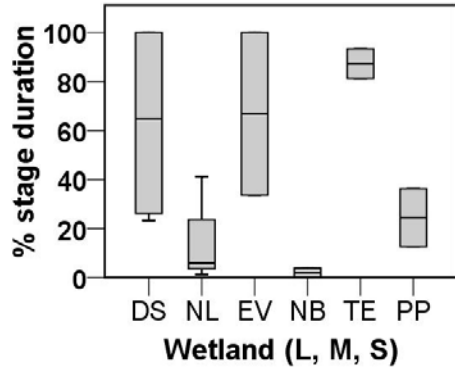


**Figure 2:** Percent stage duration for Large (DS, NL), Medium (EV, NB), and Small (TE, PP) wetlands. Aboveground flooding varied among, and within size classes.

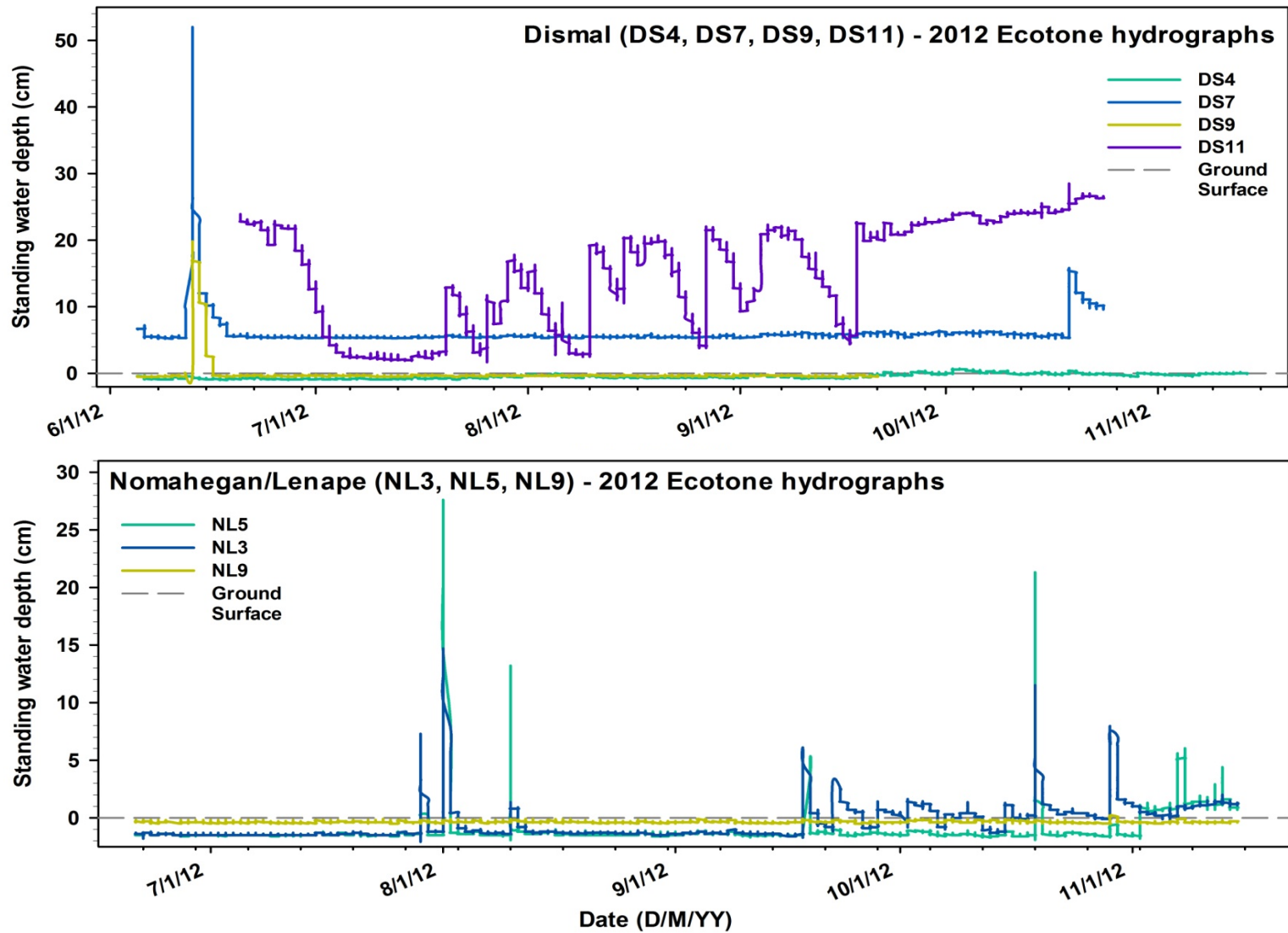
Ecotone water wells and iButton temperature sensors recorded data hourly for an average deployment duration of 145 days ( $SE \pm 2.6$  days). Hydrology monitoring equipment deployment was complete by mid-June; all equipment was retrieved by mid-November 2012. Retrieval was delayed and some data were discarded, because of complications due to Super-storm Sandy (landfall October 29-30, 2012). Descriptive summaries for each wetland are presented in **Table 1**; data therein include aboveground flooding duration, frequency, and maximum depth of flooding. Flood signatures often varied within and among wetlands. Mean percent stage duration varied greatly among wetlands and within wetland size classes (**Figure 2**). Wetland hydrographs were created for each wetland using the Ecotone water well data (Figures 3-8).

**Table 1:** Descriptive statistics of Ecotone aboveground water level monitors for each wetland. Flood depth data were calibrated with zero being soil surface. \*Monitoring days were excluded from analysis of some wells due to damage caused by Super-storm Sandy (October 29-30, 2012). N = number of Ecotone water-wells per wetland. Dismal (2), and Evergreen (1) each had site(s) flooded for the duration of the monitoring, resulting in a flood frequency of “1”.

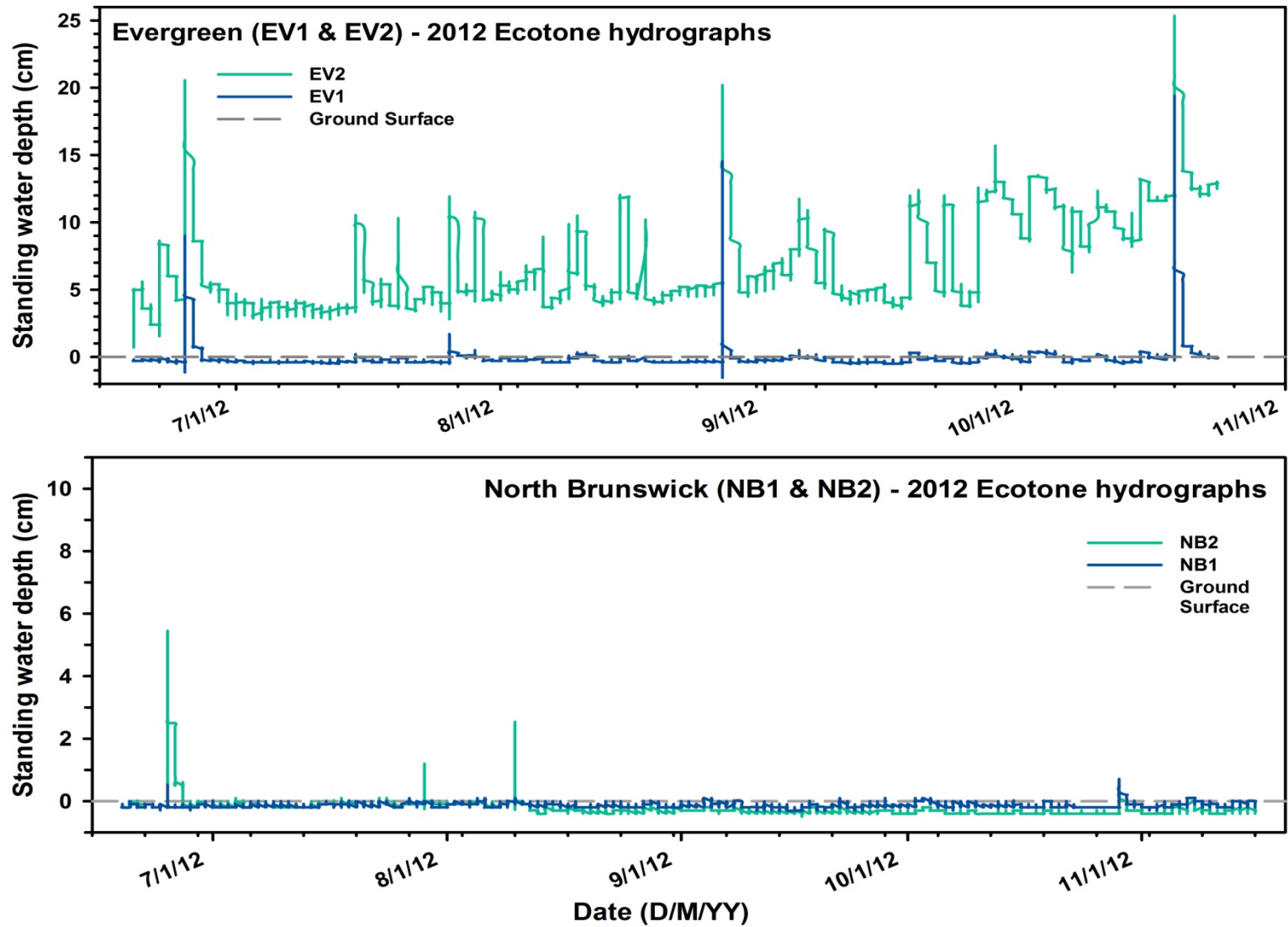
	N	Days monitored*	Flood: Duration (% days)		Frequency (days)		Max H <sub>2</sub> O depth (cm)	
			Mean $\pm$ SE	Min - Max	Mean $\pm$ SE	Min - Max	Mean $\pm$ SE	Min - Max
Dismal	4	127 - 163	63 $\pm$ 21	23 - 100	3 $\pm$ 1	1 - 7	33.8 $\pm$ 12.4	0.7 - 54.2
Nom./Lenape	3	132 - 148	16 $\pm$ 13	1 - 41	5 $\pm$ 2.0	1 - 8	14.1 $\pm$ 7.9	0.2 - 27.6
Evergreen	2	128	67 $\pm$ 33	34 - 100	6.5 $\pm$ 5.5	1 - 12	19.5 $\pm$ 5.8	13.7 - 25.3
North Bruns.	2	151	4 $\pm$ 4	0 - 8	7 $\pm$ 3	4 - 10	2.9 $\pm$ 2.2	0.7 - 5.1
Terrill	2	149	87 $\pm$ 6	81 - 93	5 $\pm$ 2	3 - 7	40.5 $\pm$ 16.7	23.8 - 57.2
Polansky	2	143	25 $\pm$ 12	13 - 36	14 $\pm$ 12	2 - 25	11.5 $\pm$ 10.9	0.6 - 22.3

These point-specific descriptive data will be used in my dissertation research to explore the relationship between vegetation composition, invasive plant species dominance, and local hydrology.

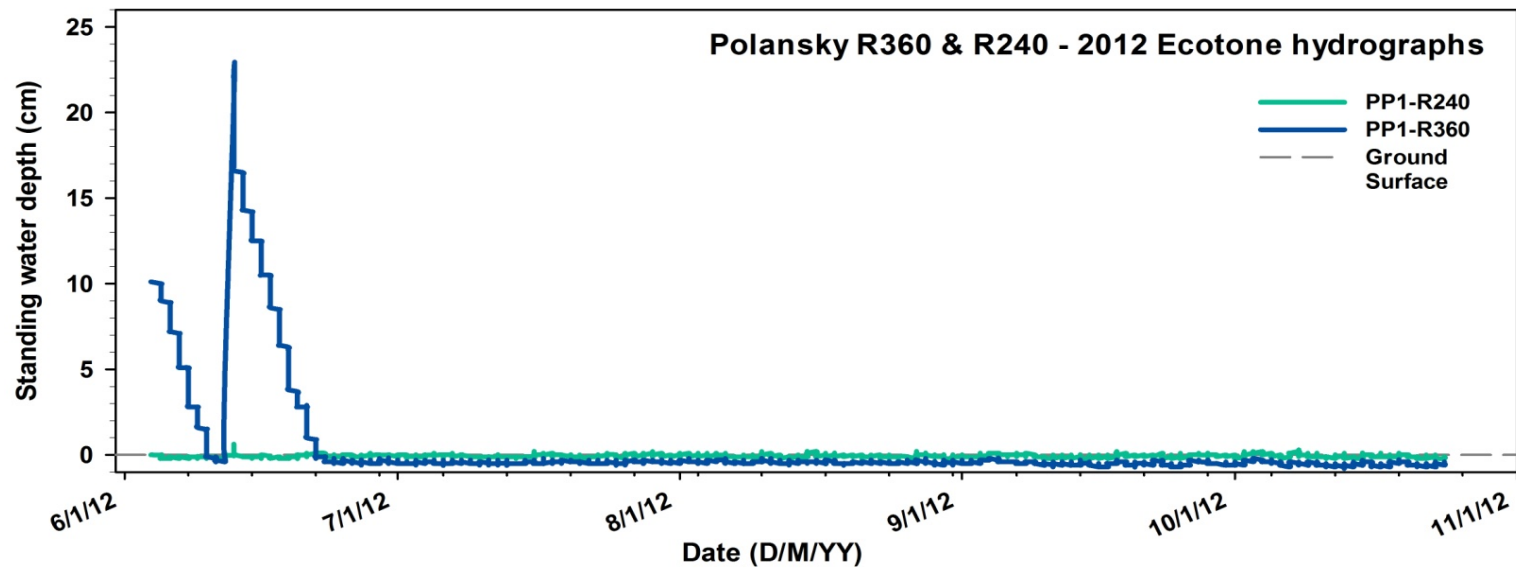
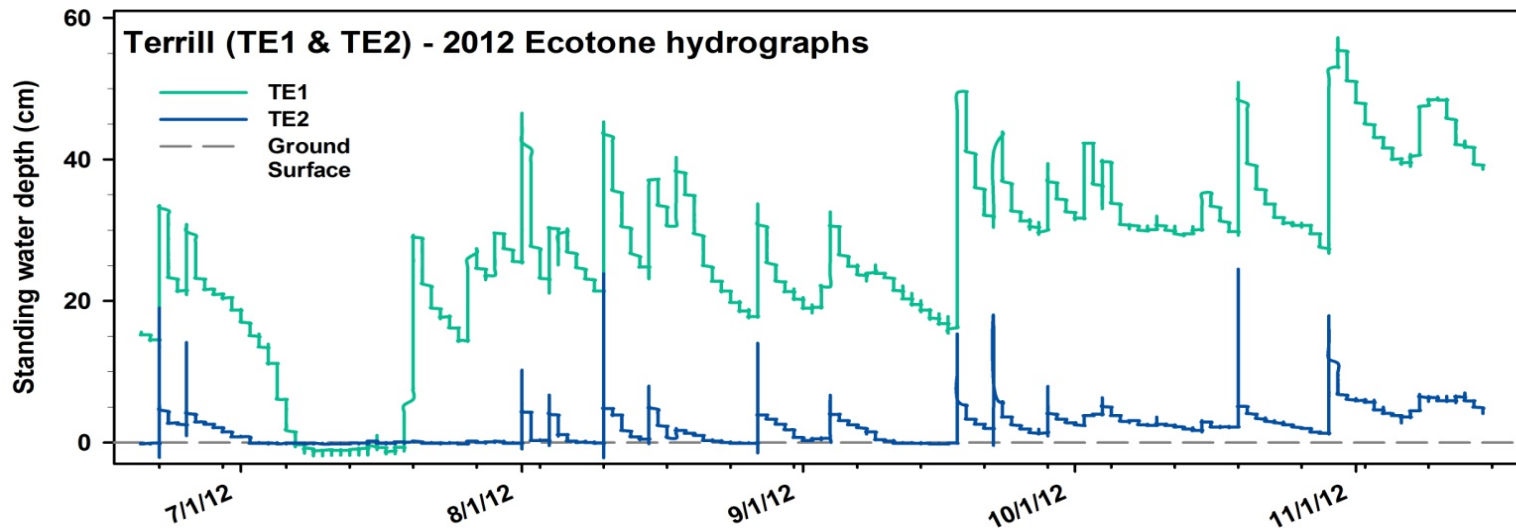
I am still processing data collected from the 120+ iButton temperature sensors deployed in 2012. The effectiveness of iButton sensors as a proxy for flooding may be seen in data from my preliminary 2011 monitoring season (**Figure 9**). Data collected from these methods provide approximate flooding duration (hours), number of flooding events, and total number of flooding episodes.



**Figures 3-4:** Hydrographs produced from data collected hourly by Ecotone water level monitors. Dismal (Figure 3) and Nomahegan/Lenape (Figure 4) are the two Large wetlands (>125 ha). Zero (dash line) delineates the ground surface; Ecotone limit is  $\leq 5$  cm below the soil surface.



**Figures 5-6:** Hydrographs produced from data collected hourly by Ecotone water level monitors. Evergreen (Figure 5) and North (Figure 6) Brunswick are the two Medium wetlands (<35 ha). Zero (dash line) delineates the ground surface; Ecotone sensor limit is  $\leq 5$  cm below the soil surface.



**Figures 7-8:** Hydrographs produced from data collected hourly by Ecotone water level monitors. Terrill (Figure 7) and Polansky (Figure 8) are the Small wetlands (<12 ha). Zero (dash line) delineates the ground surface; Ecotone sensor limit is  $\leq 5$  cm below zero.

## Above ground (AG) water flux over time - using iButton temperature sensors as a proxy for flooding with reference climate data\*

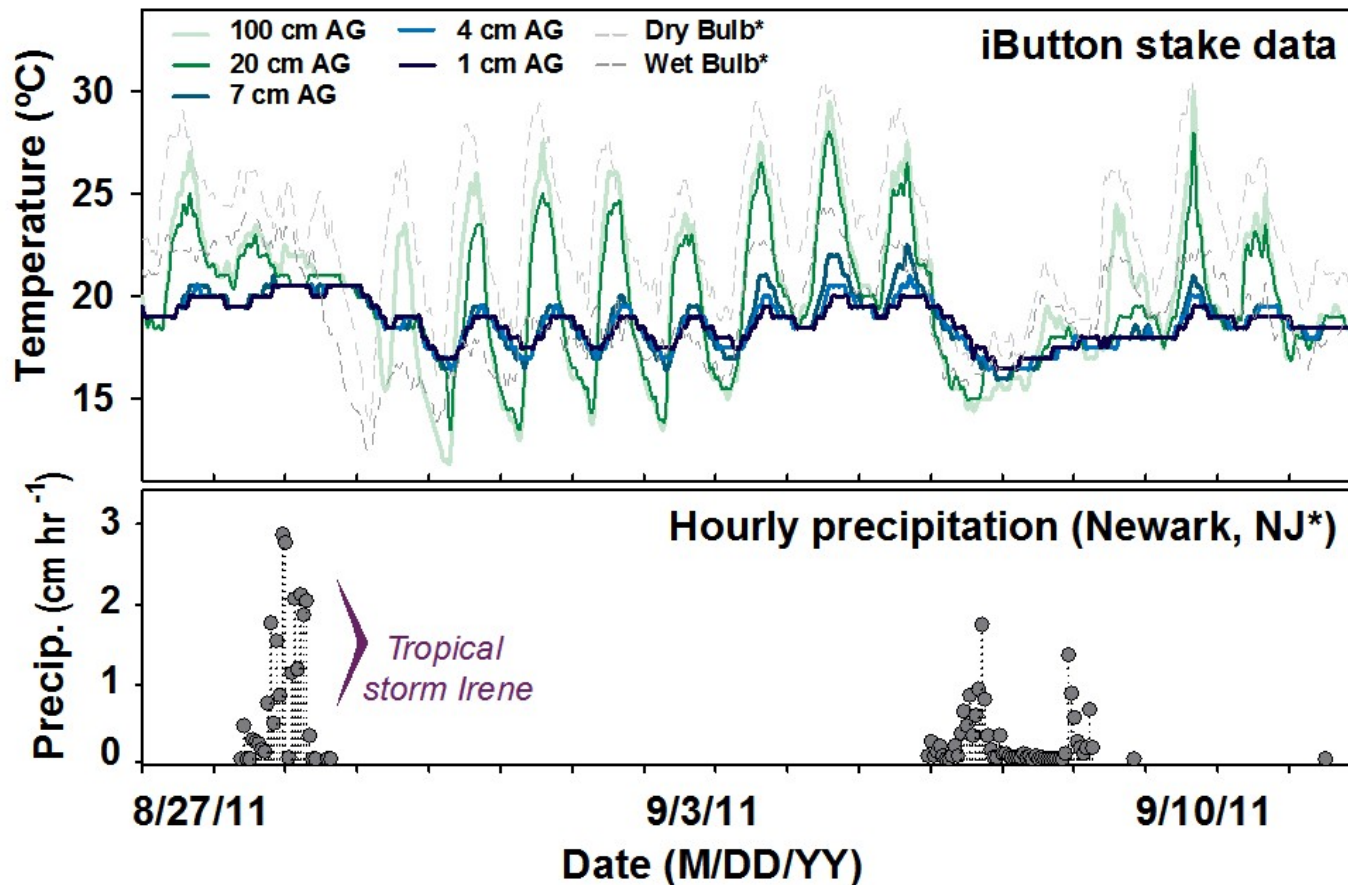


**Figure 9:** The above graph is an example of how iButtons may be used as a proxy for flooding. These data are from a plot sampled during the preliminary monitoring season in 2011. iButtons were affixed to a stake at varying intervals above the soil surface (above ground) where they logged data hourly. The dampened flood signature following Tropical Storm Irene indicates periods of flooding. A Predecessor Rainfall Event brought by Hurricane Katia and TS Lee, depicted above, occurred in early September. NOAA weather data included in the graph for comparison was collected at Newark International Airport.

*Object 2: Species composition, invasive dominance, and hydrology.*

At the sample points presented here, over 240 plant species were identified, including 16 nonnative invasive plant species. The most common invasive species, occurring in at least 20% of the sample points include Japanese stiltgrass, multiflora rose (*Rosa multiflora*), marshpepper knotweed (*Polygonum hydropiper*), and spotted ladythumb (*Polygonum persicaria*). Richness appears to have no influence on the number of invasive plant species present, as seen in Figure 10, in which sites were classified using data collected from Ecotone water wells (Environmental Laboratory, 1987). Because the relationship between expressed plant community diversity and environmental variables, such as hydrology, are so complex, more analysis is needed. I plan to do more in-depth diversity analyses that incorporate alpha and beta diversity; these vegetation and hydrology data will be incorporated into a predictive process model.

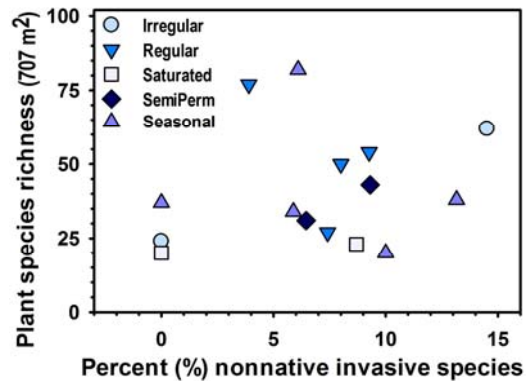


**Figure 10:** No relationship observed between plant species richness and invasive species, as coded by hydrologic zones based on flood duration (Saturated <5%; Irregularly flooded 5-12.5%; Seasonally 12.5-25%; Regularly 25-75%; and Semi-permanently 75-99%).

Japanese stiltgrass was the most prevalent invasive species, found at eight of the 15 sample points presented here. Prior to receiving NJWRRI funding I conducted extensive field surveys (84 vegetation plots), and conducted a manipulative mesocosm experiment using stiltgrass as the model species. In the experiment, I manipulated flooding depth or duration (9 treatments, including a control, 7 replicates each). Results from this experiment indicate that as little as four days of aboveground, shallow flooding can inhibit stiltgrass seedling production. These experimental results supported my field observations that the spatial distribution of stiltgrass is restricted to areas without aboveground flooding. These results have significant implications for the restoration and creation of wetlands, and maintenance of local biodiversity, as stiltgrass has been shown to alter ecosystem processes and vegetation structure (see “research problems” and citations therein). When comparing sites with and without stiltgrass, wetland alone was not a significant predictor for the species’ presence or absence (Kruskal-Wallis,  $df = 5$ ,  $p = 0.549$ ). Stiltgrass presence is significantly related to the within-plot topographic range, and maximum depth of standing water (Logistic regression,  $df = 2$ ,  $F = 4.372$ ,  $p = 0.037$ ) (Figure 11). Incorporating plot topography was an important factor because stiltgrass will persist on hummocks that do not experience flooding; this also helps correct for water well placement, which was at the lowest point within each plot. Further analyses will incorporate more environmental data and the extent to which present and past human

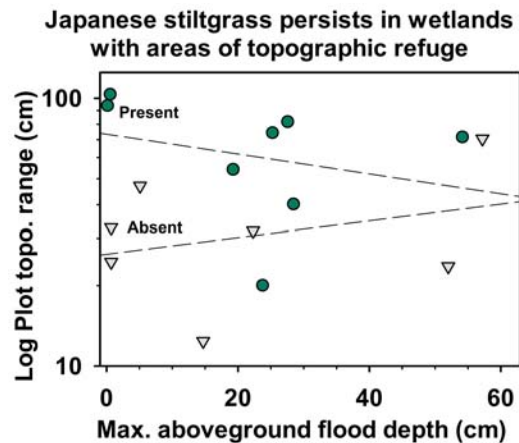


**Figure 11:** Maximum depth of aboveground flooding (cm) within the context of plot-scale topographic range, sites are color coded by stiltgrass presence (circles;  $n = 8$ ) or absence (triangles;  $n = 7$ ); lines of best fit illustrate significant differences between stiltgrass present/absence ( $df = 2$ ,  $F = 4.372$ ,  $p = 0.037$ ).

modifications such as ditching or historical land use may influence the modern expressed plant community and local flooding conditions.

## WORKS CITED

- Adams, S. N. and K. A. M. Engelhardt. 2009. Diversity declines in *Microstegium vimineum* (Japanese stiltgrass) patches. *Biological Conservation* 142:1003-1010.
- Alexander, R. B., E. W. Boyer, R. A. Smith, G. E. Schwarz and R. B. Moore. 2007. The Role of Headwater Streams in Downstream Water Quality. *Journal of the American Water Resources Association* 43:41-59.
- Alpert, P., E. Bone and C. Holzapfel. 2000. Invasiveness, invasibility and the role of environmental stress in the spread of non-native plants. *Perspectives in Plant Ecology, Evolution and Systematics* 3:52-66.
- Barden, L. S. 1987. Invasion of *Microstegium vimineum* (Poaceae), an exotic, annual, shade-tolerant, C4 grass, into a North Carolina floodplain. *American Midland Naturalist* 118:40-45.
- Chapin, F. S., III, P. A. Matson and H. A. Mooney. 2002. Terrestrial Water and Energy Balance. p. 71-96. *In Principles of Terrestrial Ecosystem Ecology*. 1st ed. Springer-Verlag, New York.
- Ehrenfeld, J. G. and J. P. Schneider. 1993. Responses of forested wetland vegetation to perturbations of water chemistry and hydrology. *Wetlands* 13:2-122.
- Ehrenfeld, J. G. 2004. The expression of multiple functions in urban forested wetlands. *Wetlands* 24:719-733.
- Ehrenfeld, J. G., P. Kourtev and W. Huang. 2001. Changes in soil functions following invasions of exotic understory plants in deciduous forests. *Ecological Applications* 11:1287-1300.
- Ehrenfeld, J. G., H. Bowman Cutway, R. Hamilton and E. Stander. 2003. Hydrologic description of forested wetlands in northeastern New Jersey, USA - an urban/suburban region. *Wetlands* 23:685-700.
- Environmental Laboratory. 1987. Corps of Engineers Wetlands Delineation Manual. U.S. Army Corps of Engineers, Washington, DC.
- Fike, J. and W. A. Niering. 1999. Four decades of old field vegetation development and the role of *Celastrus orbiculatus* in the northeastern United States. *Journal of Vegetation Science* 10:483-492.
- Flory, S. and K. Clay. 2010. Non-native grass invasion suppresses forest succession. *Oecologia* 164:1029-1038.
- Grime, J. P. 1977. Evidence for the existence of three primary strategies in plants and its relevance to ecological and evolutionary theory. *The American Naturalist* 111:1169-1194.
- Groffman, P. M., D. J. Bain, L. E. Band, K. T. Belt, G. S. Brush, J. M. Grove, R. V. Pouyat, I. C. Yesilonis and W. C. Zipperer. 2003. Down by the riverside: urban riparian ecology. *Frontiers in Ecology and the Environment* 1:315-321.
- Hogan, D. M. and M. R. Walbridge. 2007. Urbanization and nutrient retention in freshwater riparian wetlands. *Ecological Applications* 17:1142-1155.
- Kourtev, P. S., J. G. Ehrenfeld and M. Häggblom. 2003. Experimental analysis of the effect of exotic and native plant species on the structure and function of soil microbial communities. *Soil Biology and Biochemistry*, 35:895-905.
- Lockwood, J. L., M. F. Hoopes and M. P. Marchetti. 2007. *Invasion Ecology*. Blackwell Pub., Malden, MA.
- Owen, C. R. 1999. Hydrology and history: land use changes and ecological responses in an urban wetland. *Wetlands Ecology and Management* 6:209-219.
- Price, J., P. Berney, D. Ryder, R. Whalley and C. Gross. 2011. Disturbance governs dominance of an invasive forb in a temporary wetland. *Oecologia* 167:759-569.
- Rodgers, V., B. Wolfe, L. Werden and A. Finzi. 2008. The invasive species *Alliaria petiolata* (garlic mustard) increases soil nutrient availability in northern hardwood-conifer forests. *Oecologia* 157:459-471.
- Weidenhamer, J. and R. Callaway. 2010. Direct and indirect effects of invasive plants on soil chemistry and ecosystem function. *Journal of Chemical Ecology* 36:59-69.
- Woodward, R. T. and Y. Wui. 2001. The economic value of wetland services: a meta-analysis. *Ecological Economics* 37:257-270.
- Zedler, J. B. and S. Kercher. 2004. Causes and consequences of invasive plants in wetlands: Opportunities, opportunists, and outcomes. *Critical Reviews in Plant Sciences* 23:431-452.

# Reductive Dehalogenation of Brominated Organic Compounds by Nano FeS Particles

## Basic Information

<b>Title:</b>	Reductive Dehalogenation of Brominated Organic Compounds by Nano FeS Particles
<b>Project Number:</b>	2012NJ313B
<b>Start Date:</b>	3/1/2012
<b>End Date:</b>	2/28/2013
<b>Funding Source:</b>	104B
<b>Congressional District:</b>	NJ-006
<b>Research Category:</b>	Water Quality
<b>Focus Category:</b>	Toxic Substances, Treatment, Water Quality
<b>Descriptors:</b>	None
<b>Principal Investigators:</b>	Cynthia Steiner, Weilin Huang

## Publications

There are no publications.

This research project was terminated due to the student researcher's withdrawal from graduate school. The student did not spend any of the allotted funding before her withdrawal.

## **Information Transfer Program Introduction**

The information transfer program serves an important purpose to the state's water resource community. The goal is to bring timely information about critical issues in water resource sciences to the public, and to promote the importance of research in solving water resource problems. The program accomplishes this goal through a variety of means. One focus is on producing a newsletter that provides an in-depth overview of current water resource issues. The program continues to develop the NJWRRI website ([www.njwrri.rutgers.edu](http://www.njwrri.rutgers.edu)) into a comprehensive portal for water information for the state. We also collaborate with other state and regional organizations in sponsoring and producing conferences.

# Information Transfer Program

## Basic Information

<b>Title:</b>	Information Transfer Program
<b>Project Number:</b>	2012NJ314B
<b>Start Date:</b>	3/1/2012
<b>End Date:</b>	2/28/2013
<b>Funding Source:</b>	104B
<b>Congressional District:</b>	NJ-006
<b>Research Category:</b>	Not Applicable
<b>Focus Category:</b>	None, None, None
<b>Descriptors:</b>	None
<b>Principal Investigators:</b>	Christopher Obropta, Diana Morgan

## Publications

There are no publications.

## Information Transfer Program

The information transfer program has emphasized development of the website and e-based communications with stakeholder groups. It has also focused on the production of substantive newsletters addressing specific water resource issues as an effective way to communicate information to the public.

One issue of the newsletter was produced during FY 2012, and a second is in the planning process. The first issue was our annual research issue. It showcases research funded in FY 2011 by NJWRRI and NIWR/USGS, and also illustrates the importance of research in solving water-related problems. The newsletter can be found online:

<http://www.njwrri.rutgers.edu/newsletters/Summer%202012%20Newsletter.pdf> A second issue will focus on how Superstorm Sandy affected water resources in New Jersey and what changes are occurring in the aftermath of the storm. Each issue of the newsletter is approximately eight pages. It is primarily distributed via our e-mail lists to approximately 2,000 people throughout the state, as paper copies to all members of the New Jersey legislature and Congressional delegation, and it is posted on our website.

Our website ([www.njwrri.rutgers.edu/](http://www.njwrri.rutgers.edu/)) has been continually updated with information on water resource events and information in New Jersey, the U.S. and around the world. The home page and 'events' pages are regularly updated to highlight upcoming events, publications and other water-related news. For the second year in a row, we had an analysis of the traffic to the website, and a comprehensive report was compiled for us. Overall, there were more than 33,000 visits to the website from about 17,000 visitors, which is 1,000 more visitors, but 2,000 fewer visits, than last year. The pages receiving the most visits, outside of the home page, were the same as last year: the watershed organizations, new book releases and research pages. This is important information for us in terms of developing and maintaining the website. The website is our primary means of information transfer to the water community and the public, and we will continue to update and improve its functionality with the benefit of this new information.

We continue to expand and use targeted, group-specific e-mail lists to bring relevant information to specific audiences. Targeted lists include a list of scientists/principal investigators, water resource managers, non-governmental organizations and people affiliated with NGOs, and policy-makers. The lists are continuously updated and expanded, and are used to keep these groups informed of events, conferences, publications, and funding opportunities. These lists enable us to initiate and maintain frequent contact with stakeholder groups. We believe these lists are an excellent method of keeping the water-related public aware of NJWRRI, as well as informed about water-related news and information.

We also continue to participate in the New Jersey Water Monitoring Council, a statewide body representing both governmental and non-governmental organizations involved in water quality monitoring. As a member of the council, we co-sponsored the 2012 New Jersey Water Monitoring Summit, held November 28-29, 2012 at the Rutgers EcoComplex in Columbus, NJ.

[http://www.state.nj.us/dep/wms/2012\\_summit.htm](http://www.state.nj.us/dep/wms/2012_summit.htm) The Summit covered topics applicable to a broad array of water monitoring and assessment programs and projects, including monitoring of all water body types. It showcased projects, tools and programs that have been developed to inform local and state planning, protection, and restoration efforts.

NJWRRI was a co-sponsor of the 5th Passaic River Symposium held October 19, 2012 at Montclair State University, Montclair, NJ. We provided scholarships for students to attend the symposium, and an NJWRRI-funded research project was presented.

<http://www.montclair.edu/media/montclairedu/csam/passaicriverinstitute/Passaic-River-Symposium-V-Program.pdf>

# USGS Summer Intern Program

None.

<b>Student Support</b>					
<b>Category</b>	<b>Section 104 Base Grant</b>	<b>Section 104 NCGP Award</b>	<b>NIWR-USGS Internship</b>	<b>Supplemental Awards</b>	<b>Total</b>
<b>Undergraduate</b>	6	0	0	0	6
<b>Masters</b>	4	0	0	0	4
<b>Ph.D.</b>	8	1	0	0	9
<b>Post-Doc.</b>	1	2	0	0	3
<b>Total</b>	19	3	0	0	22

## Notable Awards and Achievements

For project 2008NJ161B, “Microbial Mobilization of Arsenic and Selenium Oxyanions in Subsurface Aquifers,” the following student awards are reported: 2010 Robison Award for Excellence in Graduate Studies for demonstrating “tremendous competence and accomplishment in their academic and research program while at Rutgers University, has shown an active participation in or a leadership role in the activities of the department, college, university or community, and is motivated to help and improve the human condition at this time and upon graduation.”

Also reported is the 2010 Theobald Smith Society Graduate Scholarship awarded to one graduate student in microbiology or a related field.

For project 2011NJ276B, “Assessment of Green Frog, *Lithobates clamitans*, populations as biological indicators of risk to communities near Superfund sites,” the following student presentation award is reported: Costello, Jennifer and Richard Veit, 2012, Frogs as Biological Indicators: Does Habitat Degradation Impact Prey Capture Efficiency? World Congress of Herpetology, Vancouver, B.C., Canada. Society for the Study of Amphibians and Reptiles (SSAR) Poster Award.

For project 2012NJ305B, “Performance Assessment of Bioretention for Car Wash Runoff Treatment,” the research project was submitted as part of a larger watershed implementation project to the NJ section of the American Water Resources Association for the Excellence in Water Resources Protection & Planning Award. It received an award in the Stormwater Management category. The title of the submission was “Robinson’s Branch Stormwater Management in the Township of Clark.”

For project 2012NJ321B, “Urban wetland plant assemblage species diversity and invasive species dominance as expressions of flood regime,” two student travel awards are reported: \$1000 from NJWRRI for travel to the Ecological Society of American Annual Meeting. Urban Ecosystems Ecology Springer Travel Award (\$400). August 2012. Urban Ecosystems Ecology Sections, Ecological Society of America Annual Meeting, Portland, OR.

This project also reports an invited oral presentation, titled "Invasive dominance as an expression of urban wetland hydrology," for the 2012 Society of Wetland Scientists Mid-Atlantic Chapter Conference, New Brunswick, NJ.

## Publications from Prior Years

1. 2007NJ130B ("The influence of flooding cycles and iron oxides on arsenic retention in contaminated, planted microcosms in comparison with phosphate retention.") - Dissertations - MacDonald, L.H. 2010. Microbiological and Plant-Driven Redox Systems in Groundwater and Links Between Water, Health, and Policy. "Ph.D. Dissertation." Department of Civil and Environmental Engineering, Princeton University, Princeton, NJ. 178 pages.
2. 2008NJ154B ("Volatilization of PCBs from the Tappan Zee region of the Hudson River") - Other Publications - Sandy, Andy L., Lisa A. Rodenburg, Robert J. Miskewitz, et al. 2011. Air-water exchange fluxes and mass transfer coefficients for PCBs on the Hudson River. Abstracts of Papers of the American Chemical Society. Vol. 242 Meeting Abstract 36-ENVR. Published Aug 28 2011.
3. 2008NJ154B ("Volatilization of PCBs from the Tappan Zee region of the Hudson River") - Articles in Refereed Scientific Journals - Sandy, Andy L., Jia Guo, Robert J. Miskewitz, Wade R. McGillis, Lisa A. Rodenburg. 2013. Mass transfer coefficients for volatilization of polychlorinated biphenyls from the Hudson River. *Chemosphere*. Vol. 90(5). 1637-1643.
4. 2008NJ164B ("Identifying the source of excess fine-grained sediments in New Jersey rivers using radionuclides") - Book Chapters - Feng, H., J.C. Galster, J. Lopes, N.M. Bujaski, K. Barrett, K. Olsen. 2012. Radionuclides (<sup>7</sup>Be, <sup>210</sup>Pb and <sup>137</sup>Cs) as tracers for Soil and Sediments Erosion in New Jersey stream watersheds, in Javier Guillen Gerada ed., *Radionuclides: Sources, Properties and Hazards*, Hauppauge, NY, Nova Publishers, pages 22-34.
5. 2008NJ161B ("Microbial Mobilization of Arsenic and Selenium Oxyanions in Subsurface Aquifers") - Articles in Refereed Scientific Journals - Rauschenbach, I., M.M. Haggblom, E.B. Bini, and N. Yee. 2012. Physiological response of *Desulfurispirillum indicum* S5 to arsenate and nitrate as terminal electron acceptors. *FEMS Microbiology and Ecology*. 81. 156-162.
6. 2008NJ157B ("PBDEs and Other Brominated Compounds in a Bioreactor Landfill") - Dissertations - Loudon, J.A. 2011. Reductive dehalogenation potential in a leachate recirculating bioreactor landfill and its affect on leachate toxicity. "M.S. Thesis." Department of Environmental Sciences, Graduate School, Rutgers University, New Brunswick, NJ. 101 pages.
7. 2010NJ216B ("Impact of salinization on New Jersey amphibian species: A physiological approach to water quality issues") - Other Publications - Hazard, L.C., K. Kwasek, E. Koelmel, M. Gonzalez-Abreu, and S. Gerges. 2012. Variation in salinity aversion of temperate forest amphibian species may influence response to anthropogenic saliniazation. World Congress of Herpetology, Vancouver, B.C., Canada. (poster presentation)
8. 2010NJ218B ("Evaluation of three methodologies to document improvement of water quality through stormwater management measures in an urban subwatershed") - Articles in Refereed Scientific Journals - Rector, P., C.C. Obropta, and B. Pearson. 2012. Community-scale disconnection of impervious surfaces in suburban New Jersey. *Journal of NACAA*. 5(2). Online publication: <http://www.nacaa.com/journal/>
9. 2010NJ231B ("Green Remediation of Tetracycline in Soil-Water Systems") - Other Publications - Punamiya, P., Sarkar, D., and Datta, R. 2012. Drinking water treatment residuals as a "green" sorbent for veterinary antibiotics: Results from an incubation study. Proceedings of the Annual Conferences of the Hudson Delaware Regional Chapter of the Society of Environmental Toxicology and Chemistry. Platform presentation.
10. 2011NJ273B ("An Investigation of the Water Quality of Rainwater Harvesting Systems") - Conference Proceedings - Bakacs, M. and M. Haberland. 2011. Preliminary Investigation of Roof Runoff Water Quality for Small Scale Rainwater Harvesting. Proceedings 96th Annual Meeting and Professional Improvement Conference National Association of County Agricultural Agents. Overland Park, Kansas, p. 58.
11. 2011NJ273B ("An Investigation of the Water Quality of Rainwater Harvesting Systems") - Conference Proceedings - Bakacs, M. and M. Haberland. 2012. How Healthy is Your Rain Barrel?

Water Quality of Small Scale Rainwater Harvesting Systems. Proceedings of the 2012 Land Grant/Sea Grant National Water Conference. Portland, OR. Electronic Posting:  
[http://www.usawaterquality.org/conferences/2012/abstract\\_index.html](http://www.usawaterquality.org/conferences/2012/abstract_index.html)

12. 2011NJ276B ("Assessment of Green Frog, *Lithobates clamitans*, populations as biological indicators of risk to communities near Superfund sites") - Other Publications - Costello, Jennifer and Richard Veit. 2012. Frogs as Biological Indicators: Does Habitat Degradation Impact Prey Capture Efficiency? World Congress of Herpetology, Vancouver, B.C., Canada. (poster presentation)
13. 2011NJ280B ("Development of a Push-Pull Technique to Simultaneously Characterize Volatilization and Biodegradation Rates of VOCs in Shallow Wetland Sediments") - Articles in Refereed Scientific Journals - Reid, Matthew C. and Peter R. Jaffe. 2013. A Push-Pull Test to Measure Root Uptake of Volatile Chemicals from Wetland Soils. *Environmental Science and Technology*, 47, 3190-3198.
14. 2011NJ280B ("Development of a Push-Pull Technique to Simultaneously Characterize Volatilization and Biodegradation Rates of VOCs in Shallow Wetland Sediments") - Other Publications - Reid, Matthew C. and Peter R. Jaffe. 2013. In situ measurements of dissolved gas dynamics and root uptake in the wetland rhizosphere. European Geosciences Union General Assembly, Vienna, Austria. *Geophysical Research Abstracts*, Vol. 15, EGU 2013-175. (poster presentation)
15. 2011NJ280B ("Development of a Push-Pull Technique to Simultaneously Characterize Volatilization and Biodegradation Rates of VOCs in Shallow Wetland Sediments") - Other Publications - Reid, Matthew C. and Peter R. Jaffe. 2012. Pathways for volatilization from the wetland rhizosphere. EcoSummit, Columbus, OH. (poster presentation)
16. 2011NJ281B ("Release of Hazardous Metals into Surface and Groundwater by Microbial Oxidation of Sulfide Minerals") - Other Publications - Walczak, Alexandra, Nathan Yee, and Lily Y. Young. 2012. Phosphate reaction with PbS stimulates microbial S oxidation. 22nd V.M. Goldschmidt Conference, Montreal, Quebec, Canada. Abstract number 2309. (poster presentation)